PALACKÝ UNIVERSITY OLOMOUC

Faculty of Science

Department of Biochemistry

Viola odorata L.: Identification and Characterization of Na^+,K^+-ATPase Inhibiting Component

DIPLOMA THESIS

Author:	**Bc. Tomáš Heger**
Study Programme:	N1406 Biochemistry
Field of Study:	Biochemistry
Form of Study:	Full-time
Supervisor:	**Mgr. Jiří Grúz, Ph.D.**
Year:	2021

Prohlašuji, že jsem diplomovou práci vypracoval samostatně s vyznačením všech použitých pramenů a spoluautorství. Souhlasím se zveřejněním bakalářské práce podle zákona č. 111/1998 Sb., o vysokých školách, ve znění pozdějších předpisů. Byl jsem seznámen s tím, že se na moji práci vztahují práva a povinnosti vyplývající ze zákona č. 121/2000 Sb., autorský zákon, ve znění pozdějších předpisů.

V Olomouci dne 26. 4. 2021

Tomáš Heger

Poděkování

Velmi děkuji svému vedoucímu Mgr. Jiřímu Grúzovi, Ph.D. za veškerou pomoc s vypracováním práce, za cenné konzultace a předané zkušenosti. Poděkování patří také Natalyi Fedosové, Ph.D. a doc. RNDr. Martinu Kubalovi, Ph.D. kteří mě vedli při práci na biochemické charakterizaci inhibice Na^+,K^+-ATPasy. Děkuji také Ing. Bc. Tereze Štenclové, Anežce Šindlerové, Mgr. Marii Kvasnicové, PhD a Mgr. Lucii Koplíkové za pomoc při zpracování vzorků a měření. V neposlední řadě děkuji také své rodině za podporu v průběhu studia.

Bibliografická identifikace

Jméno a příjmení autora	Tomáš Heger
Název práce	*Viola odorata* L.: Identifikace a charakterizace složky inhibující Na^+,K^+-ATPasu
Typ práce	Diplomová
Pracoviště	Laboratoř růstových regulátorů
Vedoucí práce	Mgr. Jiří Grúz, Ph.D.
Rok obhajoby práce	2021

Abstrakt

Zástupci rodu *Viola* mají důležitou roli v tradiční bylinné medicíně Asie. V této práci je zkoumána schopnost extraktu *Viola odorata* L. inhibovat Na^+,K^+-ATPasu, zvířecí enzym zodpovědný za udržování membránového potenciálu. Extrakt z kořene *V. odorata* silně inhiboval Na^+,K^+-ATPasu, zatímco extrakt ze semen nebo listů byl neúčinný. K identifikování chemického principu zapříčiňujícího aktivitu extraktu kořene byla provedena metabolomická UHPLC-QTOF-MS/MS analýza, ve které bylo detekováno 35 292 features. Kandidátní aktivní sloučeniny byly selektovány na základě korelace plochy features a biologické aktivity 14 izolovaných frakcí extraktu. Ze souboru 15 kandidátních sloučenin bylo 14 předběžně identifikováno jako procyanidiny. Následně byla proto zkoumána inhibice Na^+,K^+-ATPasy komerčně dostupnými procyanidiny (B1, B2, B3 a C1). Dimerní procyanidiny B1, B2 a B3 byly neaktivní, avšak trimerní procyanidin C1 silně inhiboval Na^+,K^+-ATPasu s IC_{50} 4,5 μmol·L^{-1}. Ještě silněji byla inhibována *p*-nitrofenylfosfatasová aktivita enzymu s IC_{50} 0,56 μmol·L^{-1}. Interakce sloučeniny s Na^+,K^+-ATPasou byla zkoumána pomocí několika fluorescenčních experimentů za využití prób eosinu a anthroylouabainu. Nově objevený inhibitor byl dokován do krystalových struktur mimikujících Na_3E_1~P·ADP a K_2E_2·P_i stavy enzymu, aby bylo možné identifikovat potenciální interakční místa s Na^+,K^+-ATPasou. Byl diskutován možný vazebný mechanismus inhibitoru a princip stojící za pozorovanou aktivitou extraktu kořene.

Klíčová slova	Na^+,K^+-ATPasa; *Viola odorata* L.; metabolomika; UHPLC-QTOF-MS/MS; procyanidin; flavan-3-ol; inhibitor; molekulový docking
Počet stran	79
Počet příloh	0
Jazyk	Anglický

Bibliographical identification

Autor's first name and surname	Tomáš Heger
Title	*Viola odorata* L.: Identification and Characterization of Na^+,K^+-ATPase Inhibiting Component
Type of thesis	Diploma
Department	Laboratory of Growth Regulators
Supervisor	Mgr. Jiří Grúz, Ph.D.
The year of presentation	2021

Abstract

Members of the *Viola* genus play important roles in traditional Asian herbal medicine. This work investigates the ability of *Viola odorata* L. extracts to inhibit Na^+,K^+-ATPase, an essential animal enzyme responsible for membrane potential maintenance. The root extract of *V. odorata* strongly inhibited Na^+,K^+-ATPase, while leaf and seeds extracts were basically inactive. A UHPLC-QTOF-MS/MS metabolomic approach was used to identify the chemical principle of the root extract's activity, resulting in the detection of 35 292 features. Candidate active compounds were selected by correlating feature area with inhibitory activity in 14 isolated fractions. This yielded a set of 15 candidate compounds, of which 14 were preliminarily identified as procyanidins. Commercially available procyanidins (B1, B2, B3 and C1) were therefore purchased and their ability to inhibit Na^+,K^+-ATPase was investigated. Dimeric procyanidins B1, B2 and B3 were found to be inactive, but the trimeric procyanidin C1 strongly inhibited Na^+,K^+-ATPase with an IC_{50} of 4.5 μmol·L^{-1}. The *p*-nitrophenyl phosphatase activity of the enzyme was inhibited even more with an IC_{50} of 0.56 μmol·L^{-1}. The interaction of the compound and Na^+,K^+-ATPase was studied using anthroyl ouabain and eosin in several fluorescence experiments. This newly discovered inhibitor was docked into crystal structures mimicking the $Na_3E_1{\sim}P{\cdot}ADP$ and $K_2E_2{\cdot}P_i$ states to identify potential interaction sites within Na^+,K^+-ATPase. Possible binding mechanisms and the principle responsible for the observed root extract activity are discussed.

Keywords	Na^+,K^+-ATPase; *Viola odorata* L.; metabolomics; UHPLC-QTOF-MS/MS; procyanidin; flavan-3-ol; inhibitor; molecular docking
Number of pages	79
Number of appendices	0
Language	English

CONTENTS

AIMS AND OBJECTIVES

Theoretical part:

1) Literature survey on approaches used for the identification of biologically active natural products.
2) Literature survey on the biochemical characterization of the Na^+,K^+-ATPase inhibiting compound from *Viola odorata* L.
3) Literature survey on structural and functional characterization of Na^+,K^+-ATPase.

Practical part:

1) Plant material extraction, fractionation, and non-targeted UHPLC-QTOF-MS/MS analysis of isolated fractions.
2) Identification of the active component by correlation of the determined Na^+,K^+-ATPase inhibition with feature/metabolite areas among isolated fractions.
3) Biochemical characterization of Na^+,K^+-ATPase-inhibiting component of *Viola odorata* L. extract focused on interactions with the enzyme of interest.

1 INTRODUCTION

Plant secondary metabolite research is being reintroduced into drug discovery programmes as modern technologies and approaches help to combat previously hard to overcome challenges related to natural product drug discovery. Advancements mainly in the field of genomics, metabolomics, proteomics, and biotechnology enable the identification of biologically active molecules from complex mixtures and elucidation of their mechanism of action (Atanasov *et al.*, 2021).

In correlation metabolomics, biological activity screening of plant extract fractions is combined with ultra-high-performance liquid chromatography coupled with high-resolution mass spectrometry. Fractions are isolated using orthogonal separation techniques to optimally distribute the chemical composition between fractions. As a result, an increased probability of candidate feature/metabolite identification is reached. The peak area is correlated with the observed biological effect to obtain a candidate feature list which should likely contain the active component (Rárová *et al.*, 2019).

Species from the *Viola* genus have their traditional place in herbal medicine of Asian nations (Akhbari *et al.*, 2012). Besides the fact that *Viola odorata* L. leaf extract is used in perfumery, our knowledge of the sweet violet phytochemistry and ethnopharmacology is limited, especially in the case of the violet root (Saint-Lary *et al.*, 2014). In the previous work, *V. odorata* root crude extract was reported to inhibit ATPase activity of Na^+,K^+-ATPase (Heger, 2019).

Translocase Na^+,K^+-ATPase (EC 7.2.2.13) not only enables essential ion transport across the plasma membrane and subsequent secondary active transport but also participates in a signalling network that is so far not well-understood. Inhibitors of the enzyme are prescribed as drugs for the treatment of heart insufficiency and irregular heartbeat. Recent research suggests a possible broader effect of Na^+,K^+-ATPase on health associated with altered signalling and not only disabled ion-transport function alone (Prassas and Diamandis, 2008). Accordingly, the inhibition of Na^+,K^+-ATPase might positively influence certain biological processes and conditions like cancer, virus infection, hypercholesterolemia, and glaucoma (Amarelle *et al.*, 2019; Katz *et al.*, 2015; Cayo *et al.*, 2017; Song *et al.*, 2020).

2 CURRENT STATE OF RESEARCH

2.1 Natural Product-Based Drug Discovery

The term "natural product" might, in the broadest context, represent any substance produced by organisms (primary or secondary metabolites, and mixtures thereof possibly containing substances with low and/or high molecular weight). However, the meaning often covers the compounds belonging to the group of secondary metabolites, specifically (Editorial, 2007; Dias *et al.*, 2012; Williams *et al.*, 1989). As organic molecules of primary metabolism, primary metabolites are found in all organisms and are essential for life processes. Secondary metabolism generates organic molecules with more diverse functions that often remain not fully understood and might fulfil specific requirements of a defined group of organisms. Secondary metabolites can be produced for symbiotic purposes (meaning either mutualistic or competitive relationship) or as metal chelators, differentiating factors, and signalling molecules (Demain and Fang, 2000).

From a medicinal chemistry point of view, natural products offer enormously wide chemical space, often referred to as going far behind synthetic chemists' imagination (Nicolaou *et al.,* 2012). Since ancient times, plenty of natural products are believed to cure various diseases, therefore they seem relevant for the drug discovery process in modern days.

The importance of natural products can easily be recognized from an analysis of the drug market. Newman and Cragg (2020) classified 1881 newly approved drugs between 1981 and 2019 based on their origin. Focusing on the group of small molecules (n = 1394) in Figure 1, there are 32% of agents falling into the group of unaltered natural products, botanical drugs, or natural product derivatives. If also synthetic mimics of natural product and synthetic drugs with natural product pharmacophore are considered, the whole group of natural product-related drugs represents 67%.

Most frequently, natural product-derived drugs belong to the group of anti-infectives or anticancer agents. This biological activity might be related to the ecological role of secondary metabolites which is often represented by the harmful effect to neighbouring organisms competing for the same resources (Cragg *et al.*, 2009; Manivasagan *et al.*, 2014; Booysen and Dicks, 2020).

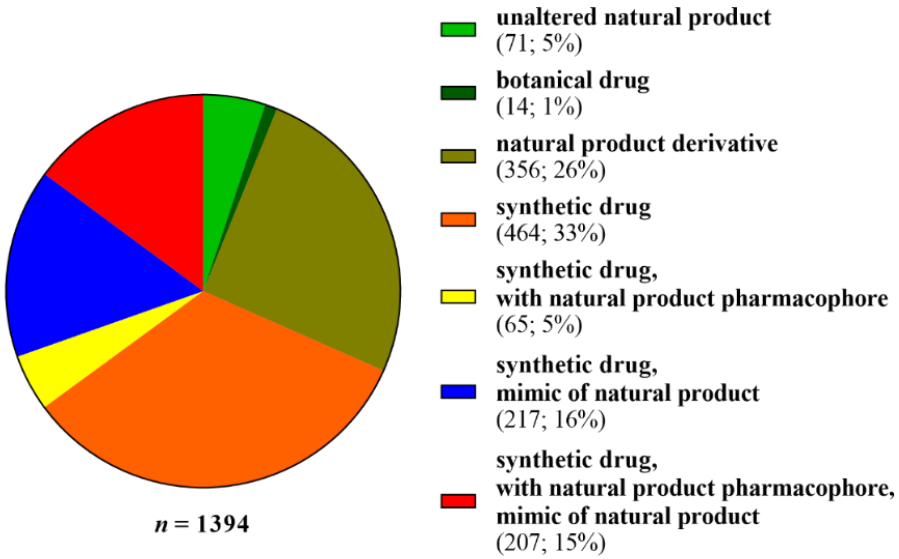

Figure 1 All small molecule drugs approved from 1. 1. 1981 to 30. 9. 2019 classified based on their origin. Adapted from Newman and Cragg (2020).

2.1.1 Properties of Biologically Active Natural Products

Compared to small molecules synthesized by medicinal chemists, natural products might have properties that are against generally accepted rules regarding ideal chemical structures in drug discovery. The most typical example of such rules was quantitatively defined by Lipinski in 1997 and nowadays the concept is known as Lipinski's rule of five (Lipinski *et al.*, 1997). The so-called rule of five was introduced to describe poor absorption or permeation of molecules, and was formulated as the presence of more than five hydrogen bond donors, more than ten hydrogen bond acceptors, the relative molecular mass greater than 500, and calculated octanol-water partition coefficient LogP greater than five.

Elimination of these features from a lead compound following Lipinski's rule of five favours drug-like structural characteristics. However, there are many other properties related to drug-likeness, and therefore, both concepts are certainly not equal (Mignani *et al.*, 2018). From the Dictionary of Natural Products database, 60% of unique molecules complied with Lipinski's rule of five (Quinn *et al.*, 2008). However, it is common among natural products that bioavailable and biologically active substances violate the rule of five although they might have high potential as leads (Ganesan, 2008). This is proved by 32% of natural products and their derivatives represented in small molecule drugs as mentioned above. Additionally, in contrast to a common rule of five violation, natural products and their derivatives were shown to exert a better drug-likeness score than the

COBRA library of synthetic and pharmacologically active compounds (Grabowski and Schneider, 2008; Schneider and Schneider, 2003).

Exploring the difference between natural products and synthetic drugs in more detail, it was shown that there are approximately three times more aromatic atoms, five times more chiral centres, twice more oxygen and four times fewer nitrogen atoms, almost twice more hydrogen bond donors and half more acceptors in natural products (Grabowski *et al.*, 2008). According to previously cited literature, the important parameter of bioavailability—the topological polar surface area—is larger compared with synthetic drugs. Based on another analysis of natural products, this parameter has broader distribution towards larger values (Grabowski *et al.*, 2008; Ertl *et al.*, 2008). In both mentioned studies, lipophilicity expressed as calculated LogP showed to be lower in natural products. The evolution-based design of natural products is mirrored in the correlation of their average molecular volume with the volumes of protein cavities extracted from Protein Data Bank (www.pdb.org) which is critical for possible molecular interactions (Koch *et al.*, 2005).

2.1.2 Challenges in Natural Product-Based Drug Discovery

In the previous chapter, it was described that natural products can offer unique chemical space which might otherwise remain unexplored due to chemist's limited synthetic possibilities and imagination usually not crossing the borders of some generally accepted drug-likeness rules in medicinal chemistry (Ganesan, 2008). Therefore, an attempt to integrate natural products in the drug discovery process can help not only investigate more diverse structures but also increase the probability of hit identification (Ertl *et al.*, 2008).

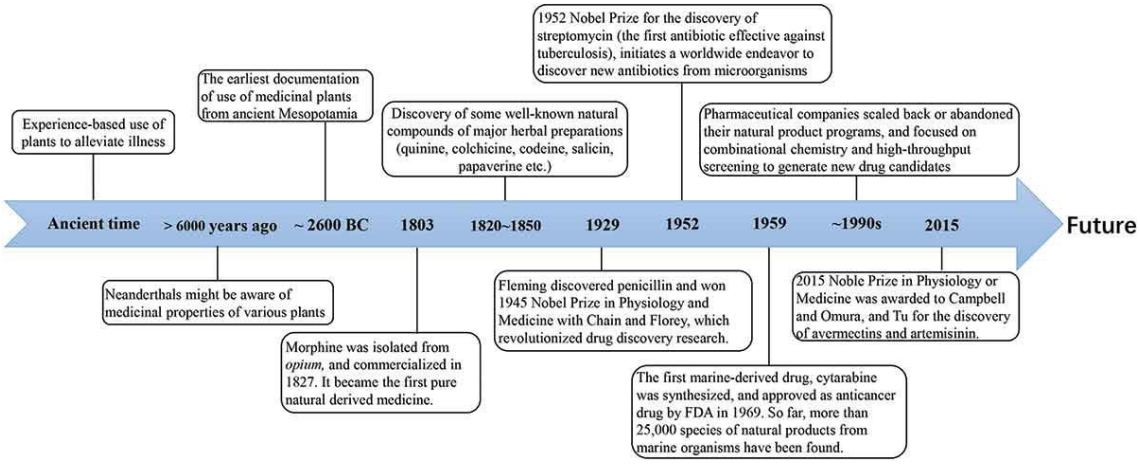

Figure 2 Selected milestones of natural product-based drug discovery. From Li *et al.* (2019).

In contrast to the theoretical benefits of natural products integration into screening campaigns, many practical problems resulted in the abandonment of natural product divisions by pharmaceutical companies in the 1990s (Figure 2). Natural product biological activity screening seemed to be a waste of effort due to the high false-positive hit rate (Jadhav *et al.*, 2010; Baell, 2016; Bisson *et al.*, 2016). Not only because of this reason, synthetic compound libraries predominated the drug discovery process. Also, rediscoveries of already known compounds, difficult isolation of pure compounds from extracts, and incompatibility with high-throughput strategies led to the decline in finding new leads among secondary metabolites (Li *et al.*, 2019).

Despite many advantageous properties, synthetic compound libraries lack structural diversity compared to the range provided by natural products. Inspiration how to enlarge chemical space in synthetic chemistry can rise from biosynthetic pathways and scaffold diversity of natural products. For example, ring-distortion strategy (Huigens *et al.*, 2013), one-pot polymer-supported synthesis (Basu and Waldmann, 2014), imino-Diels-Alder reactions (Sankar *et al.*, 2015) with several points of diversity in molecules, scaffold synthesis via andrographolide ozonolysis (Mang *et al.*, 2006), biology-oriented synthesis (BIOS) (Corrêa *et al.*, 2007), a cheminformatic approach based on structural classification of natural products (SCONP) (Koch *et al.*, 2005), and diversity-oriented synthesis with intra- and intermolecular ring rearrangement (Chauhan *et al.*, 2017) were successfully applied to find new biologically active molecules.

The testing campaign involving natural products in biochemical assays often brings many false-positive results as mentioned earlier. Artefactual hits appear due to nonspecific effects like incompatibility (e.g. compound autofluorescence) or interference of natural products with a biochemical test. Previously, a new substructure filter was introduced into libraries for high throughput screening to identify and eliminate pan assay interference compounds (PAINS) – frequent hitters in various assays sharing problematic substructural features (Baell and Holloway, 2010). In the previous review by the same author, the occurrence of PAINS motifs among natural products is discussed in detail (Baell, 2016). Some examples of secondary metabolites with problematic behaviour are demonstrated in the next subsection below.

2.1.2.1. False-Positive Results

Non-specific and non-stoichiometric inhibition is a significant source of false-positive results in natural product screenings. Jadhav *et al.* (2010) showed that 1.2% of 420 tested natural products acted as aggregate-based inhibitors on cysteine protease cruzain. Colloidal aggregation is an assay artefact commonly characterized by a steep dose-response curve with a high Hill coefficient and non-specific inhibition behaving differently from typical stoichiometric inhibition (Shoichet, 2006). Such inhibitors form aggregates observable by electron microscope as particles in tens or hundreds of nanometre range. Enzymes are inactivated by sequestration and unfolding on the surface of these colloidal particles (Simeonov *et al.*, 2008; McGovern *et al.*, 2002).

By the detergent treatment or variable preincubation period, it is possible to distinguish aggregate-based inhibitors from stoichiometric inhibitors (Feng and Shoichet, 2006; Feng *et al.*, 2007; Ryan *et al.*, 2003). Typically, dynamic light scattering measurement is used to investigate sample homogeneity and the potential presence of aggregated compound particles (Pohjala and Tammela, 2012; Seidler *et al.*, 2003). For instance, the dynamic light scattering characterization of aggregates and detergent-reversible β-lactamase and malate dehydrogenase inhibitions were performed in the study investigating secondary metabolites originating from traditional Chinese medicine formulations (Duan *et al.*, 2015). Nevertheless, this technique does not enable a high-throughput approach in its basic setup. Especially problematic aggregators are tannins due to their wide distribution in plant extracts. There are several methods to eliminate tannins, e.g. chromatographic separation, sorption, liquid-liquid extraction, and solid-phase extraction. The application of one of these techniques should be considered before activity screenings if tannins are present in samples (Wall *et al.*, 1996; Eldridge *et al.*, 2002). A useful tool for prediction of possible aggregation by a given compound based on its physical properties and structure similarity to previously reported aggregators is available online (http://advisor.bkslab.org/search/ (Irwin *et al.*, 2015)).

Besides biochemical assays with proteins in solution, aggregates also appear as problems in live cell assays where they can non-specifically trigger receptor signalling (Wang *et al.*, 2019; Sassano *et al.*, 2013). Resonant waveguide grating-based aggregation assay was shown useful in natural product aggregation screening (Wang *et al.*, 2019). Authors effectively used biosensor microplate high-throughput format to determine compound critical aggregation concentration in cell-free assay and observe dynamic mass redistribution in cell-based assay with or without detergent. Along with previously

mentioned methods, this approach can distinguish between the specific and aggregate-based activity in screening campaigns, which is a crucial step in the natural product drug discovery process.

Another example of a non-specific activity is the physical influence of phenolic phytochemicals on biological membrane properties. The amphiphilic character of phytochemicals—e.g. resveratrol, capsaicin, and genistein—results in modified bilayer function affecting integral membrane proteins. The resulting effect might be misinterpreted as a specific compound-protein interaction (Ingólfsson *et al.*, 2014). Moreover, compounds like triterpenoid saponins can even have membrane disrupting properties (Konoki and Tachibana, 1996).

Other biochemical interference can be a covalent modification of enzyme by tested phytochemical. It was demonstrated that reactive side chains of tryptophan, lysine and cysteine can be covalently modified by phenolic compounds, especially these with the ability of quinone formation (Schilling *et al.*, 2008; Rohn *et al.*, 2002). Additionally, there are other phytochemicals with electrophilic centres capable of covalent modification of proteins as well, for example, organosulfur compounds (Wilde *et al.*, 2016), isothiocyanates (Nakamura *et al.*, 2009), aldehydes and ketones (Dasari *et al.*, 2015a; Dasari *et al.*, 2015b), polyynes (Ohnuma *et al.*, 2010), lactones (De Pascale *et al.*, 2011), and epoxides (He *et al.*, 2015).

UV-Vis spectroscopic techniques offer a comfortable way of activity measurement in screening assays. However, fluorescent natural products might interfere with the activity detection based on fluorescence (Simeonov *et al.*, 2008). This problem can be solved by using red-shifted fluorescent dyes, increasing fluorophore concentration or by lifetime discriminated polarization (Turek-Etienne *et al.*, 2003; Fowler *et al.*, 2002). The study analysing potential interferences identified 11 of 29 tested flavonoids acting as strong quenchers of 4-methylumbelliferone fluorescence in the neuraminidase activity assay (Kongkamnerd *et al.*, 2011).

In reporter assays, bioluminescence produced by luciferase is commonly used for the investigation of repression or activation of target gene transcription. The fact that natural products inhibiting luciferase activity were previously described demonstrates that some secondary metabolites might be a potential source of interference as well (Somanadhan *et al.*, 2011; Cruz *et al.*, 2011). For example, some compounds with flavonoid scaffold were identified as luciferase inhibitors (Auld *et al.*, 2008). Accordingly, the general need for careful interpretation of luciferase-based assays to avoid misleading results was

emphasized in literature because it is well-known problem of established compound libraries (Pang *et al.*, 2011; Thorne *et al.*, 2012; Auld *et al.*, 2008).

2.1.2.2. Identification of Biologically Active Molecules

During the first decade of the 19th century, German pharmacist Friedrich Wilhelm Sertürner isolated morphine from opium and proved its pharmacological effect (Schmitz, 1985). Nowadays, morphine is considered the first isolated biologically active principle. The discovery influenced further development in pharmacy demonstrating the idea of natural product principle as a biologically active chemical entity that can be precisely dosed (Hamilton and Baskett, 2000). Identification of biologically active molecule in a complex mixture of naturally occurring compounds is thought to be the greatest challenge in the process of drug discovery from bioactivity screenings involving crude extracts and fractions thereof. The so-called "top-down" approach is applied in the practical part of this thesis mainly based on metabolomics study (Li *et al.*, 2019). Here, bioassay-guided fractionation and fraction libraries of natural products are discussed as one of the possible strategies in the identification of active molecule.

Traditionally, the drug discovery process from natural sources starts with testing the biological activity of crude material extracted by different solvents. Variability in solvents ensures extraction of a wide range of compounds with different polarity. After selecting the best solvent for initial extraction, the active extract is then further separated into fractions. Biological activity is tracked in the fractions while the complexity of the compound mixture is being reduced by several sub-fractionation steps (e.g. by the introduction of further polarity-differentiated fractions and/or Sephadex LH-20 fractions). This sequential process is called bioassay-guided fractionation. At the final stage, a larger amount of source material for extraction is usually needed for the purification of the target compound, typically by HPLC. Eventually, the biological activity of the isolated chemical entity is validated (Sferrazza *et al.*, 2020; Beutler *et al.*, 1993; Cantrell *et al.*, 2000; Uddin *et al.*, 2001; Schlenk *et al.*, 2005).

Re-discovery of natural product with known biological activity occurring during bioassay-guided fractionation is the drawback that wastes the whole effort for finding new biologically active molecules. Dereplication tackles the issue since the very beginning because this strategy aims to recognise and eliminate known active substances or their novel but closely related derivatives with the expected identical mechanism of action (Ito and Masubuchi, 2014). After this initial step, the discovery of novel

compounds is presumed so that resources spent during the research process are not wasted (Hou *et al.*, 2012). Preferentially, information on retention time, UV-Vis spectra, and MS(/MS) spectra obtained from LC-MS analysis are usually used for dereplication by comparing them to available databases, which is a well-established and robust approach typically carried out with crude extracts (Wolfender *et al.*, 2015; Roemer *et al.*, 2011; Nothias *et al.*, 2018). Usage of the above-mentioned detailed parameters ensures that isobaric compounds can be effectively distinguished. More recently, ion mobility (IM) drift time and calculated collision cross-section are integrated into dereplication to provide further structure-related information about the secondary metabolite (Schrimpe-Rutledge *et al.*, 2018). A detailed survey on dereplication strategies described in literature published between 1990 and 2014 provides an in-depth analysis of various methodologies (Hubert *et al.*, 2017). An interesting hypothesis was introduced describing the discovery of known natural product in different unrelated species as an indication for biological activity (Tulp and Bohlin, 2005). In this case, the rediscovery of a compound with unknown biological activity might be valuable because biosynthesis by unrelated organisms is improbable if the compound does not have any biological target.

Bioassay-guided fractionation is an exhausting process that typically requires gram quantities of source organism to be extracted. Automatization of the procedure and compatibility with modern high-throughput screenings are demanded as well. Commonly, the biological activity can be lost during the fractionation process due to its synergistic nature, a degradation of active compound or failures in compound isolation (Nothias *et al.*, 2018). Accessibility of biological material for subsequent isolation of the active principle in required quantity or too low concentration of active compound might also be a problem disabling bioassay-guided isolation. For example, the authors of the original article referring to the isolation of paclitaxel from western yew stem bark alcohol extract reported the yield of 0.02% (Wani *et al.*, 1971). However, the combination of high-resolution mass spectrometry (HRMS) with modern and sensitive NMR techniques allows the characterization of metabolites in tens of microgram quantities directly in a fraction library as described below.

To speed up the drug discovery process from natural products, the integration of instrumental techniques and direct coupling of the separation step with biological activity testing is crucial. Researchers in the pharmaceutical company Sequoia Sciences obtained a diverse plant extract-based library of 36 000 fractions containing approx. 1–5 compounds/well (Eldridge *et al.*, 2002). Authors were attentive to possible interfering

compounds like tannins and integrated steps eliminating too polar or lipophilic compounds and compounds with high molecular weight which do not have druglike properties. Scaling the whole process down and using the high-throughput format, as it was demonstrated on *Taxus brevifolia*, resulted in structure elucidation of biologically active compounds within the time and amount of plant material incomparable to traditional methods. Anticancer activity screening combined with LC-MS and NMR measurements enabled detecting minor biologically active metabolites with otherwise undetectable activity in flash fractions at the beginning of the screening.

A similar study was performed to investigate marine natural products. The authors generated 15 360-membered fraction library from desalted marine invertebrate extracts where mostly three compounds or less per fraction were detected (Bugni *et al.*, 2008). Separation was based on 2D chromatographic techniques involving HPLC fractionation protocol with online HRMS measurement. The developed methodology was tested in high-throughput phenotypic screening for selectively cytotoxic compounds in BRCA2-deficient cell line. A class of DNA-intercalating compounds plakinidines came out as hits and were further characterized directly in the active fractions using NMR. Due to the high separation level, it was possible to successfully identify minor selectively cytotoxic secondary metabolites plakinidines directly in the fraction library. The active compounds could be masked in bioassay-guided fractionation by general cytotoxicity of crellastatins, other compounds known to be present in the source organism.

Fraction libraries can also effectively facilitate the discovery of new structures without connection to biological activity in screening. LC-MS data (UV-Vis spectra, retention time and detected *m/z*) obtained during library preparation can be compared with the records in a database (Osada and Nogawa, 2012). This type of basic research in natural products can be then followed by subsequent characterization of biological activity, e.g. cytotoxicity and antimicrobial, antiparasitic, and antifungal activity as demonstrated on fraction libraries of microbial metabolites (Jang *et al.*, 2014; Lim *et al.*, 2014; Nogawa *et al.*, 2010; Nogawa *et al.*, 2012; Lim *et al.*, 2016).

Hence, above mentioned examples show some advantages of natural product fraction libraries, including reduced complexity, the discovery of minor biologically active compounds, the unmasking of active compound from more potent or oppositely acting compounds, rapid identification of active compound without the need for re-extraction, and importantly, suitability for high-throughput screenings with improved performance (Wilson *et al.*, 2020; Butler *et al.*, 2014).

Finally, as a consequence of technological development, pharmaceutical companies introduce natural products into research again since many problems can be tackled with modern approaches and technologies. Genomics and biotechnology are described in the next chapter as tools targeting challenges of identification, isolation, and production of biologically active secondary metabolites.

2.1.2.3. Biotechnology and Genomics in Natural Product Discovery

Biotechnology can facilitate natural product drug discovery at any stage. It enables the production of appreciated natural compounds in greater amounts in so-called cell factories with undemanding requirements for cultivation (Hao Guo *et al.*, 2020). Moreover, novel natural products can be generated by combinatorial biosynthesis in synthetic biology (Kim *et al.*, 2015). And importantly, biotechnology tools can uncover bioactive principle from the source organisms at the beginning of the discovery route, mainly based on the biosynthetic gene cluster identification.

Biosynthetic pathways of secondary metabolites in fungi and bacteria are regulated via biosynthetic gene clusters defined as a physically clustered group of two or more genes (Medema *et al.*, 2015). The Genomic Standards Consortium introduced the compound type-based classification of biosynthetic gene clusters into groups encoding non-ribosomal peptide synthetases, ribosomally synthesized and post-translationally modified peptides, polyketide synthases, and terpene, saccharide, or alkaloid biosynthesis enzymes. However, it was shown that also plants produce some valuable secondary metabolites via biosynthetic pathways encoded by biosynthetic gene clusters. So this phenomenon is not exclusively observed only in prokaryotes (Guo *et al.*, 2018; Qi *et al.*, 2004; Winzer *et al.*, 2012; Itkin *et al.*, 2013). Various biotechnological manipulations ranging from DNA library construction to heterologous expression are highly applicable for drug discovery purpose due to the nature of biosynthetic gene clusters, especially in the case of microorganisms exemplified below.

Genome mining and metagenomics in natural product drug discovery can be specifically useful in the identification of source organism producing desired bioactive metabolites. Almost unexplored metabolic diversity in marine microorganisms can be approached by metagenomics when cloning environmental DNA into libraries (Kennedy *et al.*, 2008). This enables the investigation of enzymatic pathways which would be otherwise impossible due to the inability to cultivate approx. 99% of microorganisms outside their natural environment (Vartoukian *et al.*, 2010). Function-based or

sequence-based metagenomics can be applied to screen environmental DNA library for the presence of biosynthetic gene clusters. Function-based metagenomics uses easily observable or measurable phenotype, whereas sequence-based metagenomics involves screening for target DNA sequence, both indicating the presence of biosynthetic gene clusters in the sample (Zhang *et al.*, 2017).

Another possibility of biosynthetic gene cluster investigation without the need for source microorganism cultivation is the synthetic biology platform called HEx (Heterologous Expression) enabling rapid and scalable production of cluster metabolites in *Saccharomyces cerevisiae* (Harvey *et al.*, 2018). Problems with microorganism cultivation, cryptic biosynthetic gene clusters or low metabolite production can be potentially all solved by heterologous expression in the suitable host organism (Luo *et al.*, 2016). Depending on biosynthetic pathway requirements and metabolic differences between source and host organisms, host metabolism must be optimized via metabolic engineering to produce as large an amount of natural product as possible (Zhang *et al.*, 2016; Bian *et al.*, 2017).

Meta-omics was successfully used for biosynthetic pathway elucidation in the case of hardly accessible anticancer compound trabectedin (Rath *et al.*, 2011). Occurring in the tunicate *Ecteinascidia turbinata*, this complex molecule is a biosynthetic product of associated intracellular bacteria *Candidatus Endoecteinascidia frumentensis*. In the different study, genome mining of *Arabidopsis thaliana* leaf microbiome in combination with imaging mass spectrometry and bioactivity-guided fractionation led to the discovery of previously unknown polyketide macrobrevin, antibiotics bearing unprecedented chemical scaffold (Helfrich *et al.*, 2018). Many other examples demonstrate that genome mining followed by analytical techniques accelerates the exploration of natural product chemical space and biological activity (Albarano *et al.*, 2020).

A modern example of biotechnological applications in natural product drug discovery is CRISPR-Cas9 mediated manipulation. The system allows gene knockout preventing rediscoveries of known bioactive compounds (Culp *et al.*, 2019) or transcription activation by the introduction of either strong promoter (gene knock-in) or transcriptional activators (CRISPR activation) (Mózsik *et al.*, 2021; Mingzi M. Zhang *et al.*, 2017). Such gene activation leads to transcription from biosynthetic gene clusters that would otherwise be silent under non-native cultivation conditions.

However, this genetic tool can also be used in plants to modulate biosynthetic pathways as demonstrated in several cases. For instance, in the opium poppy, gene encoding 3′-hydroxyl-N-methylcoclaurine 4′-O-methyltransferase (*4'OMT2*) was knocked out using the CRISPR-Cas9 system. It was previously shown that *4'OMT2* has an important role in the regulation of benzylisoquinoline alkaloid biosynthesis. Correspondingly, *4'OMT2* knockout resulted in inhibition of (*S*)-reticuline metabolic flux and led to the discovery of novel uncharacterized alkaloid (Alagoz *et al.*, 2016). Other similar examples of CRISPR-Cas9-based applications include knockout in tanshinone biosynthesis in *Salvia miltiorrhiza* (Li *et al.*, 2017), increase in γ-aminobutyric acid production by tomato (Nonaka *et al.*, 2017), and the increase of oleic acid content in *Camelina sativa* seed oil (Morineau *et al.*, 2017).

Other techniques like genome-wide drug-induced haploinsufficiency screen (Baetz *et al.*, 2004), chemical-genetic interaction profiling (Kintses *et al.*, 2019; Parsons *et al.*, 2006), CRISPR loss-of-function screen (Gonçalves *et al.*, 2020), and various integrative approaches (Lee *et al.*, 2014) can elucidate the compound mechanism of action on the basis of detailed genetic knowledge. Moreover, some studies combined the determination of the mechanism of action with bioassay-guided fractionation, which proves the applicability of the above-mentioned methods on crude extracts (Ondeyka *et al.*, 2009; Jiang *et al.*, 2008). At the opposite end of the natural product-based drug discovery, large-scale production is needed. To be able to use natural products as drugs or for further modifications, upscaled production can be optimized with genetic engineering, heterologous biosynthesis, and bioreactor cultivations. Therefore, biotechnology makes otherwise frequently difficult-to-synthesize natural products more accessible (Luo *et al.*, 2015). However, these broader aspects go beyond the main scope of the master's thesis.

2.2 *Viola* genus and Traditional Medicine

Viola is the largest genus of the *Violaceae* family, containing up to 600 species (Ballard *et al.*, 1999). Members of this genus are used in traditional herbal medicine in many regions: *V. odorata* is used in Pakistan (Rahman *et al.*, 2016), *V betonicifolia* and *V. canescens* in the Himalayas (Bhatt and Negi, 2006; Verma *et al.*, 2011), *V. hondoensis* in Korea (Chung *et al.*, 2008), and *V. yedoensis*, *V. kunawarensis*, and *V. tianschanica* in Central and East Asia (Zhu *et al.*, 2016; Wang *et al.*, 2017). Sweet violet (*V. odorata*) is applied in the traditional treatment of a wide range of diseases, including neurological disorders and hypertension (Feyzabadi *et al.*, 2017).

2.2.1 Chemical Composition of *Viola odorata* L.

Sweet violet leaf extract produced in France and Egypt is used in perfumery for its specific fragrance (Saint-Lary *et al.*, 2016). Volatile components of *V. odorata* leaf extracts include nona-2,6-dienal and (*Z*)-hex-3-enal, which are the compounds primarily responsible for its odor. Most of the other volatile components are saturated or unsaturated aliphatic hydrocarbons and related oxidized species (Cu *et al.*, 1992). Another study identified phthalate and tetrahydrobenzofuranone derivatives and monoterpenoids as the main components of leaf extracts of an Iranian chemotype of *V. odorata* (Akhbari *et al.*, 2012). In addition, cyclic peptides called cyclotides (e.g. cycloviolacins) with diverse biological activities are found in various sweet violet organs (Parsley *et al.*, 2018; Narayani *et al.*, 2017). The phytochemistry of the related species *V. betonicifolia* has been reviewed in detail (Rizwan *et al.*, 2019).

There is relatively little published information on the secondary metabolite content of root extracts of *V. odorata*, which are the subject of this work. Phenolic acids and the flavonoid compounds vitexin and rutin were quantified in the roots of *V. tricolor* during a study on mycorrhizal colonization that demonstrated the influence of mycorrhizal fungi on secondary metabolite levels (Zubek *et al.*, 2015). Similar endophyte-induced changes in phytochemical composition are well documented (Welling *et al.*, 2016; Harrison, 1999). In *V. odorata*, the diversity of endophytes in the roots was higher than in other organs (Katoch *et al.*, 2017).

2.3 Procyanidins

Procyanidins are polyphenolic compounds consisting of condensed flavan-3-ol subunits (Figure 3). Monomers of (–)-epicatechin or (+)-catechin form oligomeric or polymeric structures that are classified based on the nature of their interflavan bonds (Figure 4). Specifically, they are categorized based on the stereochemistry of the bond (α or β) and the atoms linked by the bond: bonds between atoms C-4 and C-8 or C-4 and C-6 are classified as B-type linkages, while those between C-4 and C-8 along with C-2→O→C-7 ether bond are A-type linkages (Rauf *et al.*, 2019).

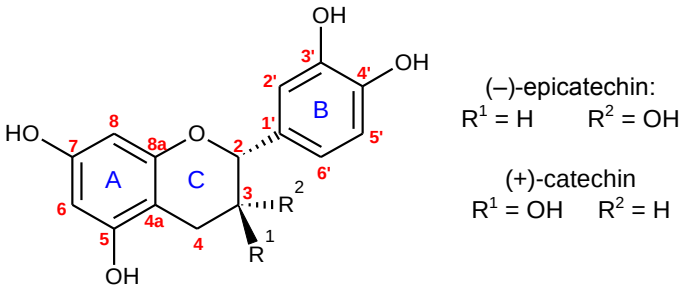

Figure 3 Structural formula of (–)-epicatechin and (+)-catechin epimers.

The broader group of condensed flavan-3-ols composed not only of (+)-catechin and (–)-epicatechin but also monomers containing a different number of hydroxyl groups is called proanthocyanidins (de la Iglesia *et al.*, 2010; Xie and Dixon, 2005). It is obvious that although there are just two types of monomers creating procyanidins, this group of natural products is very complex due to the possible number of oligomeric and isomeric states. Molecules with A-type and B-type linkages dissociate into different fragments in mass spectra, making the linkage type easily recognizable. However, this does not apply to interflavan bond isomerism (Lin *et al.*, 2014). Ion mobility-mass spectrometry can be effectively used to distinguish the degree of polymerization along with the type of interflavan linkage (Rue *et al.*, 2020).

Typically for polyphenolic compounds, proanthocyanidins act as scavengers of reactive oxygen species (Bagchi *et al.*, 1997; Bagchi *et al.*, 1998; Sato *et al.*, 1999). Its antioxidant and anti-inflammatory activities have a beneficial impact on many disease conditions. For example, proanthocyanidin intake contributes to the prevention of diseases like obesity, hypertension, diabetes, cancer, and cardiovascular disease (Izumi and Terauchi, 2020; Beecher, 2004; Corder *et al.*, 2006). From the survey of food intake conducted between 1994 and 1996 among U.S. respondents, the mean daily proanthocyanidin intake of 57.7 mg per person was estimated (Gu *et al.*, 2004). Almost three-fourths of consumed proanthocyanidin compounds contained more than three subunits.

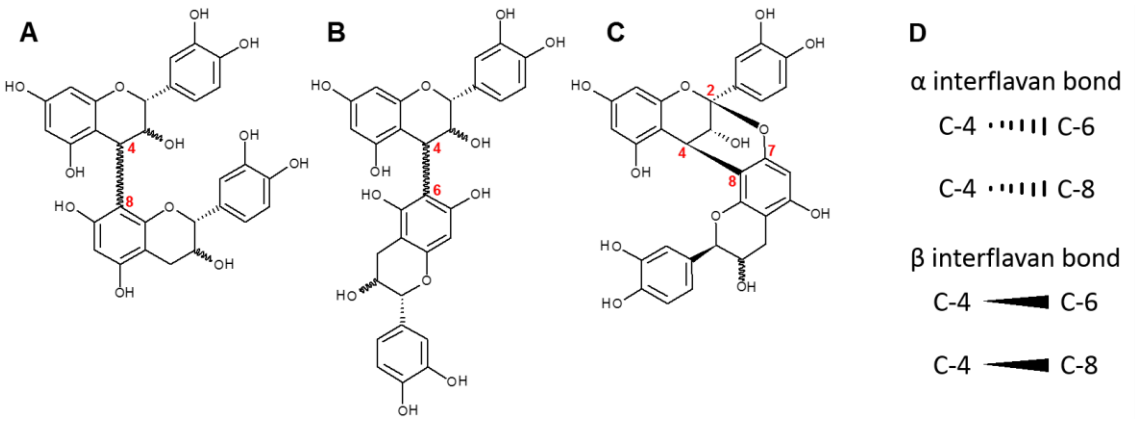

Figure 4 (A) B-type procyanidin dimer with C-4→C-8 linkage. (B) B-type procyanidin dimer with C-4→C-6 linkage. (C) A-type procyanidin dimer with C-4→C-8 and C-2→O→C-7 linkages. (D) Isomerism of interflavan bond – α and β bonds.

2.3.1 Procyanidin Biosynthesis

The biosynthetic pathway leading to procyanidins starts with the formation of monomers that are condensed together during the last step of biosynthesis. (+)-catechin and (–)-epicatechin are created via phenylpropanoid pathway from L-phenylalanine or L-tyrosine (Figure 6). Ammonia-lyase eliminates ammonia from L-tyrosine providing *p*-coumaric acid directly or from L-phenylalanine forming cinnamic acid which is subsequently hydroxylated to *p*-coumaric acid by cytochrome P450 monooxygenase (Petersen, 2003). Then, the ligase activates *p*-coumaric acid to *p*-coumaroyl-AMP undergoing thioesterification with coenzyme A (CoASH) to get *p*-coumaroyl-CoA (Li and Nair, 2015). Chalcone synthase belonging to the polyketide synthase enzyme family performs decarboxylative condensation of three malonyl-CoA molecules with the substrate providing tetraketide intermediate proceeding Claisen-type of cyclization in naringenin chalcone (Abe and Morita, 2010). The second intramolecular cyclization occurs via chalcone isomerase reaction with the mechanism of nucleophilic conjugate addition forming naringenin (Jez and Noel, 2002). Two mechanistically different types of hydroxylation—mediated by monooxygenase and dioxygenase—follow. Firstly, cytochrome P450-dependent enzyme flavonoid 3'-hydroxylase uses NADPH and O_2 to oxidize the phenyl B-ring of naringenin creating eriodictyol (Schoenbohm *et al.*, 2000). The second enzyme, flavonoid 3-hydroxylase, catalyses the reaction with non-haem iron using 2-oxoglutarate, O_2 and cofactor ascorbate introducing hydroxyl group into the O-heterocyclic ring of chromane skeleton. This reaction leading to dihydroquercetin (also called (+)-taxifolin) is an important regulation point of the flavan-3-ol biosynthesis (Turnbull *et al.*, 2004). Oxo group of dihydroquercetin is reduced by dihydroflavonol

4-reductase which gives leucoanthocyanidin. This substrate can undergo reactions catalysed by anthocyanidin synthase and reductase to obtain (–)-epicatechin or can be further reduced by leucoanthocyanidin reductase in position C-4 to get (+)-catechin.

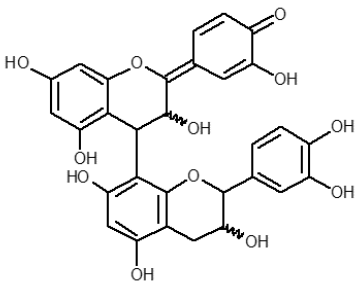

Figure 5 Quinone methide derived from B-type procyanidin dimer (Tanaka *et al.*, 2000)

The exact mechanism of how flavan-3-ols are connected to form procyanidins is not known (He *et al.*, 2008). Even whether the process is catalysed by enzymes or if it is of non-enzymatic nature is not clear. Similarly, the possibility of further procyanidin metabolization also remains an unanswered question (Suvanto *et al.*, 2020). Nevertheless, a few hypotheses are trying to address this issue. A common mechanism of interflavan bond formation is believed to be based on the nucleophilic attack of monomers or pre-existing procyanidin on (–)-epicatechin, resp. (+)-catechin carbocation intermediate (Figure 7). One hypothesis proposes that such carbocations can be generated from quinone methides synthesized by polyphenol oxidase. Carbocations are then formed via flav-3-en-3-ol or reduced intermediates of quinone methides. Additionally, flav-3-en-3-ols might be released during enzymatic conversions or non-enzymatic reactions of intermediates derived from leucoanthocyanidin (Xie and Dixon, 2005). Flav-3-en-3-ols have their tautomeric forms in *p*-quinone methides of the A-ring, and under acidic conditions, carbocations can appear (Pfeiffer *et al.*, 2006). Proposed reaction conditions correspond well with the finding that H^+-ATPase is essential for procyanidin biosynthesis (Baxter *et al.*, 2005). However, the mechanism behind the importance of H^+-ATPase for procyanidin biosynthesis has not been elucidated (He *et al.*, 2008).

The formation of the A-type linkage in procyanidin structure was proposed to be related to polyphenol oxidase activity (Dixon *et al.*, 2004). Firstly, the hydroxylated phenyl B-ring is oxidized by the enzyme to form a quinone methide intermediate (Figure 5). Then, the C-7 hydroxyl group attacks the C-2 position of quinone methide intermediate, which results in the formation of the C-2→O→C-7 ether bond. It is not clear if the ether bond is formed initially before the biosynthesis of large A-type procyanidins or is created later in the final structure (Tanaka *et al.*, 2000).

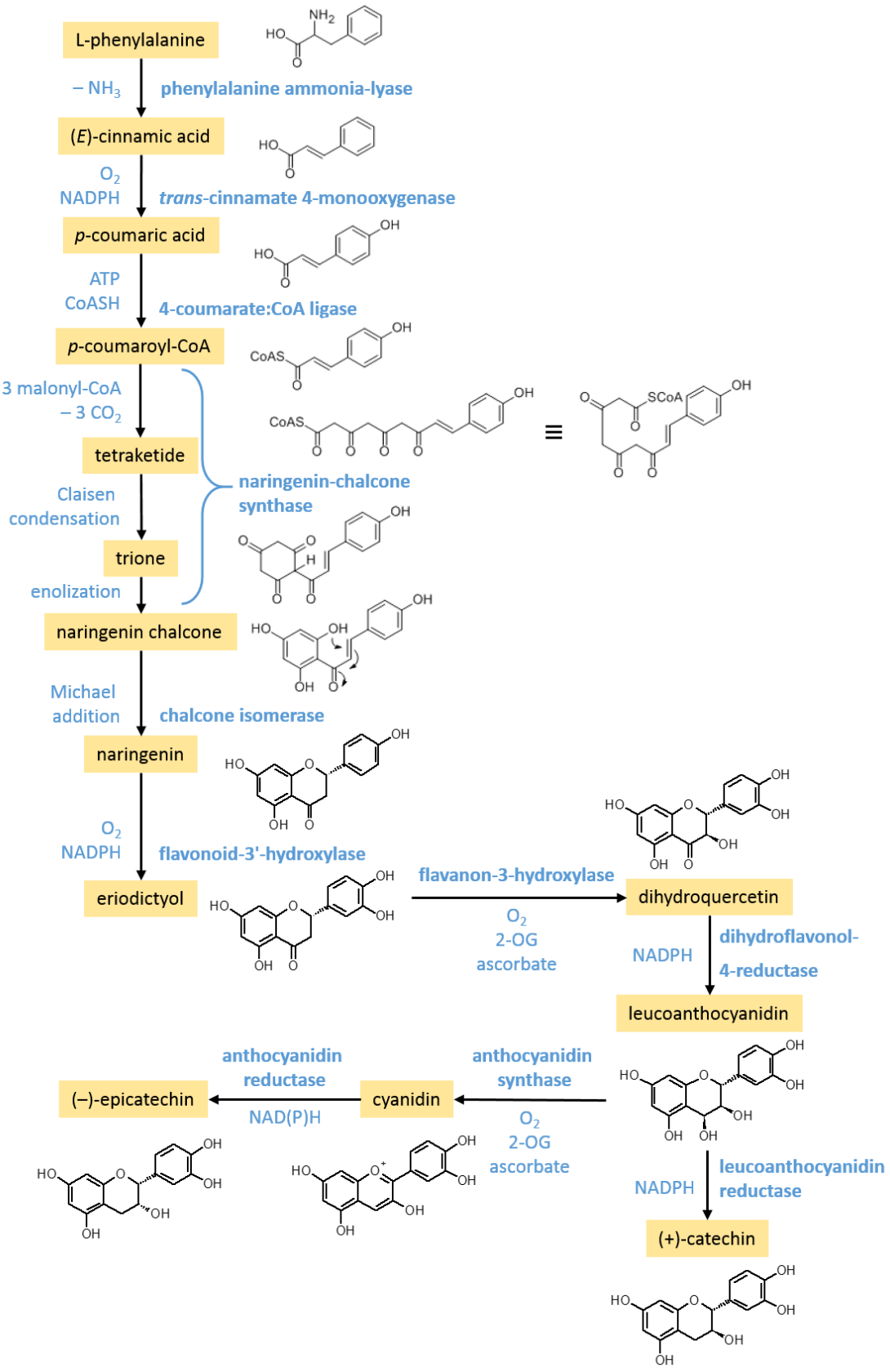

Figure 6 Schematic biosynthesis of flavan-3-ol via phenylpropanoid pathway and flavonoid-related enzymes. Adapted from He *et al.* (2008) and Wikimedia Commons (1. 6. 2011; Biosynthesis of (-)-epicatechin; by Amulloa)

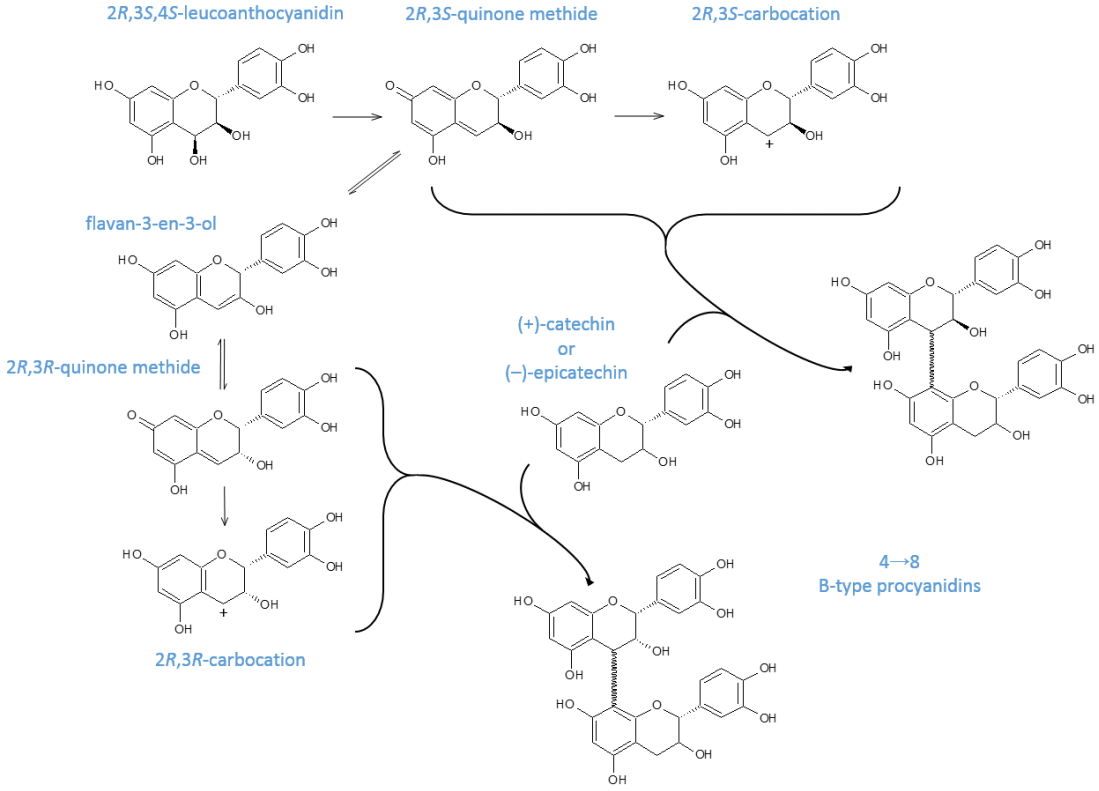

Figure 7 Suggested mechanism of interflavan bond formation in procyanidins. Adapted from Marles *et al.* (2003).

2.3.2 A-type Procyanidins

A-type procyanidins were identified, for example, in cranberries (Prior *et al.*, 2001; Ou *et al.*, 2012), peanut skin (Appeldoorn *et al.*, 2009; Dudek *et al.*, 2017), chocolate (Cambrai *et al.*, 2017), plum, avocado, curry (Gu *et al.*, 2003), cinnamon (Lu *et al.*, 2011), and litchi pericarp (Liu *et al.*, 2007).

A-type procyanidin dimers and trimers inhibited α-glucosidase (Zhao *et al.*, 2020) while α-amylase was not inhibited by procyanidin dimer A1 as another study proved (Tamura *et al.*, 2015). A-type trimers and pentamers isolated from cinnamon displayed anti-HIV-1 activity (Connell *et al.*, 2016). Procyanidin A1 prevented degranulation of basophilic leukaemia cells (Tomochika *et al.*, 2011). *In vitro* experiments showed that procyanidin A2 but not B-type procyanidin dimers B1 and B2 decreased the production of eotaxin-1, chemokine associated with asthma and inflammation (Coleman *et al.*, 2016). Also, complex downregulation of pro-inflammatory signalling induced by lipopolysaccharide and upregulation of Nrf2 signalling were observed in RAW264.7 cells after procyanidin A2 treatment (Wang *et al.*, 2020). Another example of the difference in the activity of the compounds with A- and B-type linkages can be demonstrated on

cranberry procyanidins. A-type trimers from cranberries possessed anti-adherence activity against uropathogenic P-fimbriated *Escherichia coli*, whereas B-type dimer procyanidin B2 was inactive (Foo *et al.*, 2000).

Regarding possible metabolic transformation products of A-type procyanidins, compounds can undergo degradation by intestinal microbiota *in vitro* (Engemann *et al.*, 2012). It was shown that A-type procyanidins dimers, trimers, and tetramers can be transported across Caco-2 cell monolayer (Ou *et al.*, 2012). In an animal experiment with rats, the A-type dimers were slightly absorbed from the intestine and were detected neither methylated nor conjugated in plasma, whereas trimers were not absorbed (Appeldoorn *et al.*, 2009). In contrast, another rat experiment where A-type procyanidins were administrated provided the data demonstrating that intact procyanidins were not found in rat plasma while the microbial degradation products of the compounds were significantly elevated (Li *et al.*, 2013).

2.3.3 B-type Procyanidins

The dietary sources of B-type procyanidins are larger than these of A-type procyanidins and include, e.g. various berries and common fruit, legumes, cereals, and nuts (Prior and Gu, 2005; Bittner *et al.*, 2013; Gu *et al.*, 2004). According to epidemiological studies, apples are the major source of flavonoid compounds in the human diet (Gu *et al.*, 2004). The analysis of six apple cultivars provided the average concentration of phenolic compounds where procyanidin B2 was the second most abundant among phenolics after quercetin glucosides (Lee *et al.*, 2003).

B-type dimers and trimers are potent inhibitors of lectin-like oxidized receptor-1 involved in inflammation and atherogenesis (Nishizuka *et al.*, 2011). In the same study, administration of oligomeric complex containing mainly B-type procyanidins purified from apple led to less arterial lipid deposition in rats. Procyanidin dimers B1 and B2 but not A1 or A2 inhibited the transactivation of nuclear factor κB (Mackenzie *et al.*, 2009). The activity of angiotensin I converting enzyme was inhibited by cocoa B-type procyanidins not only in the assay with the isolated enzyme but also when determined in treated cells (Ottaviani *et al.*, 2006). Procyanidin B1 decreased migration and proliferation of liver cancer cells and was found to be a specific inhibitor of tumorigenesis-related potassium channel Kv10.1 (Na *et al.*, 2020). The proteomic analysis explored the effect of procyanidin B2 treatment on liver mitochondria of diabetic

mice finding that observed change in the protein profile might have a positive effect on diabetic liver damage (Yu *et al.*, 2020).

The study investigating the absorption of (+)-catechin, B-type procyanidins B3 (dimer) and C2 (trimer), and polymeric proanthocyanidins using the Caco-2 cell monolayer model suggested the paracellular route of the intestinal absorption. The permeability for polymeric proanthocyanidins with the average degree of polymerization of 6 was approx. ten times lower compared to the permeability of monomeric, dimeric, and trimeric compounds (Deprez *et al.*, 2001). The fact that an increased degree of polymerization results in poor absorption is well-known (Yang *et al.*, 2021). Despite the low bioavailability in general, in several animal and human studies, too, B-type procyanidins were detected in plasma after dietary administration (Holt *et al.*, 2002; Tanaka *et al.*, 2003; Wang *et al.*, 2018; Shoji *et al.*, 2006; Sano *et al.*, 2003).

2.4 Na^+,K^+-ATPase

Na^+,K^+-ATPase (NKA; EC 7.2.2.13) is a transmembrane enzyme found in every animal cell. It is responsible for maintaining the plasma membrane potential and sodium gradient necessary for the function of many secondary active transporters (Kaplan, 2002; Zdravkovic *et al.*, 2012). Its importance in clinical practice is demonstrated by the frequent prescription of NKA inhibitors such as digoxin, which is used against cardiac insufficiency (Adams *et al.*, 2014). Moreover, rare mutations of NKA cause severe diseases including familiar hemiplegic migraine type 2 and rapid-onset dystonia-parkinsonism (De Carvalho Aguiar *et al.*, 2004; Segall *et al.*, 2005).

Two hundred and thirty-six years after the first publication of William Withering's book *An Account of the Foxglove, and Some of Its Medical Uses*, which describes medical uses of digitalis, the pharmacology of NKA remains interesting but incompletely understood. In addition to its role in heart failure management, recent high-throughput screening efforts suggest that NKA inhibition may have positive effects on hypercholesterolemia, several types of cancer, and viral infections (Li *et al.*, 2020; Wha Jun *et al.*, 2013; Nilubol *et al.*, 2012; Jiao Guo *et al.*, 2020; Prassas *et al.*, 2008; Rupaimoole *et al.*, 2020; Zhang *et al.*, 2012; Cayo *et al.*, 2017; Song *et al.*, 2020; Simpson *et al.*, 2009).

2.4.1 Structure of P-Type ATPases

The first discovery of P-type ATPase was made by danish physiologist Jens Christian Skou who discovered NKA in 1957 (Skou, 1957). In 2000, the first crystallographic structure of the protein belonging to the same family, sarco/endoplasmic reticulum Ca^{2+}-ATPase (SERCA), was obtained at 2.6 Å resolution (Toyoshima *et al.*, 2000). However, low-resolution structures were known from previous experiments done with SERCA (Ogawa *et al.*, 1998; Zhang *et al.*, 1998; Toyoshima *et al.*, 1993) and NKA, too (Herbert *et al.*, 1985; Hebert *et al.*, 1988).

When phylogenetically analysed, five distinct P-type ATPase main subfamilies can be distinguished (P1–P5) with minor subtypes denoted by upper-case letter making 11 classification classes in total (P1A, P1B, P2A, P2B, P2C, P2D, P3A, P3B, P4, P5A, and P5B). P1 ATPases are mostly heavy metal pumps, and P2 ATPases include Ca^{2+}-ATPases, Na^{+}-ATPases, H^{+},K^{+}-ATPase, and NKA. P3 ATPases are H^{+} and Mg^{2+} plasma membrane pumps, P4 ATPases are phospholipid flippases, and the molecular function of the P5 subfamily is unknown (Axelsen and Palmgren, 1998; Søndergaard and Pedersen, 2015; Sørensen *et al.*, 2019; Corradi *et al.*, 2020).

The P-type ATPase family, to which NKA belongs, is characterized by common structural and catalytical features. The letter P in the protein family name refers to the phosphoenzyme intermediate that is crucial for conformational changes driving the transport of ions across membranes. P-type ATPases exert a common transport mechanism based on alternating access involving cytoplasm-facing E1 states and outward-facing E2 states (Pedersen and Carafoli, 1987). The minimal functional part of the enzyme—the catalytically active α subunit—has at least six membrane-spanning helices (M1–M6) called the membrane (M) domain and the cytoplasmic part composed of three globular domains (abbreviated as the N-, P-, and A-domain). This topology is conserved among P-type ATPases ensuring a common catalytical mechanism and the binding of transported ions.

The nucleotide-binding (N) domain has the Rossmann fold typical in proteins binding nucleotide cofactors (Kaplan, 2002). Among all three cytoplasmic domains, the N-domain is the least conserved, however, the core structure does not vary across P-type ATPases (Palmgren and Nissen, 2011). The N-domain binds the adenine base of ATP into the pocket while the phospho-ribosyl moiety bridges the N- and P-domain interface during the phosphoryl transfer reaction (Sørensen *et al.*, 2004a). The overall highly conserved phosphorylation (P) domain has the same fold as the catalytic domain of the

haloacid dehalogenase protein superfamily (abbreviated as the HAD domain) (Kaplan, 2002). The aspartyl phosphate residue of the phosphoenzyme intermediate is located in the conserved DKTG sequence in the P-domain. Interestingly, a conserved intracellular binding site for the K^+ ion is localized in the P-domain, too. Co-ordinated K^+ ion enhances enzyme dephosphorylation by modulating the A- and P-domain interaction and stabilizes dephosphorylated enzyme state (Ekberg *et al.*, 2010; Schack *et al.*, 2008; Sørensen *et al.*, 2004b). During the catalysis, the flexible domain linkers enable the cytoplasmic actuator (A) domain to rotate by ~120° so it can be brought towards and outwards the phosphorylation site. The wide rotation of the A-domain is also associated with helices M1–M4 up and down movements and is important for the enzyme autophosphatase activity described later (Morth *et al.*, 2011).

The transmembrane region of the α subunit can be divided into support (S) and transport (T) domains. The auxiliary S-domain is more rigid than the highly flexible T-domain and has specialized functions including, e.g. coordination of transported ion in Ca^{2+}-ATPases or NKA. The S-domain exerts higher sequence variability, and the number and the position of alpha helices forming the S-domain differ across P-type ATPases. The T-domain is formed by six transmembrane helices and its main function is ion binding and oscillatory opening of ion pathways from the intracellular and extracellular side. Structural features of the T-domain suggest that the mechanism of ion binding is the same in all P-type ATPases. C- or N-terminal tail, or both ends form regulatory (R) domains in most P-type ATPases acting as sensors for transported cation or activity modulators (Palmgren and Nissen, 2011).

2.4.2 Na^+,K^+-ATPase Subunits

NKA (Figure 8) consists of a ~112kDa catalytic α subunit with ten transmembrane segments and four isoforms (α_{1-4}), and a ~55 kDa glycosylated β subunit with one transmembrane segment and three isoforms (β_{1-3}) that acts as a chaperone and modulatory protein (Blanco and Mercer, 1998; Kaplan, 2002; Toyoshima *et al.*, 2011). The catalytically active αβ heterodimer can also associate with one of the regulatory and stabilizing FXYD proteins (Clausen *et al.*, 2017; Yap *et al.*, 2021).

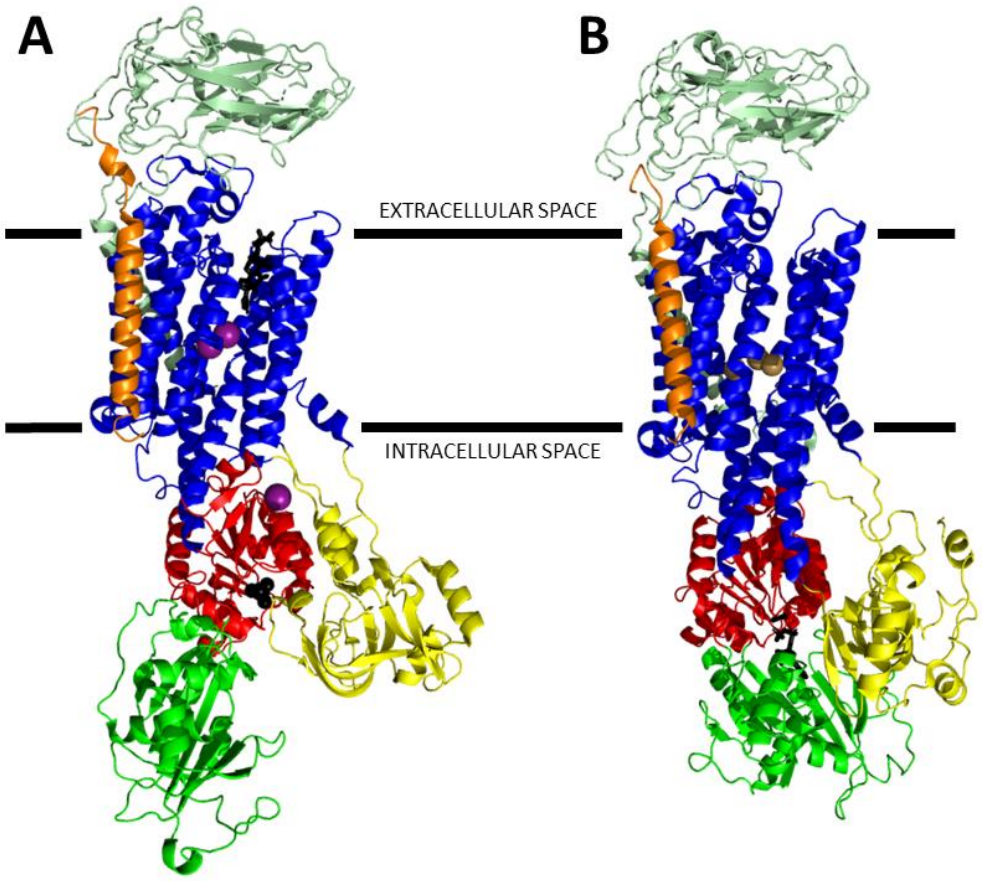

Figure 8 The structure of Na^+,K^+-ATPase (NKA). The common colour code: the FXYD protein in orange; the β subunit in pale green; the α subunit – transmembrane part (the M-domain) with short loops in blue, the P-domain in red, the N-domain in green, the A-domain in yellow. (A) The NKA structure of the $K_2E_2{\cdot}P_i$ state analogue; purple dots represent K^+ ions (non-transported K^+ ion located in the cytoplasm occupies modulatory binding site), ouabain bound to the α subunit from the extracellular side represented by black sticks, phosphate (P_i) analogue $[MgF_4]^{2-}$ located in the P-domain represented by black spheres; PDB ID 3A3Y. (B) The NKA structure of the $Na_3E_1{\sim}P{\cdot}ADP$ state analogue mimicking the phosphoryl transfer reaction from ATP; brown dots represent Na^+ ions, $ADP{\cdot}[AlF_4]^-$ mimicking the phosphoryl transfer reaction from ATP represented by black sticks between the P- and N-domains; PDB ID 3WGU. The figure was prepared in the PyMOL Molecular Graphics System, Version 1.6, Schrödinger, LLC.

Regulation of NKA in the context of different physiological processes and conditions occurs via assembly of NKA of variable subunit composition. Besides housekeeping $\alpha_1\beta_1$ NKA, concrete αβ heterodimers can be specifically found in certain tissues (Tokhtaeva *et al.*, 2012). For example, astrocytes express $\alpha_2\beta_2$ NKA with kinetic properties that allow responding to elevated extracellular K^+ concentration associated with neuronal activity (Cameron *et al.*, 1994; Larsen *et al.*, 2014). Another example of the importance of the specific αβ isoform in the context of the physiological environment can be demonstrated on the retina. The heterodimers containing the β_2 subunit were shown to anchor

extracellular protein retinoschisin expressed in photoreceptor and bipolar cells with possible consequences for intracellular signalling pathways playing role in the X-linked juvenile retinoschisis disease (Plössl *et al.*, 2017; Friedrich *et al.*, 2011; Molday *et al.*, 2007).

The subunit α (~112 kDa) is the catalytic subunit of P-type ATPases that has been extensively described from a structural point of view in chapter 2.4.1 dedicated to the general structure of P-type ATPases. In NKA, the α subunit has ten transmembrane helices of which six helices form the T-domain, and four helices form the S-domain. The C-terminus acts as the R-domain controlling Na^+ affinity (Kaplan, 2002; Palmgren and Nissen, 2011; Toustrup-Jensen *et al.*, 2009). Importantly, NKA highly selective inhibitors called cardiotonic steroids—such as ouabain or digoxin—bind to the α subunit and inhibit the enzyme with high affinity in the E_2-P state, plugging the ion pathway to prevent K^+ binding (Cornelius *et al.*, 2011; Yatime *et al.*, 2011). The ubiquitously expressed α_1 subunit helps to maintain the housekeeping activity of NKA. Expression of the α_2 subunit occurs mainly in the heart and skeletal muscle, glial cells, and astrocytes. The α_3 isoform is found in neurons and photoreceptors (Clausen *et al.*, 2017; Benarroch, 2011). The subunits α_2 and α_3 maintain specific roles in the brain associated with neuronal activity, therefore mutations of these isoforms lead to severe neuronal diseases. Mutations in the α_2 subunit cause familial hemiplegic migraine type 2, whereas diseases like rapid-onset dystonia-parkinsonism, alternating hemiplegia of childhood, and CAPOS syndrome are rooted in mutations of the α_3 subunit (Larsen *et al.*, 2016; Salles and Fernandez, 2020). Sperm cells express the α_1 and α_4 subunits, while the occurrence of the α_4 subunit is almost exclusive to sperms and is essential for their motility and fertility (Jimenez *et al.*, 2011).

The subunit β (~55 kDa) is a single-pass type II membrane protein with cytoplasmic N-terminus and large ectodomain. Heavily glycosylated ectodomain containing three disulfide bridges covers the α subunit from the top. Among the P-type ATPases, only NKA and H^+,K^+-ATPase (P2C-ATPases) require the β subunit to be functional. However, most lipid flippases belonging to the P4-ATPase family are also binary complexes, but a protein from the CDC50 family maintains functions similar to the β subunit in P2C ATPases (Timcenko *et al.*, 2019). The subunit β has two main functions: (a) it acts as a chaperon, assists translation, and helps membrane integration of the α subunit, and (b) it modulates transport properties of NKA (Geering, 2001; Rajasekaran *et al.*, 2004; Hilbers *et al.*, 2016). There are three isoforms of the β subunit (β_1– β_3) in human expressed differently across various tissues. The isoform β_1 is expressed ubiquitously, the

β_2 is present in muscles and astrocytes, and the β_3 is found mainly in lung, testis, oligodendrocytes, and skeletal muscle (Tokhtaeva *et al.*, 2012; Larsen *et al.*, 2016; Benarroch, 2011). Interestingly, interactions with the specific β subunit can be used to design NKA isoform-selective inhibitors based on a cardiotonic steroid scaffold (Habeck *et al.*, 2016; Katz *et al.*, 2015).

FXYD proteins have their name for the common phenylalanyl-X-tyrosyl-aspartyl region in the N-terminal extracellular part of the sequence. Also, the shared sequence pattern includes two glycine and one serin residues located in the transmembrane helix (Crambert and Geering, 2003; Arystarkhova *et al.*, 2007). There are seven single-span membrane proteins from the FXYD family (FXYD1–FXYD7) with type I topology and molecular weight of 6.5–17 kDa (glycosylated FXYD5 up to 50 kDa) occurring in humans with the tissue-specific distribution. One exception is Mat-8 (FXYD3) with two splice variants – the longer one gives the protein with two transmembrane helices and intracellular N-terminus while the shorter variant has the same topology of type I transmembrane protein as other FXYD proteins (Bibert *et al.*, 2006). Functional aspects of the α and β subunits are discussed mainly in chapter 2.4.4. However, the function of FXYD proteins is not further described there because of the non-essential importance of the FXYD subunit for the NKA activity. Nevertheless, selected interesting aspects of FXYD-mediated regulation of NKA are briefly mentioned here below to demonstrate how complex the whole problematics is.

Association of the auxiliary FXYD subunit with αβ heterodimer is not essential for the NKA activity but, additionally to specific NKA isoform formation, it further modulates NKA kinetic properties. For example, phospholemman (FXYD1)—found in the heart and skeletal muscle—can two-fold decrease apparent Na^+ affinity or oppositely, corticosteroid hormone-induced factor (CHIF or FXYD4) expressed in kidneys can increase the affinity two to three times (Crambert *et al.*, 2002; Garty *et al.*, 2002). Furthermore, the NKA function can be modulated by posttranslational modifications of its three possible subunits. A well-known example of the functional role of FXYD protein posttranslational modifications is the phosphorylation of two serine residues in phospholemman. Phospholemman decreases the activity of NKA, and this inhibition effect can be relieved by phosphorylation at S63 or S68 (Mishra *et al.*, 2015). Additionally, single nucleotide polymorphism in phospholemman leading to R70C amino acid substitution *in vitro* decreases phosphorylation at S68 by protein kinase C. This polymorphism was found to be associated with a significant blood pressure increase in

middle-aged men (Boguslavskyi *et al.*, 2021). Another example of dysadherin (FXYD5) shows how posttranslational modifications of the subunits can influence NKA function with the impact on roles unrelated to ion exchange. Dysadherin is considered not only as an NKA-modulating subunit (Miller and Davis, 2008) but also as a cancer-associated membrane glycoprotein that reduces cell-cell adhesiveness and promotes metastasis (Ino *et al.*, 2002). Adhesion impairment was suggested to occur via reduction of intercellular β_1-β_1 dimerization of the $\beta_1\alpha_1$ NKA heterodimer as a result of increased O-glycosylation of dysadherin in cancer cells (Tokhtaeva *et al.*, 2016).

Tissue and physiological conditions interacting with the regulation of NKA—involving posttranslational modifications and isoenzyme assembly along with auxiliary FXYD subunit—demonstrate the complexity of this protein pump. Therefore, many details undoubtedly remain to be discovered to further explain the NKA importance in health and disease.

2.4.3 Catalytic Cycle of Na^+,K^+-ATPase

A catalytic cycle of the alternating-access type of ion transport is common to all P-type ATPases and includes series of large conformational changes in the α subunit partially described above in connection with the domain functions. The overall catalytic cycle involves the E_1-E_2 conformational states oscillation and results in ping-pong ion exchange explained below in details (Monti *et al.*, 2018). The first mechanism of ion transport by P-type ATPase was proposed by Post and Albers for NKA (Post *et al.*, 1969; Albers, 1967). In a broader sense, the so-called Albers-Post model (Figure 9) applies to all P-type ATPases and can be understood in the atomistic details with currently available structural data.

The E_1 conformation opened to the cytoplasm has a high affinity for three sodium ions, while extracellularly facing E_2 conformation favours two potassium ions. Ions bind to the binding sites with a high affinity from one side of the membrane, whereas the affinity is much lower when the enzyme changes its conformation and opens to the other side of the membrane facilitating ion dissociation (Heyse *et al.*, 1994). Vectorial ion transport coupled with ATP hydrolysis enables conformational changes associated with the phosphoenzyme formation. This needs the cytoplasmic domains of the α subunit to perform a phosphoryl transfer reaction.

Before the phosphoryl transfer reaction, ATP binds to the enzyme in a modulatory mode in which ATP helps enzyme conformational transition and is uncoupled from lately

phosphorylated aspartate D376 (rat α_1 numbering; residue from the ^{376}DKTG^{379} motif in the P-domain). Such binding where ATP acts as a cofactor accelerates the $[K_2]E_2$ to Na_3E_1 states transition (Jensen *et al.*, 2006; Glynn and Richards, 1982; Forbush, 1987). After the association of the E_1-enzyme with Na^+ ions, a new Mg^{2+} binding site in the P-domain is created near D376, where the Mg^{2+} ion acts as a phosphorylation cofactor. Bound ATP switches to the catalytical mode of binding, initiating the S_N2 phosphoryl transfer reaction with the assistance of two Mg^{2+} ions of which one weakens electrostatic repulsion of aspartate and ATP γ-phosphate (Zhang and Zhang, 2019). This causes the break of the ATP/P-domain bridge, and the A-domain can now rotate, which leads to the E_1-P to E_2-P transition, the rate-limiting step of the catalytic cycle (Sørensen *et al.*, 2004a; Palmgren and Nissen, 2011). In the $[Na_3]E_1$-P stage, Na^+ ions are occluded, which means they are inaccessible from either side of the membrane. Occluded states prevent ion channel-like short circuit and are the basis of vectorial ion transport (Toyoshima *et al.*, 2011).

In the E_2-P conformation, Na^+ ions dissociate from the enzyme via a newly formed access channel and the affinity for K^+ ions is greatly increased (Gadsby *et al.*, 2012; Babes and Fendler, 2000; Castillo *et al.*, 2015). This reversal in the ion affinities drives the catalytic cycle in the forward direction. The K^+ ions binding facilitates dephosphorylation of the K_2E_2-P enzyme, which leads to the rapid occlusion of K^+ ions (Castillo *et al.*, 2015). The autophosphatase activity of NKA is maintained by the A-domain. The interaction between the A- and P-domains, resulting in the aspartyl phosphate hydrolysis, is modulated by a cytoplasmic K^+ binding site. Occupancy of the site by the K^+ ion also stabilizes the dephosphorylated enzyme intermediate (Schack *et al.*, 2008). The A-domain contains the a conserved ^{219}TGES^{222} sequence, which reaches close proximity to phosphorylated aspartate in the E_2 state but is brought away in the E_1 state due to the domain rotation (Horisberger, 2004; Clausen *et al.*, 2004). Bringing the TGES motif to the chemical microenvironment of the P-/N-domain interface causes glutamyl pK_a increase leading to the subtraction of a proton from the water molecule attacking aspartyl phosphate (Toyoshima *et al.*, 2004). Finally, the water in-line attack releases inorganic phosphate from the phosphoenzyme intermediate in an S_N2 manner, and the cycle as described is completed.

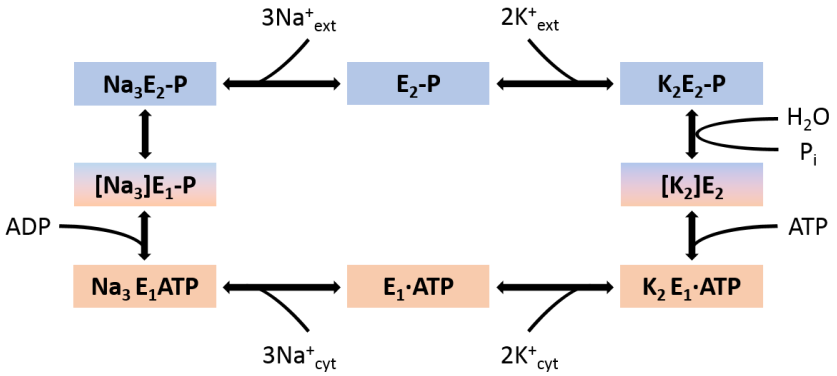

Figure 9 The Albers-Post scheme of the ion transport by Na^+,K^+-ATPase (NKA). The occluded states with ions inaccessible from any side of the membrane are denoted by square brackets. The space from where ions are transported is indicated by the ion subscript "ext" or "cyt" as extracellular space or cytoplasm, respectively. The binding of ATP in the modulatory mode is marked by the dot (·), whereas the catalytical mode is denoted without the dot. The scheme was adapted from Heyse *et al.* (1994) and Dyla *et al.* (2019).

For the basic research in the field of P-type ATPases, and especially in the structural studies shedding light on the ion transport mechanism, it is important to be able to obtain isolated catalytic states of enzymes. Otherwise, it would be too difficult to investigate, e.g. possible interactions with ligands or ions under turnover conditions. Phosphoenzyme analogues can be obtained under appropriate ion substrate conditions by the treatment of P-type ATPases with various metal fluorides mimicking phosphate states in the phosphorylation site. Tetrahedral $[MgF_4]^{2-}$ is analogous to released inorganic phosphate (P_i) in the active site. $[BeF_3]^-$ bound to aspartyl carboxyl oxygen also exerts tetrahedral geometry but in this case mimics aspartylphosphate residue. Octahedral analogues with $[AlF_4]^-$ represent either the phosphoryl transfer transition state or the hydrolysis reaction transition state. With this metal fluoride coordinated by catalytic aspartate from one side, the analogue of the phosphorylation step can be obtained if terminal phosphate oxygen of ADP coordinates the other side of the $[AlF4]^-$ complex. Aspartyl phosphate hydrolysis transition state is mimicked when ADP is replaced by water molecule being nucleophilically activated by glutamyl residue from the TGES motif in the desired enzyme conformation (Cornelius *et al.*, 2011).

2.4.4 Function of Na^+,K^+-ATPase

As a translocase, NKA hydrolyzes ATP to transfer three Na^+ ions to the extracellular space and two K^+ ions to the cytoplasm (Kubala, 2006). The resulting ion gradient across the plasma membrane is central to the physiology of excitable cells. Additionally, the sodium gradient drives secondary active transport (Glitsch, 2001).

Other important functions of NKA include thermogenesis (Clarke *et al.*, 2013) and promotion of cell adhesion and interaction via its β_1 subunit (Páez *et al.*, 2019; Tokhtaeva *et al.*, 2011; Vagin *et al.*, 2006). It was also shown that the β_1 subunit can act as a general K^+-dependent lectin that binds to GlcNAc-terminating oligosaccharides (Kitamura *et al.*, 2005), and that its expression suppresses the motility and invasiveness of carcinoma cells (Rajasekaran *et al.*, 2001). In addition to these functions, NKA is part of a complex signaling network that is currently under investigation.

In signal transduction pathways, NKA acts as a receptor for cardiotonic steroids, which are highly selective inhibitors that bind in a cavity accessible from the extracellular side (Laursen *et al.*, 2013). Many studies have shown that upon cardiotonic steroid binding, NKA interacts with several downstream proteins via its intracellular side and triggers a signaling cascade (Aperia *et al.*, 2016; Xie and Askari, 2002). The identification of these signaling pathways and the highly conserved cardiotonic steroid-binding site prompted efforts to identify naturally occurring endogenous ligands of NKA (Dostanic-Larson *et al.*, 2005). The first report describing an endogenous cardiotonic steroid was published in 1991 (Hamlyn *et al.*, 1991), and endogenous cardiotonic steroids are now regarded as a distinct class of hormones (Schoner, 2002; Bagrov *et al.*, 2009). However, uncertainties remain concerning their biosynthesis and distribution (Lewis *et al.*, 1994; Baecher *et al.*, 2014).

A wide range of proteins that are directly or indirectly involved in signaling pathways can interact with NKA, including caveolin-1 (Cai *et al.*, 2008), inositol 1,4,5-trisphosphate receptor (Zhang *et al.*, 2006), adducin (Ferrandi *et al.*, 1999), G protein-coupled receptor 35 (Schneditz *et al.*, 2019), and ankyrin (Devarajan *et al.*, 1994). The N-terminal proline-rich motif of NKA, which is unique among P-type ATPases, may act as a docking site for SH3 domains of downstream proteins like phosphoinositide-3 kinase (Yudowski *et al.*, 2000) or Src kinase (Banerjee *et al.*, 2015; Tian *et al.*, 2006; Nie *et al.*, 2020). Conformational changes of this proline-rich region upon ouabain binding may influence such protein-protein interactions (Yatime *et al.*, 2011). Unfortunately, despite extensive studies, the mechanism of signal transduction mediated by Src kinase is not fully understood (Yosef *et al.*, 2016).

3 EXPERIMENTAL PART

3.1 Chemicals

Procyanidin B1, B2, B3 and C1 standards were purchased from PhytoLab (Germany). Stock solutions were prepared by dissolving procyanidins in 50% methanol to a final concentration of 10 mM and stored at -80 °C. The NKA inhibitor ouabain was purchased from Merck (Germany). All solutions were prepared using Milli-Q water with a resistivity above 18.2 MΩ·cm (25 °C).

3.2 Isolation of Na^+,K^+-ATPase

SDS-solubilized NKA was isolated using the protocol of Fedosova (Fedosova, 2016), with the following modifications: excess buffer I was poured out from the dissected outer medulla, and the soaked tissue was transferred into a blender. The outer medulla was then homogenized in buffer II with a tissue : buffer ratio of 1 : 3 while ¾ of buffer II was in the form of ice cubes. Aliquots of SDS-solubilized NKA isolate in buffer II were stored at –80 °C, and were determined to have a protein concentration of 0.44 $mg \cdot mL^{-1}$ by the Lowry method.

3.3 Na^+,K^+-ATPase (NKA) Activity Assay

Authentic standards (procyanidins B1, B2, B3, and C1; (+)-catechin and (–)-epicatechin) dissolved in 50% methanol with a stock concentration of 10 $mmol \cdot L^{-1}$ were diluted to a final concentration of 100 $\mu mol \cdot L^{-1}$ for use in assays. Crude extracts of *Viola odorat* L. seed, root, and leaf with concentration of 240 mg $DW \cdot mL^{-1}$ in dimethyl sulfoxide were diluted to a final concentration of 600 $\mu g\ DW \cdot mL^{-1}$. Fractions of crude *V. odorata* L. root extract with stock concentrations of 240 mg $DW \cdot mL^{-1}$ in 20% methanol with 0.1% HCOOH were diluted to a final concentration of 480 $\mu g\ DW \cdot mL^{-1}$.

Inorganic phosphate (P_i) quantification was conducted in microplates using a previously reported method (Kubala *et al.*, 2016). Each ATPase reaction was performed in four wells without ouabain to determine total liberated P_i and in four wells with ouabain to quantify P_i not generated by ouabain-sensitive NKA activity.

The ouabain-sensitive ATPase activity of NKA (henceforth referred to as NKA activity) was measured by adding 30 μL of a 1.67x concentrated buffered NKA solution to 10 μL of pre-concentrated inhibitor solution diluted in water. NKA was pre-incubated with the inhibitor for 5 min, then the ATPase reaction was started by adding 10 μL of 15 mmol·L^{-1} Na_2ATP dissolved in 25 mmol·L^{-1} Tris base. The final buffered (pH 7.2) NKA solution contained 4 mmol·L^{-1} $MgCl_2$, 20 mmol·L^{-1} KCl, 130 mmol·L^{-1} NaCl, 30 mmol·L^{-1} L-histidine, and 26 μg·mL^{-1} of NKA protein with or without 1 mmol·L^{-1} ouabain. The ATPase reaction lasted for 6 min after which 75 μL of solution II was added to develop color (2.9% (w/v) sodium dodecyl sulfate, 0.5% (w/v) ammonium heptamolybdate tetrahydrate, 163 mmol·L^{-1} ascorbic acid, and 3.7% (w/v) HCl). After 8 min, color development was stopped by adding 125 μL of solution III (3.5% (w/v) bismuth citrate, 3.5% (w/v) trisodium citrate dihydrate, 3.7% (w/v) HCl). Finally, the absorbance was measured at 710 nm using an Infinite 200 microplate reader (Tecan, Switzerland).

The NKA activity observed in the presence of each inhibitor was normalized against a control activity determined by mixing the NKA solution with water instead of an inhibitor solution in order to obtain the relative NKA activity (%) for each inhibitor. NKA activity was calculated by subtracting the average absorbance of ouabain containing samples from that of samples without ouabain. Dose-response curves were generated by using a four-parameter logistic function (fixed 0–100 % range) to fit the experimental data.

3.4 Plant Collection and Extraction

Viola odorata L., collected in Bělkovice Valley (Olomouc Region, Czech Republic), was identified by Michal Hroneš, Ph.D. (Department of Botany, Palacký University Olomouc). Plants were freeze-dried and homogenized using blade grinder. 30 mg of dried plant material (DW) was extracted in a microtube using 1 mL of 0.1% HCOOH in methanol. Glass balls were added to the microtube and the plant material was homogenized for 5 min using an MM 400 oscillatory ball mill (RETSCH, Germany) operating at 27 Hz. An ultrasound-assisted extraction (10 min, 45 kHz) in a USC100T ultrasonic bath (VWR, USA) and subsequent centrifugation (21 300 g, 25 °C, 10 min) followed. The supernatant was collected and evaporated at 37 °C in a TurboVap Classic LV nitrogen evaporator (Biotage, Sweden).

3.5 Plant Extract Fractionation

Methanol, aqueous ammonia and HCOOH used for fractionation were of LC-MS grade.

Reverse phase C18 SPE fractionation. A solid-phase extraction (SPE) C18 sorbent cartridge (*Spe-ed* 6 mL octadecyl/18; Applied Separations, USA) was conditioned with 12 mL of methanol and equilibrated with 2 mL of 0.1% HCOOH. Evaporated crude *Viola odorata* root extract (24 mg DW) dissolved in 2 mL of 0.1% HCOOH was loaded onto the column. Fractions RP0, RP1, RP2, RP3, RP4, RP5, RP6, and RP7 were obtained by eluting the crude extract from the sorbent with 2 mL of 0.1% HCOOH in aqueous methanol of gradually increasing concentration (0, 10, 20, 30, 50, 60, 70, and 100 %).

Mixed-mode anion exchange SPE fractionation. A mixed-mode anion exchange (MAX) SPE sorbent cartridge (Oasis MAX, 150 mg, 6 mL; Waters, USA) was conditioned with 12 mL of methanol and equilibrated first with 6 mL of water followed by 6 mL of 5% aqueous ammonia. Evaporated crude *V. odorata* root extract (24 mg DW) dissolved in 5% aqueous ammonia was loaded onto the column and washed with 5 mL of the loading solvent (eluting fraction MA0). Fractions obtained by elution with 4 mL of methanol (MA1) and 4 mL of 2% methanolic HCOOH (MA2) were then collected.

Mixed-mode cation exchange SPE fractionation. A mixed-mode cation exchange (MCX) SPE sorbent cartridge (Oasis MCX, 150 mg, 6 mL; Waters, USA) was conditioned with 12 mL of methanol and equilibrated firstly with 6 mL of water, then with 6 mL of 2% aqueous HCOOH. Evaporated crude *V. odorata* root extract (24 mg DW) dissolved in 2% aqueous HCOOH was loaded onto the column and washed with 5 mL of loading solvent (eluting fraction MC0). Fractions obtained by elution with 4 mL of methanol (MC1) and 4 mL of 5% methanolic ammonia (MC2) were collected.

Each collected fraction was evaporated at 37 °C in a nitrogen evaporator and then redissolved in 100 μL of 20% methanol with 0.1% HCOOH. Aliquots were taken for use in LC-MS analyses and NKA inhibition assays.

3.6 UHPLC-QTOF-MS/MS

UHPLC-QTOF-MS/MS analyses were performed as described previously (Rárová *et al.*, 2019). Briefly, samples dissolved in 20% methanol with 0.1% HCOOH were filtered through a 0.2 μm regenerated cellulose membrane microfilter (Grace, USA) prior to UHPLC analysis. 5 μL of each sample was injected onto a reversed-phase column (BEH C18, 1.7 μm, 2.1 × 150 mm, Waters, USA) maintained at 30 °C. Elution was performed over 22 minutes using the following binary gradient of acetonitrile (A) and 5 $mmol \cdot L^{-1}$ aqueous HCOOH (B): 0 min 5% A, 1 min 10% A, 12 min 35% A, 17 min 70% A, 17.5 min 100% A. The nebulizer gas pressure was set to 6 bar, desolvation temperature to 500 °C, and desolvation gas flow to 600 $L \cdot h^{-1}$. Analytes were ionized using an ESI source (120 °C, capillary 2 kV, cone voltage 25 V, cone gas flow 30 $L \cdot h^{-1}$) operating in both negative and positive ion modes. MS data were recorded in the *m/z* range of 70−1500. MS/MS experiments were performed using a collision energy of 20 eV.

In-house developed MATLAB algorithms were applied to raw LC-MS data generated by MassLynx software to produce a list of features characterized by retention time, *m/z*, and peak area. Only features with retention times between 2 and 18 min and a peak area above 5000 AU in at least one sample were considered. Pearson correlation coefficients were computed between feature area and inhibitory activity (expressed in μmol of ouabain equivalents per 1 g of DW). Features with the highest correlation coefficients were manually processed using Masslynx 4.1 software (Waters, USA) to identify candidate pseudo-molecular ions, their elemental compositions, and the corresponding mass accuracy. Procyanidins B1, B2, B3 and C1 were identified based on their retention times and comparisons to the fragmentation patterns of authentic standards.

3.7 Anthroyl Ouabain Fluorescence Assay

The buffer for the 9-anthroyl ouabain fluorescence assay was composed of 30 $mmol \cdot L^{-1}$ Tris-HCl (pH 7.4), 4 $mmol \cdot L^{-1}$ $MgCl_2$, 4 $mmol \cdot L^{-1}$ KH_2PO_4, and 50 $\mu g \cdot mL^{-1}$ NKA. In a cuvette with a stir bar, the buffer with NKA was incubated with or without 25 $\mu mol \cdot L^{-1}$ procyanidin C1 on magnetic stirrer for 5 min. In the samples used for the estimation of the anthroyl ouabain baseline fluorescence, 1 $mmol \cdot L^{-1}$ ouabain was added before procyanidin C1. Then, the fluorescence measurement started with recording the baseline after which anthroyl ouabain at the concentration of 1 $\mu mol \cdot L^{-1}$ was added, and the fluorescence intensity increase was recorded until reaching a plateau level.

Spex Fluorolog-3 fluorometer (HORIBA; Japan) equipped with a thermostated cell compartment and a magnetic stirrer was used for the experiment. The instrument was set to the following parameters of a kinetic mode of acquisition: excitation wavelength 370 nm (bandpass 5 nm), emission wavelength 485 nm (bandpass 14 nm), total time 600 s, number of points 1000.

3.8 Eosin Fluorescence Assay

The reaction buffer for the eosin fluorescence assay contained 10 mmol·L^{-1} L-histidine (pH 7.4), 1 mmol·L^{-1} *trans*-1,2-cyclohexanediaminetetraacetic acid (CDTA), and 50 µg·mL^{-1} NKA. Before the experiment, the eosin dissociation constant (K_d^{eosin}) was determined to be 67 nmol·L^{-1} under the same conditions. Therefore, the concentration of 150 and 300 nmol·L^{-1} eosin was chosen for the following experiments with procyanidin C1. These conditions enable observing the possible change in the procyanidin C1 apparent dissociation constant with varying eosin concentration.

The titration procedure involved:

1) recording of the baseline fluorescence of eosin with NKA in the buffer solution (NKA conformation: E_1 and E_2)
2) addition of KCl up to the concentration of 20 µmol·L^{-1} (NKA conformation: E_2; the free eosin fluorescence is recorded)
3) addition of NaCl up to the concentration of 30 mmol·L^{-1} (NKA conformation: E_1; maximum eosin bound)
4) titration of procyanidin C1: 5 / 10 / 15 / 20 / 25 / 30 / 35 µmol·L^{-1}
5) addition of ADP up to the concentration of 100 µmol·L^{-1} (eosin binding is competitively inhibited; the free eosin fluorescence is recorded)

Spex Fluorolog-3 fluorometer (HORIBA; Japan) was used for fluorescence experiment with following parameters: excitation wavelength 530 nm (slit 1 mm), emission wavelength 550 nm (slit 10 mm), total time 600 s, increment 0.2 s. The points in the titration curve were expressed as a residual fluorescence F_R (%) calculated according to the following equation:

$$F_R = \frac{F_{X\ \mu mol\cdot L^{-1}\ PC1} - F_{100\ \mu mol\cdot L^{-1}\ ADP}}{F_{30\ mmol\cdot L^{-1}\ Na^+} - F_{100\ \mu mol\cdot L^{-1}\ ADP}} \cdot 100\ \%$$

$F_{X\ \mu mol\cdot L^{-1}\ PC1}$ represents the fluorescence level at a given concentration of procyanidin C1, $F_{100\ \mu mol\cdot L^{-1}\ ADP}$ the fluorescence level after the addition of ADP up to

the concentration of 100 μmol·L^{-1} (free eosin fluorescence), and $F_{30\ mmol\cdot L^{-1}\ Na^{+}}$ the fluorescence level after the addition of NaCl up to the concentration of 30 mmol·L^{-1} (bound eosin fluorescence).

The residual fluorescence was plotted against the procyanidin C1 concentration and the data were fitted by four parameter logistic function (A_1, A_2, and x_0 set as free and p fixed as 1).

3.9 *p*-Nitrophenyl Phosphatase (pNPPase) Assay

The buffer for the pNPPase activity assay was composed of 30 mmol·L^{-1} L-histidine (pH 7.4), 150 mmol·L^{-1} KCl, 20 mmol·L^{-1} $MgCl_2$, and 10 mmol·L^{-1} *p*-nitrophenyl phosphate (pNPP). A cuvette containing the buffer solution with pNPP substrate was inserted into the spectrophotometer UV-1800 (Shimadzu Corporation; Japan). After the baseline recording at 410 nm, NKA was added at the final concentration of 50 μg·mL^{-1} (total time 3 600 s with 4 s cycles). The reaction was monitored at the same absorbance value corresponding to the production of *p*-nitrophenolate anion. The linear absorbance increase was observed, then procyanidin C1 at varying concentrations (0 / 6.25 / 12.5 / 25 μmol·L^{-1}) was added resulting in the change of absorbance slope. Kinetic experiments were performed for each inhibitor concentration separately.

The relative pNPPase activity (the specific activity with inhibitor divided by the specific activity without inhibitor) expressed in percent was plotted against procyanidin C1 concentration to create the inhibition curve. Data were fitted by four parameter logistic function (A_1, A_2, and x_0 set as free and p fixed as 1).

3.10 Determination of K^+ Ions Deocclusion Rate Constant

The determination of the K^+ ions deocclusion rate constant was performed with DX 17MV stopped-flow spectrofluorometer (Applied Photophysics; UK). Eosin fluorescence was recorded at excitation wavelength 530 nm (bandpass 10 nm) and emission wavelength above 550 nm (cut-off filter) during the time interval of 4 s with 4 ms increments.

Syringe A contained the enzyme solution composed of 10 mmol·L^{-1} L-histidine (pH 7.4), 1 mmol·L^{-1} *trans*-1,2-cyclohexanediaminetetraacetic acid (CDTA), 100 nmol·L^{-1} eosin Y, varying concentration of KCl (10 / 500 / 2 000 μmol·L^{-1}), and 140 μg·mL^{-1} NKA with or without 25 mmol·L^{-1} procyanidin C1. Syringe B was filled with the buffer containing the same L-histidine, CDTA, eosin, and varying KCl

concentrations with or without procyanidin C1, but also contained 60 mmol·L^{-1} NaCl. The data from 3–9 kinetic experiments were used to calculate the fast and slow rate constants from a double exponential model in KyPlot 5 software (Kyence; Japan).

3.11 Molecular Docking

The structure of procyanidin C1 obtained from the PubChem database was optimized using Avogadro (Avogadro: an open-source molecular builder and visualization tool. Version 1.2. http://avogadro.cc/; doi.org/10.1186/1758-2946-4-17) using the energy minimizing tool with the General Amber Force Field. Ligands and NKA crystal structures 3WGU (Kanai *et al.*, 2013) and 2ZXE (Shinoda *et al.*, 2009) without heteroatoms were prepared for docking using Autodock Tools (https://dx.doi.org/10.1002/jcc.21256, version 1.5.6). Ligand bonds whose rotation generated different conformers were allowed to rotate freely in accordance with the software's default settings. Docking was performed using Autodock Vina (Trott and Olson, 2009), with a grid box covering the whole protein. Exhaustiveness was set to 100 and available 20 binding modes were obtained. Redocking was performed with grid box limited to frequently occupied binding sites.

Protein-ligand interactions of redocked binding modes were analyzed using the Protein-Ligand Interaction Profiler (PLIP) (Salentin *et al.*, 2015). Residue numbering remained the same as in the original crystal structures. Figures for publication were prepared using PyMOL (The PyMOL Molecular Graphics System, Version 2.4.1, Schrödinger, LLC.).

3.12 Statistical Analysis

All statistical analyses were performed using GraphPad Prism 8.0 software (GraphPad Software, Inc; USA). Data on NKA activity were analyzed by one-way ANOVA followed by Tukey's *post hoc* test. Values are given as mean ± SD. Statistical significance is reported as **** $p < 0.0001$, *** $p < 0.001$, ** $p < 0.01$ and * $p < 0.05$.

4 RESULTS

Over 50 plant species were extracted and screened for NKA inhibiting activity (data not shown). Individual parts of the most promising candidate, *Viola odorata* L., were then analyzed separately to evaluate their activity (Figure 10A). Interestingly, although seed and leaf extracts showed no significant activity, root extracts inhibited NKA by over 90% at a concentration of 600 µg DW·mL^{-1}. Therefore, the root extract was further investigated by separating it into fractions using C18, mixed-mode anion, and cation exchange SPE columns. This separatory process yielded 14 fractions, of which two (RP2 and MC2) were significantly active (Figure 10B). A recently published correlation-metabolomic approach was then applied to these fractions to identify candidate features possibly responsible for the observed NKA-inhibiting activity (Rárová *et al.*, 2019).

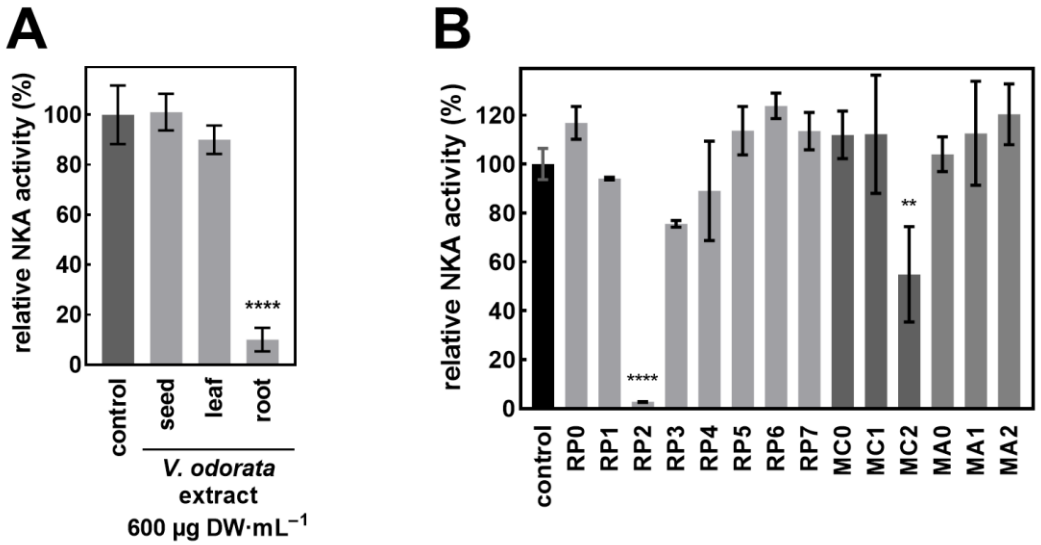

Figure 10 (A) Relative NKA activity (%) of Na^+,K^+-ATPase treated with crude methanolic *Viola odorata* extracts. Data are expressed as means ± SD (n = 3–4); Statistical significance based on Tukey's test is indicated by **** for $p < 0.0001$. (B) Relative NKA activity (%) of Na^+,K^+-ATPase treated with *V. odorata* root extract fractions. Data are expressed as means ± SD (n = 3–4); Statistical significances based on Tukey's test are indicated by **** and ** for $p < 0.0001$ and for $p < 0.005$, respectively. The original data were published as a part of the bachelor's thesis (Heger, 2019).

All isolated fractions were analyzed by non-targeted UHPLC-QTOF-MS/MS, which revealed 15 331 features in negative and 19 961 features in positive ion modes. Combined features from both modes were filtered based on their abundance and retention time, resulting in 2 748 features in total. These features were correlated with the inhibitory activity of each fraction and sorted according to the calculated correlation coefficients. The dimensionality of the data was further reduced by manual identification of the molecular ions of adducts, fragments, and isotopic peaks. Data from positive and negative modes were processed separately, which typically resulted in the presence of two rows independently referring to the same metabolite (see for example rows 1 and 2 in Table 1). The highly correlated candidate metabolites are shown in Table 1. Briefly, the higher the r value, the greater the likelihood that the row represents the active component. The majority of the candidate metabolites were annotated as B-type procyanidins, with the exception of one that was putatively identified as feruloyl putrescine. The commercially available procyanidins B1, B2, B3 and C1 were purchased and analyzed, allowing two candidates to be unambiguously identified as procyanidins C1 and B2. The NKA inhibitory activities of all available procyanidins (B1, B2, B3 and C1) were also determined (Figure 11A), revealing that procyanidin C1 is a strong inhibitor with an IC_{50} of 4.5 ± 0.8 µmol·L^{-1} (Figure 11B).

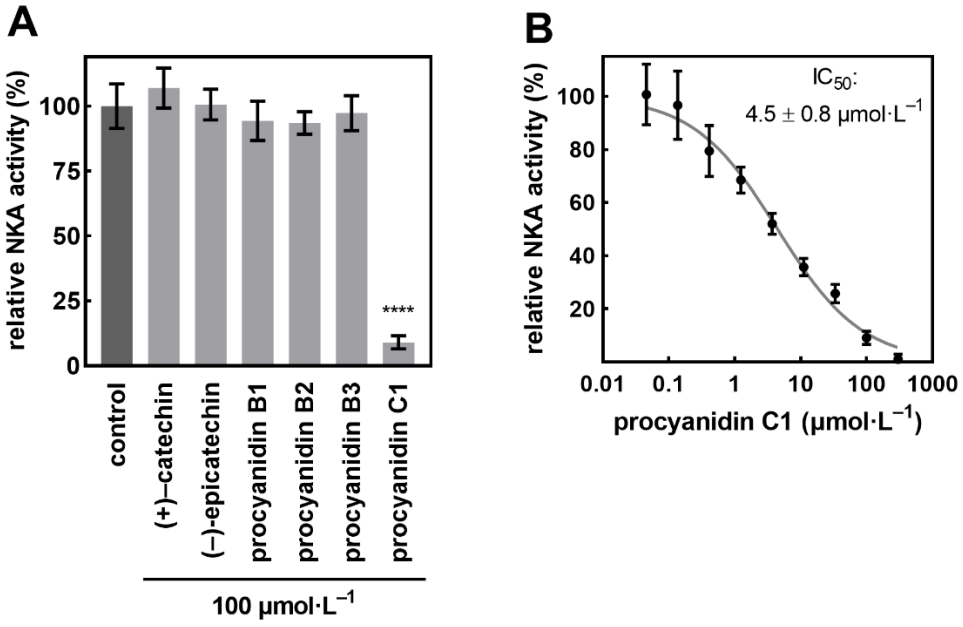

Figure 11 (A) Relative NKA activity (%) of Na^+,K^+-ATPase treated with flavan-3-ols and B-type procyanidin dimers and trimer. Data are expressed as means ± SD (n = 4); procyanidin C1 data taken from part B. Statistical significance based on Tukey's test is indicated by **** for $p < 0.0001$. (B) Dose-response curve for NKA inhibition by procyanidin C1. Data are expressed as means ± SD (n = 8).

Table 1 Top 15 candidate features from the metabolomic analysis of *Viola odorata* root fractions based on the Pearson correlation coefficient r. Metabolites were putatively identified (annotated) by analyzing their MS^2 spectra with the exception of procyanidins B2 and C1, which were identified by direct comparison with authentic standards.

no.	measured *m/z*	theoretical *m/z*	mode	Δppm	RT (min)	r	annotation
1	867.2136	867.2136	pos	0.0	5.89	0.9599	B-type procyanidin trimer 1
2	865.1971	865.1980	neg	–1.0	5.88	0.9581	B-type procyanidin trimer 1
3	577.1348	577.1346	neg	0.3	7.61	0.9562	B-type procyanidin dimer
4	579.1508	579.1503	pos	0.9	7.61	0.9540	B-type procyanidin dimer
5	867.2133	867.2136	pos	–0.3	7.12	0.9474	B-type procyanidin trimer 2
6	579.1501	579.1503	pos	–0.3	6.33	0.9463	procyanidin B2
7	1155.2785	1155.2614	pos	0.2	5.86	0.9403	B-type procyanidin tetramer
8	865.196	865.1980	neg	–2.3	7.09	0.9392	B-type procyanidin trimer 2
9	577.1346	577.1346	neg	0.0	6.33	0.9367	procyanidin B2
10	867.2137	867.2136	pos	0.1	7.25	0.9343	procyanidin C1
11	1153.2585	1153.2614	neg	–2.5	5.86	0.9324	B-type procyanidin tetramer
12	865.1966	865.1980	neg	–1.6	7.24	0.9306	procyanidin C1
13	867.2137	867.2136	pos	0.1	5.74	0.9253	B-type procyanidin trimer 3
14	265.1551	265.1552	pos	–0.4	5.00	0.9196	feruloyl putrescine
15	865.1977	865.1980	neg	–0.3	7.72	0.9118	B-type procyanidin trimer 4

Due to the complexity of the *V. odorata* extracts, it was not possible to structurally identify the other B-type procyanidins from the candidate list. The diversity of B-type procyanidins in *Viola odorata* root is illustrated by the number of peaks with *m/z* 865 showing fragmentation patterns characteristic of B-type procyanidin trimers (Figure 12).

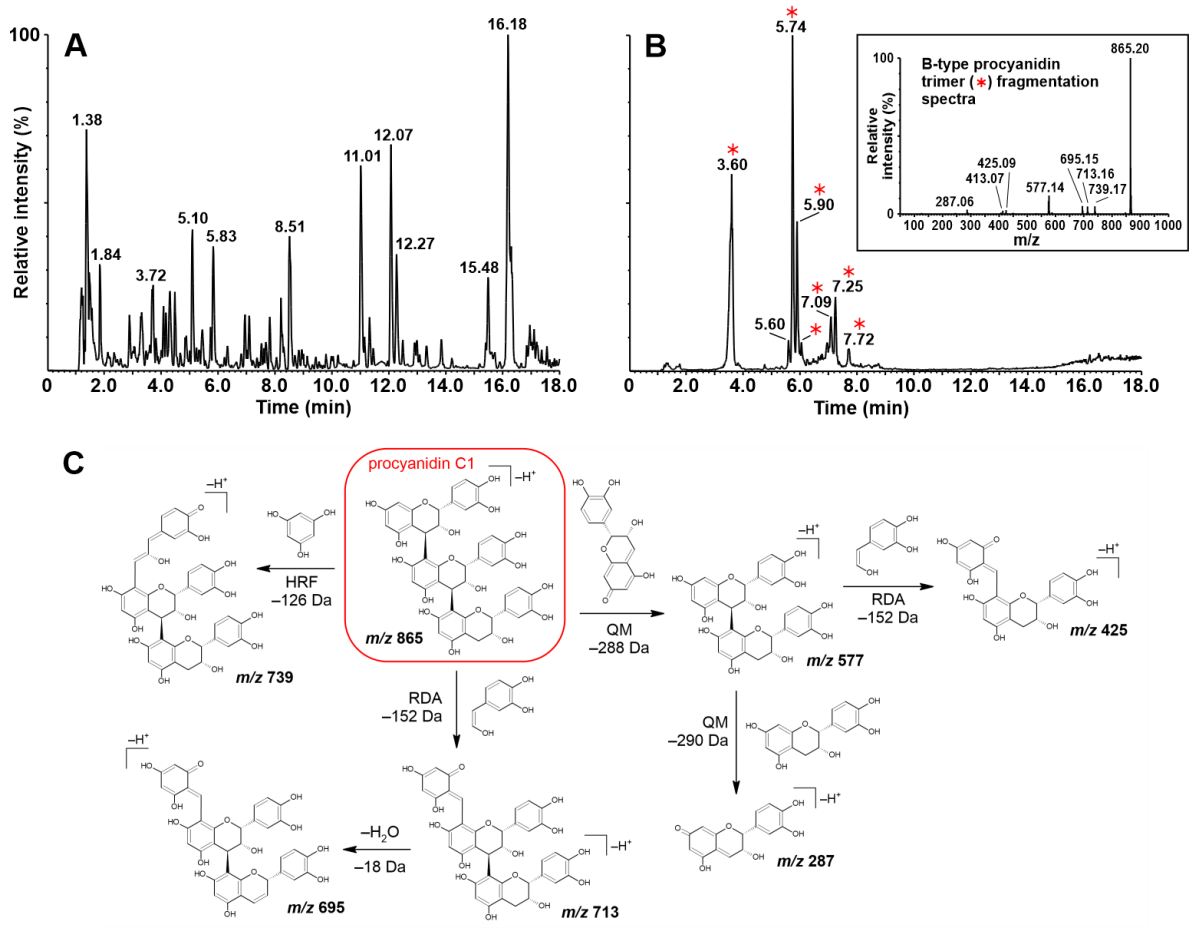

Figure 12 (A) UHPLC-ESI-MS base peak chromatogram of a crude *Viola odorata* root extract (160 mg DW·mL^{-1}) recorded in negative ion mode. (B) Extracted ion chromatogram recorded in negative ion mode (*m/z* 865). Analytes showing fragmentation patterns characteristic of B-type procyanidin trimers are indicated by red asterisks. Inset: B-type procyanidin trimer fragmentation spectrum obtained in negative ion mode with a collision energy of 20 eV. (C) B-type procyanidin trimer fragmentation pathways of procyanidin C1 (Enomoto *et al.*, 2019); QM quinone methide cleavage; HRF heterocyclic ring fission; RDA retro-Diels–Alder cleavage.

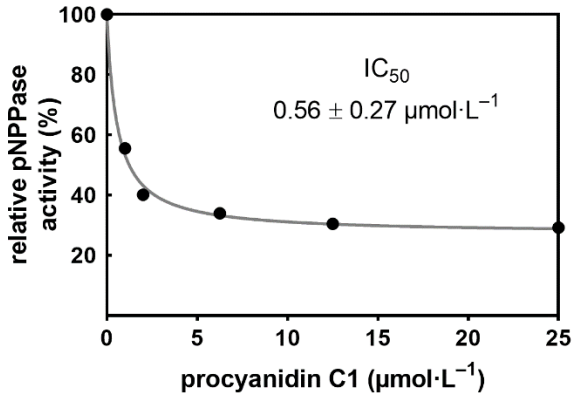

Figure 13 Dose-response curve of the NKA pNPPase activity inhibition by procyanidin C1. Data represent preliminarily singlicate measurement.

Remarkably, procyanidin C1 showed more potent activity in the *p*-nitrophenyl phosphatase (pNPPase) assay. According to the preliminary results, the NKA pNPPase activity was inhibited with one order magnitude lower IC_{50} (0.56 ± 0.27 µmol·L^{-1}) compared to ATPase activity (Figure 13).

Fluorescence experiments were performed to further investigate the interaction of procyanidin C1 and NKA. The effect of procyanidin C1 on eosin Y and 9-anthroyl ouabain fluorescence activation was analysed under various conditions. A typical titration curve of the eosin fluorescence experiment is shown in Figure 14A, while a similar experiment with two procyanidin C1 additions is shown on the right part of the figure (14B). The concentration of 20 µmol·L^{-1} KCl forced the enzyme to the E_2 conformation where the unbound probe had a low fluorescence yield. The opposite effect was induced by 30 mmol·L^{-1} NaCl causing the binding of the probe to the E_1 enzyme characterized by the fluorescence increase. The final addition of 100 µmol·L^{-1} ADP brought the curve back to the baseline level due to the competitive displacement of eosin by ADP. Obviously, procyanidin C1 rapidly decreases the bound eosin fluorescence. The raw data of experiments with and without procyanidin C1 indicate that the free eosin fluorescence is not decreased by the tested compound (not presented).

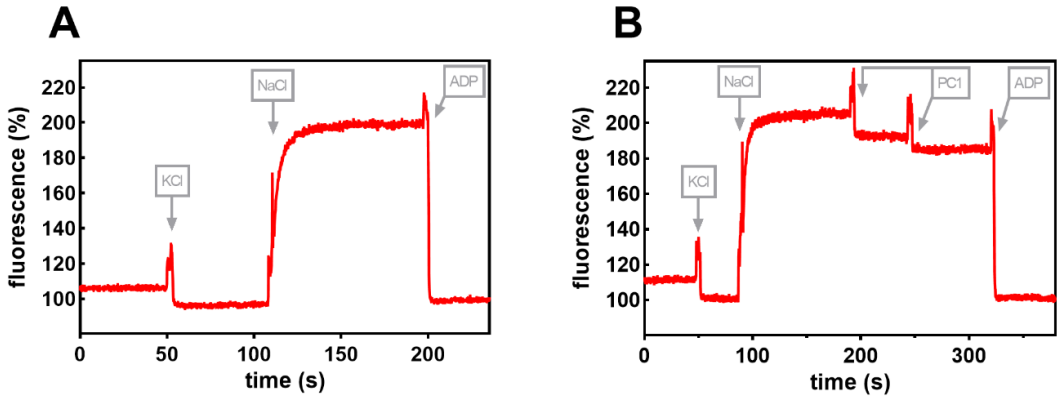

Figure 14 (A) Typical eosin fluorescence curve. Arrows indicate the additions of 20 µmol·L^{-1} KCl, 30 mmol·L^{-1} NaCl, and 100 µmol·L^{-1} ADP. (B) Eosin fluorescence experiment showing the influence of procyanidin C1 (PC1) on the bound eosin fluorescence. Arrows indicate the same steps described in A plus the two consecutive additions of PC1 up to 13 and 26 µmol·L^{-1}, respectively.

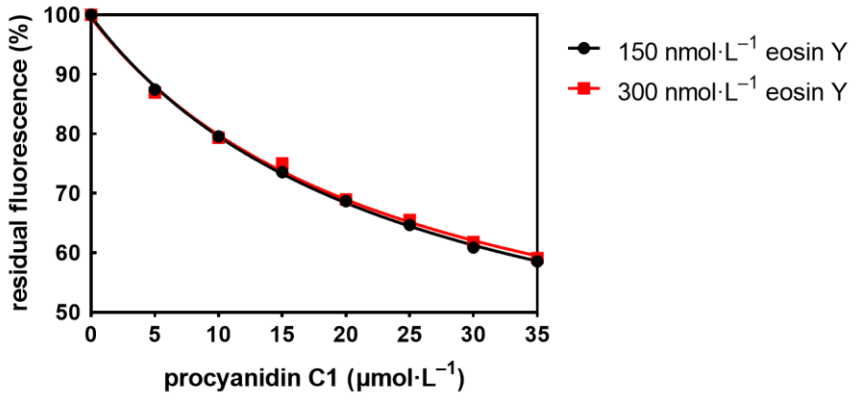

Figure 15 Residual fluorescence of eosin obtained from the titration curve of procyanidin C1 under the conditions with 150 and 300 nmol·L^{-1} eosin Y, respectively.

The following experiment proved that although a fluorescence yield decreases upon procyanidin C1 addition, the apparent dissociation constant (K_d^{app}) of procyanidin C1 is not changed under the conditions of 150 and 300 nmol·L^{-1} eosin, respectively (K_d^{eosin} was determined as 67 nmol·L^{-1}). The corresponding K_d^{app} values of procyanidin C1 were 24.8 ± 1.5 and 24.6 ± 3.4 µmol·L^{-1}, respectively (Figure 15). The next eosin fluorescence experiment involved the titration of NaCl into the assay buffer containing various K^+ concentrations with or without 25 µmol·L^{-1} procyanidin C1 (Figure 16). The apparent affinity of NKA for Na^+ ions was investigated showing the expected decrease with increasing K^+ concentration. However, the presence of procyanidin C1 left-shifted the curves mitigating the effect of K^+ ions on the bound eosin fluorescence.

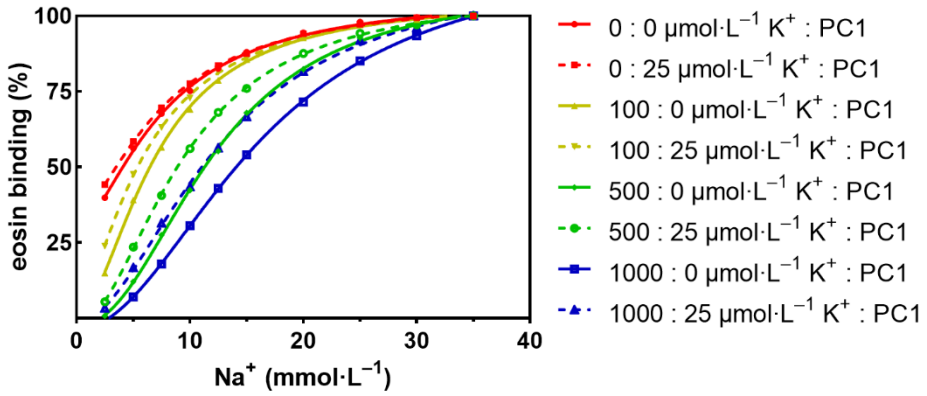

Figure 16 Eosin fluorescence experiments of the Na^+ titration with varying K^+ concentration and with or without procyanidin C1 (PC1) added.

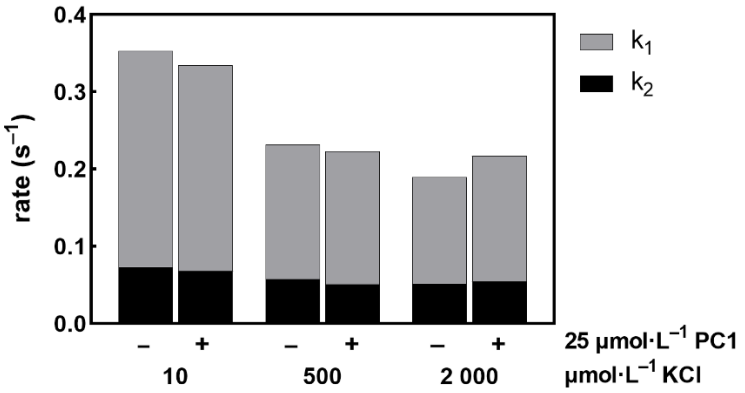

Figure 17 K^+ ions deocclusion rate constants determined by the stopped-flow eosin fluorescence experiments (n = 3–9).

The K^+ ions deocclusion rate constants were determined by stopped-flow experiments (Figure 17). The NKA solution in one syringe with varying KCl concentration and with or without 25 µmol·L^{-1} procyanidin C1 was mixed with 60 mmol·L^{-1} NaCl and 100 nmol·L^{-1} eosin in the second syringe. The concentrations of buffer, procyanidin C1, and K^+ ions were kept constant. The simplified scheme of conformational changes is as follows (the number of bound ions is omitted):

$$E_2K <=> E_1K <=> E_1 <=> E_1Na <=> E_1Na\text{-eosin}$$

The process is described with a double exponential function where the slow component (k_2) corresponds to the K^+ deocclusion by the $E_2K <=> E_1K$ transition, and the fast component (k_1) describes Na^+ binding. As expected, the rate constant k_1 of the fast phase decreased with increasing K^+ concentration. Neither k_2 nor k_1 does not seem to be affected by procyanidin C1.

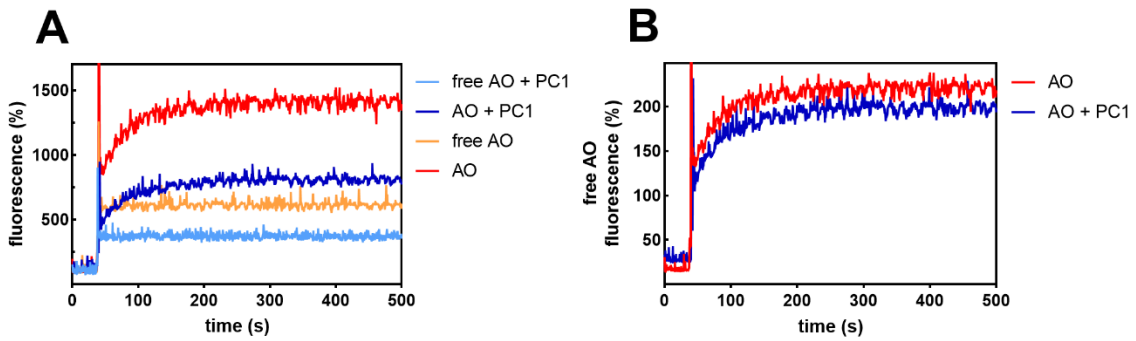

Figure 18 (A) Fluorescence experiment of 9-anthroyl ouabain (AO) binding to the E_2-P enzyme under the conditions with or without 25 μmol·L^{-1} procyanidin C1 (PC1). The AO and AO + PC1 lines show the fluorescence increase upon AO addition, whereas the free AO and free AO + PC1 represent the same experiments but pre-incubated with unlabelled ouabain before the measurement. (B) 9-anthroyl ouabain (AO) fluorescence with or without procyanidin C1 (PC1) normalized to the corresponding level of free AO fluorescence (the data from A).

The last performed fluorescence experiment was the anthroyl ouabain binding assay (Figure 18). The fluorescence was largely increased upon anthroyl ouabain binding to the E_2-P enzyme. The fluorescence records of anthroyl ouabain binding and unbound anthroyl ouabain are shown in part 18A. The data in part 18B of the figure represent another normalization of the 18A dataset. The anthroyl ouabain fluorescence record from the experiment with or without procyanidin C1 was normalized to the corresponding baseline fluorescence of unbound anthroyl ouabain. Procyanidin C1 decreased the fluorescence of both free and bound anthroyl ouabain.

Finally, molecular docking of procyanidin C1 to NKA was performed to identify possible interaction sites. Two crystal structures of NKA representing different catalytic intermediates were selected for the docking study: 3WGU ($Na_3E_1[AlF_4]^-$·ADP), which has a resolution of 2.80 Å and is an analogue of the Na_3E_1~P·ADP state, and 2ZXE (K_2E_2·$[MgF_4]^{2-}$), which has a resolution of 2.40 Å and is analogous to the K_2E_2·P_i state.

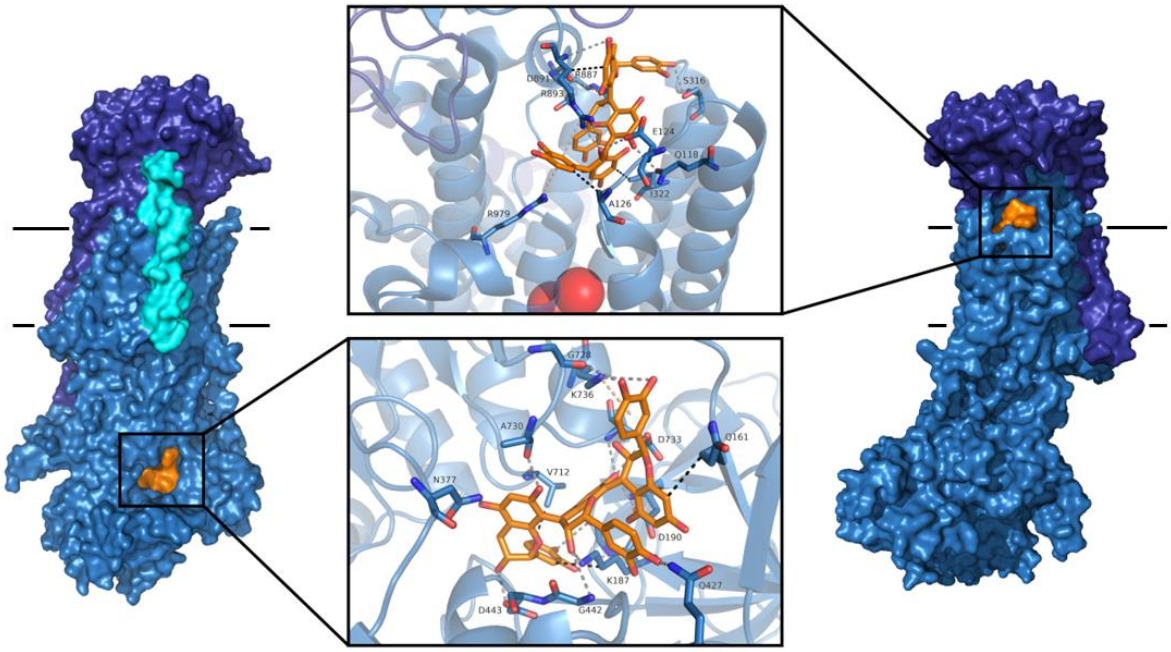

Figure 19 Binding modes of procyanidin C1 in the structures mimicking the $Na_3E_1{\sim}P{\cdot}ADP$ state (left; 3WGU) and the $K_2E_2{\cdot}P_i$ state (right; 2ZXE). The membrane region is indicated by horizontal lines. Surface representation color code: subunit α – sky-blue; subunit β – deep blue; FXYD protein – cyan; procyanidin C1 – orange. Non-covalent interactions are shown in the middle using the following color code: hydrophobic – black; hydrogen bonding – grey; cation-π – beige. Potassium ions are represented as red spheres.

Docking of procyanidin C1 into the structural analogue of the NKA of $Na_3E_1{\sim}P{\cdot}ADP$ state (3WGU) yielded lower binding energies than those for docking into the $K_2E_2{\cdot}P_i$ state analogue. The binding site with the highest affinity for procyanidin C1 (binding energy: –11.5 kcal·mol^{-1}) was located in close proximity to the nucleotide binding site (Figure 19, left). For the $K_2E_2{\cdot}P_i$ state analogue (2ZXE), the lowest energy binding site of procyanidin C1 (binding energy: –9.9 kcal·mol^{-1}) was in the extracellular part of the protein (Figure 19, right). In this case, key protein-ligand interactions included two cation-π bonds between arginine guanidinium groups and the *ortho*-dihydroxyphenyl rings of procyanidin C1.

5 DISCUSSION

A modern approach based on correlation metabolomics was used to identify active compounds in a plant extract. This procedure led to a few candidate compounds and ultimately to the root extract constituent procyanidin C1, which strongly inhibited ATPase activity of NKA (IC_{50} 4.5 $\mu mol \cdot L^{-1}$). In contrast to the strong biological activity of the trimer procyanidin C1, commercially available procyanidin dimers (B1, B2 and B3) were inactive (IC_{50} > 100 $\mu mol \cdot L^{-1}$). The NKA-inhibiting activity of procyanidin C1 was previously unknown, although a procyanidin-rich hawthorn extract WS® 1442 with a procyanidin content of 17.3–20.1% was previously shown to inhibit NKA (Willer *et al.*, 2012; Schwinger *et al.*, 2000; Koch and Malek, 2011). Potential antiarrhythmic and positive ionotropic effects of WS® 1442 were also reported. However, it remains unclear whether procyanidins or other components of hawthorn extract are primarily responsible for the activity of WS® 1442. For example, ursolic and oleanolic acids, which constitute roughly 0.6% of WS® 1442, are also moderate inhibitors of NKA, with IC_{50} values of 25 to 100 $\mu mol \cdot L^{-1}$ (Yokomichi *et al.*, 2011; Chen *et al.*, 2010). In this work, the data on procyanidin C1 suggest that its strong NKA-inhibitory activity together with its high abundance in hawthorn extract may explain the cardiac glycoside-like properties of WS® 1442 (Svedström *et al.*, 2002; Hellenbrand *et al.*, 2015; Svedström *et al.*, 2006; CuiLi*et al.*, 2006; CuiNakamura*et al.*, 2006; Yang and Liu, 2012; Zumdick *et al.*, 2009).

Besides, procyanidin C1 was also shown to inhibit gastric H^+,K^+-ATPase, which is another P-type ATPase with an E_1–E_2 catalytic mechanism like NKA. The gastric H^+,K^+-ATPase was inhibited by an extract from the aerial part of *Cecropia glaziovii* Snethl. as well as by its chemical constituents procyanidins C1 and B2, whose IC_{50}'s were determined to be 46.5 and 40.6 $\mu mol \cdot L^{-1}$, respectively (Souccar *et al.*, 2008). Due to the presence of other phenolics and the relatively low activity of the identified constituents, the chemical principle of H^+,K^+-ATPase inhibition by *Cecropia glaziovii* extract remains unclear.

In this work, the only commercially available trimer, procyanidin C1, was investigated and showed NKA inhibition. Despite its strong activity, procyanidin C1 was present at relatively low concentrations in *V. odorata* (data not shown), suggesting that other compounds may contribute to the extract's activity. It should be noted that the top scoring metabolite given by correlation approach was an unknown trimeric B–type procyanidin, the isomer of procyanidin C1. Due to their similar chemical structures, the procyanidins

inevitably coeluted from the SPE cartridges used in this work (C18, MAX and MCX). Therefore, their individual contributions to the overall extract activity are not readily distinguished by correlation alone. However, the metabolomic and biochemical data suggest that procyanidin C1 is responsible for the observed activity of *V. odorata* root extracts, either alone or in combination with its isomer(s). Contributions of extract components other than procyanidin metabolites is unlikely because the only non-procyanidin compound correlated with NKA activity was annotated as feruloyl putrescine, a mono-conjugated phenolamide present in many species that have never been reported to inhibit NKA, including *Salsola subaphylla, Zea mays, Oryza sativa, and Nicotiana tabacum* (Mizukasi *et al.*, 1971; Li *et al.*, 2018; Ryabinin and Il'Ina, 1949). It should also be noted that the presence of procyanidins in the root, the only active *V. odorata* part, might be associated with their role in the nitrogen cycle in the soil (Bardon *et al.*, 2017; Kraus *et al.*, 2004).

In contrast to the strongly active trimeric procyanidin C1, the dimeric procyanidins B1, B2 and B3 were completely inactive towards NKA. Possible binding modes of procyanidin C1 were identified by molecular docking using the 3WGU and 2ZXE crystal structures of NKA proteins originating from *Sus scrofa* and *Squalus acanthias*, respectively. Both of these structures are available at considerably higher resolutions than other published NKA structures and were therefore the only catalytic state analogs investigated in this work. Two interesting bifacial cation-π interactions between arginine guanidinium groups and the *ortho*-dihydroxyphenyl rings of procyanidin C1 were found in the structure mimicking $K_2E_2{\cdot}P_i$ state (2ZXE). This interaction causes the ion pathway (which is formed by residues including one of the interacting arginines, R979) to become inaccessible from the extracellular side (Čechová *et al.*, 2016). This binding mode may thus sterically impede ion exchange. It should be noted that residues R979 in loop L9-10 and D128 in loop L1-2 form a salt bridge in the E_2-P state, but separation of these residues is believed to be required for the motion of the TM2 transmembrane helix during the catalytic cycle (Chebrolu *et al.*, 2014; Young and Artigas, 2021). Other residues from L1-2 are also important for the protein's translocase function, so their interactions with the ligand could have additional effects on its conformational transitions (Chebrolu *et al.*, 2014).

In the best docking pose of the $Na_3E_1{\sim}P{\cdot}$ADP-mimicking structure (3WGU), the ligand plugged the whole hydrophilic cavity in front of the nucleotide-binding site in the cleft between the nucleotide-binding (N) and actuator (A) domains. In this case, the

binding energy (–11.5 kcal·mol^{-1}) was lower than that for the previously discussed 2ZXE structure (–9.9 kcal·mol^{-1}). Due to the interdomain location of the binding site, residues from all three cytoplasmic domains are involved in procyanidin C1 binding. The interdomain space in the intracellular part of the protein was previously suggested to be a possible binding site for flavonolignans based on a docking study (Kubala *et al.*, 2016). A subsequent fluorescence spectroscopy experiment proved that flavonolignans interact with the cytoplasmic segment connecting transmembrane helices TM4 and TM5, providing experimental evidence for a binding mode that may contribute to the inhibition of NKA by flavonolignans. Therefore, the identification of a similarly located binding pose in this work may help explain the inhibitory activity of procyanidin C1.

Compared to the ATPase activity of NKA, the *p*-nitrophenyl phosphatase activity of the enzyme was inhibited even more with an IC_{50} of 0.56 μmol·L^{-1}. However, the interpretation of the pNPPase assay is limited by the fact that the exact mechanism of this non-physiological reaction is unknown. The enzyme exerts this phosphatase activity in E_2-dependent and ouabain inhibition sensitive manner (Berberián and Beaugé, 1985). Nevertheless, the inhibition of pNPPase activity by procyanidin C1 provides information about a strong interaction of the compound with the E_2 enzyme (Satoh *et al.*, 1996).

Eosin, the established fluorescent probe for the nucleotide-binding site and the E_1-E_2 transition, was used to further characterize the interaction between the NKA and procyanidin C1 (Esmann and Fedosova, 1997). The experiments showed that procyanidin C1 decreases the bound eosin fluorescence yield and its K_d is independent of the eosin concentration. Therefore, the inhibitor interacted with the NKA while not competing with eosin binding. The K^+-dependence of procyanidin C1 effect on the Na^+ titration curve was described. It seemed that the inhibitor either increases apparent affinity for Na^+ or prevents K^+ binding.

The detailed insight into the part of the NKA reaction cycle was enabled by the eosin experiment focused on K^+-deocclusion in the stopped-flow setup. The obtained data on deocclusion kinetics were in good agreement with the values previously published in the literature (Heyse *et al.*, 1994). It was shown that procyanidin C1 did not significantly affect neither the slow nor fast phase of the kinetics. Therefore, the E_2-E_1 transition and the exchange of ions followed by the association of the Na-bound E1 enzyme with eosin were not disrupted by procyanidin C1 present during this part of the catalytic cycle.

The important interaction site found in NKA is the cardiotonic steroid-binding site accessible from the extracellular side of the enzyme. The inhibitor ouabain binds to this

site with the high affinity in the E_2-P state disabling further progression of the catalytic cycle. The derivative anthroyl ouabain binds to the cardiotonic steroid-binding site, and this interaction is associated with the large fluorescence increase (Cornelius *et al.*, 2011). The performed experiments showed that procyanidin C1 decreases both fluorescences of bound and free anthroyl ouabain. The slight decrease in bound probe fluorescence indicated that procyanidin C1 is able to interact with the phosphoenzyme intermediate, too. However, the overall inhibitor quenching effect complicated the possibilities and interpretation of the binding experiments.

Regarding the occurrence of procyanidins in the human diet, these compounds are highly abundant with an estimated daily intake of 57.7 mg per person (Gu *et al.*, 2004). On the basis of cell monolayer penetration studies, they are believed to undergo paracellular absorption from the intestine (Kosińska and Andlauer, 2012; Mendoza-Wilson *et al.*, 2016; Deprez *et al.*, 2001). *In vivo* animal and human studies have also shown that procyanidin dimers and trimers are stable under gastric conditions, are not degraded into monomers, and can be detected in rat plasma and urine after ingestion (Serra *et al.*, 2013; Prasain *et al.*, 2009; Tsang *et al.*, 2005; Serra *et al.*, 2009; Serra *et al.*, 2010; Shoji *et al.*, 2006) (Tsang *et al.*, 2005; Serra *et al.*, 2010; Ottaviani *et al.*, 2012; Rios *et al.*, 2002). While quantitative data on the plasma concentrations of procyanidins in humans are limited, procyanidin B2 was detected in plasma at a concentration of 4.0 ± 0.6 nmol·L^{-1} after the consumption of 1.8 mg dimeric procyanidins per kg of body weight. Interestingly, treatment of the plasma samples with sulfatases and β-glucuronidases did not increase the measured procyanidin B2 concentration, suggesting that it was not conjugated (Ottaviani *et al.*, 2012). Procyanidins were also detected in human plasma from individuals who had recently consumed procyanidin-rich plant foods/extracts. For example, administration of 0.375 g of cocoa per kg of body weight and 2 g of proanthocyanidin-rich grape seed extract per person resulted in the detection of procyanidins B2 at 41 ± 4 nmol·L^{-1} and B1 at 10.6 ± 2.5 nmol·L^{-1} in human plasma (Holt *et al.*, 2002; Sano *et al.*, 2003). Ingested procyanidins thus seem to be readily absorbed in humans, resulting in detectable levels in human plasma. As such, they are both dietary compounds capable of inhibiting NKA and also potential sources of novel molecular structures that could be used as alternatives to cardiac glycosides in the treatment of congestive heart failure and cardiac arrhythmia.

6 CONCLUSION

Procyanidin C1 is a newly discovered Na^+,K^+-ATPase (NKA) inhibitor whose molecular architecture could potentially be optimized to develop analogues with greater druglikeness. Its low micromolar IC_{50} makes all trimeric B-type procyanidins interesting targets for further mechanistic investigation and analysis of structure-activity relationships. Such studies could enable the development of novel NKA inhibitors with previously unexplored modes of action and/or binding sites. The successful application of correlation metabolomics in this work further demonstrates the high effectivity of this approach for identifying biologically active compounds in complex extracts.

7 LITERATURE

Abe I., Morita H. (2010): Structure and function of the chalcone synthase superfamily of plant type III polyketide synthases. *Natural Product Reports* **27**, 809–838.

Adams K.F., Ghali J.K., Herbert Patterson J., Stough W.G., Butler J., Bauman J.L., Ventura H.O., Sabbah H., MacKowiak J.I., Van Veldhuisen D.J. (2014): A perspective on re-evaluating digoxin's role in the current management of patients with chronic systolic heart failure: Targeting serum concentration to reduce hospitalization and improve safety profile. *European Journal of Heart Failure* **16**, 483–493.

Akhbari M., Batooli H., Kashi F.J. (2012): Composition of essential oil and biological activity of extracts of *Viola odorata* L. from central Iran. *Natural Product Research* **26**, 802–809.

Alagoz Y., Gurkok T., Zhang B., Unver T. (2016): Manipulating the biosynthesis of bioactive compound alkaloids for next-generation metabolic engineering in opium poppy Using CRISPR-Cas 9 genome editing technology. *Scientific Reports* **6**.

Albarano L., Esposito R., Ruocco N., Costantini M. (2020): Genome Mining as New Challenge in Natural Products Discovery. *Marine Drugs* **18**, 199.

Albers R.W. (1967): Biochemical Aspects of Active Transport. *Annual Review of Biochemistry* **36**, 727–756.

Amarelle L., Katzen J., Shigemura M., Welch L.C., Cajigas H., Peteranderl C., Celli D., Herold S., Lecuona E., Sznajder J.I. (2019): Cardiac glycosides decrease influenza virus replication by inhibiting cell protein translational machinery. *Am J Physiol Lung Cell Mol Physiol* **316**, 1094–1106.

Aperia A., Akkuratov E.E., Fontana J.M., Brismar H. (2016): Na+-k+-ATPase, a new class of plasma membrane receptors. *American Journal of Physiology - Cell Physiology* **310**, C491–C495.

Appeldoorn M.M., Vincken J.P., Gruppen H., Hollman P.C.H. (2009): Procyanidin dimers A1, A2, and B2 are absorbed without conjugation or methylation from the small intestine of rats. *Journal of Nutrition* **139**, 1469–1473.

Appeldoorn M.M., Vincken J.P., Sanders M., Hollman P.C.H., Gruppen H. (2009): Combined normal-phase and reversed-phase liquid chromatography/ESI-MS as a tool to determine the molecular diversity of A-type procyanidins in peanut skins. *Journal of Agricultural and Food Chemistry* **57**, 6007–6013.

Arystarkhova E., Donnet C., Muñoz-Matta A., Specht S.C., Sweadner K.J. (2007): Multiplicity of expression of FXYD proteins in mammalian cells: Dynamic exchange of phospholemman and γ-subunit in response to stress. *American Journal of Physiology - Cell Physiology* **292**.

Atanasov A.G., Zotchev S.B., Dirsch V.M., Orhan I.E., Banach M., Rollinger J.M., Barreca D., Weckwerth W., Bauer R., Bayer E.A., Majeed M., Bishayee A., Bochkov V., Bonn G.K., Braidy N., Bucar F., Cifuentes A., D'Onofrio G., Bodkin M., Diederich M., Dinkova-Kostova A.T., Efferth T., El Bairi K., Arkells N., Fan T.P., Fiebich B.L., Freissmuth M., Georgiev M.I., Gibbons S., Godfrey K.M., Gruber C.W., Heer J., Huber L.A., Ibanez E., Kijjoa A., Kiss A.K., Lu A., Macias F.A., Miller M.J.S., Mocan A., Müller R., Nicoletti F., Perry G., Pittalà V., Rastrelli L., Ristow M., Russo G.L., Silva A.S., Schuster D., Sheridan H., Skalicka-Woźniak K., Skaltsounis L., Sobarzo-Sánchez E., Bredt D.S., Stuppner H., Sureda A., Tzvetkov N.T., Vacca R.A., Aggarwal B.B., Battino M., Giampieri F., Wink M., Wolfender J.L., Xiao J., Yeung A.W.K., Lizard G., Popp M.A., Heinrich M., Berindan-Neagoe I., Stadler M., Daglia M., Verpoorte R., Supuran C.T. (2021): Natural products in drug discovery: advances and opportunities. *Nature Reviews Drug Discovery* **20**, 200–216.

Auld D.S., Southall N.T., Jadhav A., Johnson R.L., Diller D.J., Simeonov A., Austin C.P., Inglese J. (2008): Characterization of chemical libraries for luciferase inhibitory activity. *Journal of Medicinal Chemistry* **51**, 2372–2386.

Axelsen K.B., Palmgren M.G. (1998): Evolution of substrate specificities in the P-type ATPase superfamily. *Journal of Molecular Evolution* **46**, 84–101.

Babes A., Fendler K. (2000): Na^+ transport, and the E_1P-E_2P conformational transition of the Na+/K+-ATPase. *Biophysical Journal* **79**, 2557–2571.

Baecher S., Kroiss M., Fassnacht M., Vogeser M. (2014): No endogenous ouabain is detectable in human plasma by ultra-sensitive UPLC-MS/MS. *Clinica Chimica Acta* **431**, 87–92.

Baell J.B. (2016): Feeling Nature's PAINS: Natural Products, Natural Product Drugs, and Pan Assay Interference Compounds (PAINS). *Journal of Natural Products* **79**, 616–628.

Baell J.B., Holloway G.A. (2010): New substructure filters for removal of pan assay interference compounds (PAINS) from screening libraries and for their exclusion in bioassays. *Journal of Medicinal Chemistry* **53**, 2719–2740.

Baetz K., McHardy L., Gable K., Tarling T., Rebérioux D., Bryan J., Andersen R.J., Dunn T., Hieter P., Roberge M. (2004): Yeast genome-wide drug-induced haploinsufficiency screen to determine drug mode of action. *Proceedings of the National Academy of Sciences of the United States of America* **101**, 4525–4530.

Bagchi D., Garg A., Krohn R.L., Bagchi M., Tran M.X., Stohs S.J. (1997): Oxygen free radical scavenging abilities of vitamins C and E, and a grape seed proanthocyanidin extract *in vitro*. *Research Communications in Molecular Pathology and Pharmacology* **95**, 179–189.

Bagchi D., Kuszynski C., Balmoori J., Bagchi M., Stohs S.J. (1998): Hydrogen peroxide-induced modulation of intracellular oxidized states in cultured macrophage J774A.1 and neuroactive PC-12 cells, and protection by a novel grape seed proanthocyanidin extract. *Phytotherapy Research* **12**, 568–571.

Bagrov A.Y., Shapiro J.I., Fedorova O. V. (2009): Endogenous cardiotonic steroids: Physiology, pharmacology, and novel therapeutic targets. *Pharmacological Reviews* **61**, 9–38.

Ballard H.E., Sytsma K.J., Kowal R.R. (1999): Shrinking the Violets: Phylogenetic Relationships of Infrageneric Groups in Viola (Violaceae) Based on Internal Transcribed Spacer DNA Sequences. *Systematic Botany* **23**, 458.

Banerjee M., Duan Q., Xie Z. (2015): SH2 Ligand-Like Effects of Second Cytosolic Domain of Na/K-ATPase α1 Subunit on Src Kinase J. W. Lee, ed. *PLOS ONE* **10**, e0142119.

Bardon C., Poly F., Haichar F. el Z., Le Roux X., Simon L., Meiffren G., Comte G., Rouifed S., Piola F. (2017): Biological denitrification inhibition (BDI) with procyanidins induces modification of root traits, growth and N status in *Fallopia* x *bohemica*. *Soil Biology and Biochemistry* **107**, 41–49.

Basu S., Waldmann H. (2014): Polymer supported synthesis of a natural product-inspired oxepane library. *Bioorganic and Medicinal Chemistry* **22**, 4430–4444.

Baxter I.R., Young J.C., Armstrong G., Foster N., Bogenschutz N., Cordova T., Peer W.A., Hazen S.P., Murphy A.S., Harper J.F. (2005): A plasma membrane H^+-ATPase is required for the formation of proanthocyanidins in the seed coat endothelium of *Arabidopsis thaliana*. *Proceedings of the National Academy of Sciences of the United States of America* **102**, 2649–2654.

Beecher G.R. (2004): Proanthocyanidins: Biological Activities Associated with Human Health. *Pharmaceutical Biology* **42**, 2–20.

Benarroch E.E. (2011): Na^+,K^+-ATPase: Functions in the nervous system and involvement in neurologic disease. *Neurology* **76**, 287–293.

Berberián G., Beaugé L. (1985): Phosphatase activity of (Na^+ + K^+)-ATPase. Ligand interactions and related enzyme forms. *BBA - Biomembranes* **821**, 17–29.

Beutler J.A., Cardellina J.H., Lin C.M., Hamel E., Cragg G.M., Boyd M.R. (1993): Centaureidin, a cytotoxic flavone from *Polymnia fruticosa*, inhibits tubulin polymerization. *Bioorganic and Medicinal Chemistry Letters* **3**, 581–584.

Bhatt V.P., Negi G.C.S. (2006): Ethnomedicinal plant resources of Jaunsari tribe of Garhwal Himalaya, Uttaranchal. *Indian Journal of Traditional Knowledge* **5**, 331–335.

Bian X., Tang B., Yu Y., Tu Q., Gross F., Wang H., Li A., Fu J., Shen Y., Li Y.Z., Stewart A.F., Zhao G., Ding X., Müller R., Zhang Y. (2017): Heterologous Production and Yield Improvement of Epothilones in *Burkholderiales* Strain DSM 7029. *ACS Chemical Biology* **12**, 1805–1812.

Bibert S., Roy S., Schaer D., Felley-Bosco E., Geering K. (2006): Structural and functional properties of two human FXYD3 (Mat-8) isoforms. *Journal of Biological Chemistry* **281**, 39142–39151.

Bisson J., McAlpine J.B., Friesen J.B., Chen S.N., Graham J., Pauli G.F. (2016): Can Invalid Bioactives Undermine Natural Product-Based Drug Discovery? *Journal of Medicinal Chemistry* **59**, 1671–1690.

Bittner K., Rzeppa S., Humpf H.U. (2013): Distribution and quantification of flavan-3-ols and procyanidins with low degree of polymerization in nuts, cereals, and legumes. *Journal of Agricultural and Food Chemistry* **61**, 9148–9154.

Blanco G., Mercer R.W. (1998): Isozymes of the Na-K-ATPase: Heterogeneity in structure, diversity in function. *American Journal of Physiology - Renal Physiology* **275**.

Boguslavskyi A., Tokar S., Prysyazhna O., Rudyk O., Sanchez-Tatay D., Lemmey H.A.L., Dora K.A., Garland C.J., Warren H.R., Doney A., Palmer C.N.A., Caulfield M.J., Vlachaki Walker J., Howie J., Fuller W., Shattock M.J. (2021): Phospholemman Phosphorylation Regulates Vascular Tone, Blood Pressure, and Hypertension in Mice and Humans. *Circulation* **143**, 1123–1138.

Booysen E., Dicks L.M.T. (2020): Does the Future of Antibiotics Lie in Secondary Metabolites Produced by *Xenorhabdus* spp.? A Review. *Probiotics and Antimicrobial Proteins* **12**, 1310–1320.

Bugni T.S., Richards B., Bhoite L., Cimbora D., Harper M.K., Ireland C.M. (2008): Marine natural product libraries for high-throughput screening and rapid drug discovery. *Journal of Natural Products* **71**, 1095–1098.

Butler M.S., Fontaine F., Cooper M.A. (2014): Natural product libraries: Assembly, maintenance, and screening. *Planta Medica* **80**, 1161–1170.

Cai T., Wang H., Chen Y., Liu L., Gunning W.T., Quintas L.E.M., Xie Z.J. (2008): Regulation of caveolin-1 membrane trafficking by the Na/K-ATPase. *Journal of Cell Biology* **182**, 1153–1169.

Cambrai A., Marchioni E., Julien-David D., Marcic C. (2017): Discrimination of Cocoa Bean Origin by Chocolate Polyphenol Chromatographic Analysis and Chemometrics. *Food Analytical Methods* **10**, 1991–2000.

Cameron R., Klein L., Shyjan A.W., Rakic P., Levenson R. (1994): Neurons and astroglia express distinct subsets of Na,K-ATPase α and β subunits. *Molecular Brain Research* **21**, 333–343.

Cantrell C.L., Gustafson K.R., Cecere M.R., Pannell L.K., Boyd M.R. (2000): Chondropsins A and B: Novel tumor cell growth-inhibitory macrolide lactams from the marine sponge Chondropsis sp. *Journal of the American Chemical Society* **122**, 8825–8829.

De Carvalho Aguiar P., Sweadner K.J., Penniston J.T., Zaremba J., Liu L., Caton M., Linazasoro G., Borg M., Tijssen M.A.J., Bressman S.B., Dobyns W.B., Brashear A., Ozelius L.J. (2004): Mutations in the Na^+/K^+-ATPase α3 gene ATP1A3 are associated with rapid-onset dystonia parkinsonism. *Neuron* **43**, 169–175.

Castillo J.P., Rui H., Basilio D., Das A., Roux B., Latorre R., Bezanilla F., Holmgren M. (2015): Mechanism of potassium ion uptake by the Na^+/K^+-ATPase. *Nature Communications* **6**, 1–8.

Cayo M.A., Mallanna S.K., Di Furio F., Jing R., Tolliver L.B., Bures M., Urick A., Noto F.K., Pashos E.E., Greseth M.D., Czarnecki M., Traktman P., Yang W., Morrisey E.E., Grompe M., Rader D.J., Duncan S.A. (2017): A Drug Screen using Human iPSC-Derived Hepatocyte-like Cells Reveals Cardiac Glycosides as a Potential Treatment for Hypercholesterolemia. *Cell Stem Cell* **20**, 478-489.e5.

Čechová P., Berka K., Kubala M. (2016): Ion Pathways in the Na^+/K^+-ATPase. *Journal of Chemical Information and Modeling* **56**, 2434–2444.

Chauhan J., Luthra T., Gundla R., Ferraro A., Holzgrabe U., Sen S. (2017): A diversity oriented synthesis of natural product inspired molecular libraries. *Organic and Biomolecular Chemistry* **15**, 9108–9120.

Chebrolu S., Ma H., Artigas P. (2014): State-Dependent Movement between the First and Last External Loops of the Na/K Pump α Subunit. *Biophysical Journal* **106**, 582a.

Chen R.J.Y., Chung T.Y., Li F.Y., Yang W.H., Jinn T.R., Tzen J.T.C. (2010): Steroid-like compounds in Chinese medicines promote blood circulation via inhibition of Na^+/K^+-ATPase. *Acta Pharmacologica Sinica* **31**, 696–702.

Chung I.M., Kim M.Y., Park W.H., Moon H.I. (2008): Aldose reductase inhibitors from *Viola hondoensis* W. Becker et H Boss. *American Journal of Chinese Medicine* **36**, 799–803.

Clarke R.J., Catauro M., Rasmussen H.H., Apell H.J. (2013): Quantitative calculation of the role of the Na^+,K^+-ATPase in thermogenesis. *Biochimica et Biophysica Acta - Bioenergetics* **1827**, 1205–1212.

Clausen J.D., Vilsen B., McIntosh D.B., Einholm A.P., Andersen J.P. (2004): Glutamate-183 in conserved TGES motif of domain A of sarcoplasmic reticulum Ca^{2+}-ATPase assists in catalysis of E_2/E_2P partial reactions. *Proceedings of the National Academy of Sciences of the United States of America* **101**, 2776–2781.

Clausen M. V, Hilbers F., Poulsen H. (2017): The Structure and Function of the Na,K-ATPase Isoforms in Health and Disease. *Frontiers in physiology* **8**, 371.

Coleman S.L., Hurst R.D., Sawyer G.M., Kruger M.C. (2016): The *in vitro* evaluation of isolated procyanidins as modulators of cytokine-induced eotaxin production in human alveolar epithelial cells. *Journal of Berry Research* **6**, 115–124.

Connell B.J., Chang S.-Y., Prakash E., Yousfi R., Mohan V., Posch W., Wilflingseder D., Moog C., Kodama E.N., Clayette P., Lortat-Jacob H. (2016): A Cinnamon-Derived Procyanidin Compound Displays Anti-HIV-1 Activity by Blocking Heparan Sulfate- and Co-Receptor-Binding Sites on gp120 and Reverses T Cell Exhaustion via Impeding Tim-3 and PD-1 Upregulation Y. Wu, ed. *PLOS ONE* **11**, e0165386.

Corder R., Mullen W., Khan N.Q., Marks S.C., Wood E.G., Carrier M.J., Crozier A. (2006): Red wine procyanidins and vascular health. *Nature* **444**, 566.

Cornelius F., Mahmmoud Y.A., Toyoshima C. (2011): Metal fluoride complexes of Na,K-ATPase: Characterization of fluoride-stabilized phosphoenzyme analogues and their interaction with cardiotonic steroids. *Journal of Biological Chemistry* **286**, 29882–29892.

Corradi G.R., Mazzitelli L.R., Petrovich G.D., Grenon P., Sørensen D.M., Palmgren M., De Tezanos Pinto F., Adamo H.P. (2020): Reduction of the P5A-ATPase Spf1p phosphoenzyme by a Ca^{2+}-dependent phosphatase. *PLoS ONE* **15**.

Corrêa I.R., Nören-Müller A., Ambrosi H.D., Jakupovic S., Saxena K., Schwalbe H., Kaiser M., Waldmann H. (2007): Identification of inhibitors for mycobacterial protein tyrosine phosphatase B (MptpB) by biology-oriented synthesis (BIOS). *Chemistry - An Asian Journal* **2**, 1109–1126.

Cragg G.M., Grothaus P.G., Newman D.J. (2009): Impact of natural products on developing new anti-cancer agents. *Chemical Reviews* **109**, 3012–3043.

Crambert G., Füzesi M., Garty H., Karlish S., Geering K. (2002): Phospholemman (FXYD1) associates with Na,K-ATpase and regulates its transport properties. *Proceedings of the National Academy of Sciences of the United States of America* **99**, 11476–11481.

Crambert G., Geering K. (2003): FXYD Proteins: New Tissue-Specific Regulators of the Ubiquitous Na,K-ATPase. *Science Signaling* **2003**, 1–9 (re1).

Cruz P.G., Auld D.S., Schultz P.J., Lovell S., Battaile K.P., MacArthur R., Shen M., Tamayo-Castillo G., Inglese J., Sherman D.H. (2011): Titration-based screening for evaluation of natural product extracts: Identification of an Aspulvinone family of luciferase inhibitors. *Chemistry and Biology* **18**, 1442–1452.

Cu J.Q., Perineau F., Gaset A. (1992): Volatile components of violet leaves. *Phytochemistry* **31**, 571–573.

Cui T., Li J.Z., Kayahara H., Ma L., Wu L.X., Nakamura K. (2006): Quantification of the polyphenols and triterpene acids in Chinese hawthorn fruit by high-performance liquid chromatography. *Journal of Agricultural and Food Chemistry* **54**, 4574–4581.

Cui T., Nakamura K., Tian S., Kayahara H., Tian Y.-L. (2006): Polyphenolic Content and Physiological Activities of Chinese Hawthorn Extracts. *Bioscience, Biotechnology, and Biochemistry* **70**, 2948–2956.

Culp E.J., Yim G., Waglechner N., Wang W., Pawlowski A.C., Wright G.D. (2019): Hidden antibiotics in actinomycetes can be identified by inactivation of gene clusters for common antibiotics. *Nature Biotechnology* **37**, 1149–1154.

Dasari R., De Carvalho A., Medellin D.C., Middleton K.N., Hague F., Volmar M.N.M., Frolova L. V., Rossato M.F., De La Chapa J.J., Dybdal-Hargreaves N.F., Pillai A., Mathieu V., Rogelj S., Gonzales C.B., Calixto J.B., Evidente A., Gautier M., Munirathinam G., Glass R., Burth P., Pelly S.C., van Otterlo W.A.L., Kiss R., Kornienko A. (2015): Synthetic and Biological Studies of Sesquiterpene Polygodial: Activity of 9-Epipolygodial against Drug-Resistant Cancer Cells. *ChemMedChem* **10**, 2014–2026.

Dasari R., Masi M., Lisy R., Ferdérin M., English L.R., Cimmino A., Mathieu V., Brenner A.J., Kuhn J.G., Whitten S.T., Evidente A., Kiss R., Kornienko A. (2015): Fungal metabolite ophiobolin A as a promising anti-glioma agent: *In vivo* evaluation, structure-activity relationship and unique pyrrolylation of primary amines. *Bioorganic and Medicinal Chemistry Letters* **25**, 4544–4548.

Demain A.L., Fang A. (2000): The natural functions of secondary metabolites. In: *Advances in biochemical engineering/biotechnology*. (A. Fiechter, ed.), Springer Nature, Berlin, Heidelberg, 1–39.

Deprez S., Mila I., Huneau J.F., Tome D., Scalbert A. (2001): Transport of proanthocyanidin dimer, trimer, and polymer across monolayers of human intestinal epithelial Caco-2 cells. *Antioxidants and Redox Signaling* **3**, 957–967.

Devarajan P., Scaramuzzino D.A., Morrow J.S. (1994): Ankyrin binds to two distinct cytoplasmic domains of Na,K-ATPase α subunit. *Proceedings of the National Academy of Sciences of the United States of America* **91**, 2965–2969.

Dias D.A., Urban S., Roessner U. (2012): A Historical Overview of Natural Products in Drug Discovery. *Metabolites* **2**, 303–336.

Dixon R.A., Xie D.-Y., Sharma S.B. (2004): Proanthocyanidins - a final frontier in flavonoid research? *New Phytologist* **165**, 9–28.

Dostanic-Larson I., Van Huysse J.W., Lorenz J.N., Lingrel J.B. (2005): The highly conserved cardiac glycoside binding site of Na,K-ATPase plays a role in blood pressure regulation. *Proceedings of the National Academy of Sciences of the United States of America* **102**, 15845–15850.

Duan D., Doak A.K., Nedyalkova L., Shoichet B.K. (2015): Colloidal aggregation and the *in vitro* activity of traditional Chinese medicines. *ACS Chemical Biology* **10**, 978–988.

Dudek M.K., Gliński V.B., Davey M.H., Sliva D., Kaźmierski S., Gliński J.A. (2017): Trimeric and Tetrameric A-Type Procyanidins from Peanut Skins. *Journal of Natural Products* **80**, 415–426.

Dyla M., Hansen S.B., Nissen P., Kjaergaard M. (2019): Structural dynamics of P-type ATPase ion pumps. *Biochemical Society Transactions* **47**, 1247–1257.

Editorial (2007): All natural. *Nature Chemical Biology* **3**, 351–351.

Ekberg K., Pedersen B.P., Sørensen D.M., Nielsen A.K., Veierskov B., Nissen P., Palmgren M.G., Buch-Pedersen M.J. (2010): Structural identification of cation binding pockets in the plasma membrane proton pump. *Proceedings of the National Academy of Sciences of the United States of America* **107**, 21400–21405.

Eldridge G.R., Vervoort H.C., Lee C.M., Cremin P.A., Williams C.T., Hart S.M., Goering M.G., O'Neil-Johnson M., Zeng L. (2002): High-throughput method for the production and analysis of large natural product libraries for drug discovery. *Analytical Chemistry* **74**, 3963–3971.

Engemann A., Hübner F., Rzeppa S., Humpf H.U. (2012): Intestinal metabolism of two A-type procyanidins using the pig cecum model: Detailed structure elucidation of unknown catabolites with Fourier transform mass spectrometry (FTMS). *Journal of Agricultural and Food Chemistry* **60**, 749–757.

Enomoto H., Takahashi S., Takeda S., Hatta H. (2019): Distribution of Flavan-3-ol Species in Ripe Strawberry Fruit Revealed by Matrix-Assisted Laser Desorption/Ionization-Mass Spectrometry Imaging. *Molecules* **25**, 103.

Ertl P., Roggo S., Schuffenhauer A. (2008): Natural product-likeness score and its application for prioritization of compound libraries. *Journal of Chemical Information and Modeling* **48**, 68–74.

Esmann M., Fedosova N.U. (1997): Eosin as a probe for conformational transitions and

nucleotide binding in Na,K-ATPase. In: *Annals of the New York Academy of Sciences*. Blackwell Publishing Inc., Malden, USA, 310–321.

Fedosova N.U. (2016): Purification of Na,K-ATPase from pig kidney. In: *Methods in Molecular Biology*. Totowa, New Jersey, USA, Humana Press Inc., 5–10.

Feng B.Y., Shoichet B.K. (2006): A detergent-based assay for the detection of promiscuous inhibitors. *Nature Protocols* **1**, 550–553.

Feng B.Y., Simeonov A., Jadhav A., Babaoglu K., Inglese J., Shoichet B.K., Austin C.P. (2007): A high-throughput screen for aggregation-based inhibition in a large compound library. *Journal of Medicinal Chemistry* **50**, 2385–2390.

Ferrandi M., Salardi S., Tripodi G., Barassi P., Rivera R., Manunta P., Goldshleger R., Ferrari P., Bianchi G., Karlish S.J.D. (1999): Evidence for an interaction between adducin and Na^+-K^+-ATPase: relation to genetic hypertension. *American Journal of Physiology-Heart and Circulatory Physiology* **277**, H1338–H1349.

Feyzabadi Z., Ghorbani F., Vazani Y., Zarshenas M.M. (2017): A Critical Review on Phytochemistry, Pharmacology of *Viola odorata* L. and Related Multipotential Products in Traditional Persian Medicine. *Phytotherapy Research* **31**, 1669–1675.

Foo L.Y., Lu Y., Howell A.B., Vorsa N. (2000): A-type proanthocyanidin trimers from cranberry that inhibit adherence of uropathogenic P-fimbriated *Escherichia coli*. *Journal of Natural Products* **63**, 1225–1228.

Forbush B. (1987): Rapid release of ^{42}K and ^{86}Rb from an occluded state of the Na,K-pump in the presence of ATP or ADP. *Journal of Biological Chemistry* **262**, 11104–11115.

Fowler A., Swift D., Longman E., Acornley A., Hemsley P., Murray D., Unitt J., Dale I., Sullivan E., Coldwell M. (2002): An evaluation of fluorescence polarization and lifetime discriminated polarization for high throughput screening of serine/threonine kinases. *Analytical Biochemistry* **308**, 223–231.

Friedrich U., Stöhr H., Hilfinger D., Loenhardt T., Schachner M., Langmann T., Weber B.H.F. (2011): The Na/K-ATPase is obligatory for membrane anchorage of retinoschisin, the protein involved in the pathogenesis of X-linked juvenile retinoschisis. *Human Molecular Genetics* **20**, 1132–1142.

Gadsby D.C., Bezanilla F., Rakowski R.F., De Weer P., Holmgren M. (2012): The dynamic relationships between the three events that release individual Na^+ ions from the Na^+/K^+-ATPase. *Nature Communications* **3**, 1–6.

Ganesan A. (2008): The impact of natural products upon modern drug discovery. *Current Opinion in Chemical Biology* **12**, 306–317.

Garty H., Lindzen M., Scanzano R., Aizman R., Füzesi M., Goldshleger R., Farman N., Blostein R., Karlish S.J.D. (2002): A functional interaction between CHIF and Na-K-ATPase: implication for regulation by FXYD proteins. *American Journal of Physiology-Renal Physiology* **283**, F607–F615.

Geering K. (2001): The functional role of β subunits in oligomeric P-type ATPases. *Journal of Bioenergetics and Biomembranes* **33**, 425–438.

Glitsch H.G. (2001): Electrophysiology of the Sodium-Potassium-ATPase in Cardiac Cells. *Physiological Reviews* **81**, 1791–1826.

Glynn I.M., Richards D.E. (1982): Occlusion of rubidium ions by the sodium-potassium pump: its implications for the mechanism of potassium transport. *The Journal of Physiology* **330**, 17–43.

Gonçalves E., Segura-Cabrera A., Pacini C., Picco G., Behan F.M., Jaaks P., Coker E.A., Meer D., Barthorpe A., Lightfoot H., Mironenko T., Beck A., Richardson L., Yang W., Lleshi E., Hall J., Tolley C., Hall C., Mali I., Thomas F., Morris J., Leach A.R., Lynch J.T., Sidders B., Crafter C., Iorio F., Fawell S., Garnett M.J. (2020): Drug mechanism-of-action discovery through the integration of pharmacological and CRISPR screens. *Molecular Systems Biology* **16**, e9405.

Grabowski K., Baringhaus K.H., Schneider G. (2008): Scaffold diversity of natural products: Inspiration for combinatorial library design. *Natural Product Reports* **25**, 892–904.

Grabowski K., Schneider G. (2008): Properties and Architecture of Drugs and Natural Products Revisited. *Current Chemical Biology* **1**, 115–127.

Gu L., Kelm M.A., Hammerstone J.F., Beecher G., Holden J., Haytowitz D., Gebhardt S., Prior R.L. (2004): Concentrations of Proanthocyanidins in Common Foods and Estimations of Normal Consumption. *Journal of Nutrition*, **134**, 613–617.

Gu L., Kelm M.A., Hammerstone J.F., Beecher G., Holden J., Haytowitz D., Prior R.L. (2003): Screening of Foods Containing Proanthocyanidins and Their Structural Characterization Using LC-MS/MS and Thiolytic Degradation. *Journal of Agricultural and Food Chemistry* **51**, 7513–7521.

Guo Hao, Wang H., Huo Y.X. (2020): Engineering Critical Enzymes and Pathways for Improved Triterpenoid Biosynthesis in Yeast. *ACS Synthetic Biology* **9**, 2214–2227.

Guo Jiao, Jia X., Liu Y., Wang S., Cao J., Zhang B., Xiao G., Wang W. (2020): Screening of natural extracts for inhibitors against Japanese encephalitis virus infection. *Antimicrobial Agents and Chemotherapy* **64**.

Guo L., Winzer T., Yang X., Li Y., Ning Z., He Z., Teodor R., Lu Y., Bowser T.A., Graham I.A., Ye K. (2018): The opium poppy genome and morphinan production. *Science* **362**, 343–347.

Habeck M., Tokhtaeva E., Nadav Y., Ben Zeev E., Ferris S.P., Kaufman R.J., Bab-Dinitz E., Kaplan J.H., Dada L.A., Farfel Z., Tal D.M., Katz A., Sachs G., Vagin O., Karlish S.J.D. (2016): Selective Assembly of Na,K-ATPase α2β2 Heterodimers in the Heart. *Journal of Biological Chemistry* **291**, 23159–23174.

Hamilton G.R., Baskett T.F. (2000): In the arms of morpheus: The development of morphine for postoperative pain relief. *Canadian Journal of Anesthesia* **47**, 367–374.

Hamlyn J.M., Blaustein M.P., Bova S., Ducharme D.W., Harris D.W., Mandel F., Mathews W.R., Ludens J.H. (1991): Identification and characterization of a ouabain-like compound from human plasma. *Proceedings of the National Academy of Sciences of the United States of America* **88**, 6259–6263.

Harrison M.J. (1999): MOLECULAR AND CELLULAR ASPECTS OF THE ARBUSCULAR MYCORRHIZAL SYMBIOSIS. *Annual Review of Plant Physiology and Plant Molecular Biology* **50**, 361–389.

Harvey C.J.B., Tang M., Schlecht U., Horecka J., Fischer C.R., Lin H.C., Li J., Naughton B., Cherry J., Miranda M., Li Y.F., Chu A.M., Hennessy J.R., Vandova G.A., Inglis D., Aiyar R.S., Steinmetz L.M., Davis R.W., Medema M.H., Sattely E., Khosla C., Onge R.P.S., Tang Y., Hillenmeyer M.E. (2018): HEx: A heterologous expression platform for the discovery of fungal natural products. *Science Advances* **4**, eaar5459.

He F., Pan Q.H., Shi Y., Duan C.Q. (2008): Biosynthesis and genetic regulation of proanthocyanidins in plants. *Molecules* **13**, 2674–2703.

He Q.-L., Titov D. V., Li J., Tan M., Ye Z., Zhao Y., Romo D., Liu J.O. (2015): Covalent Modification of a Cysteine Residue in the XPB Subunit of the General Transcription Factor TFIIH Through Single Epoxide Cleavage of the Transcription Inhibitor Triptolide. *Angewandte Chemie International Edition* **54**, 1859–1863.

Hebert H., Skriver E., Söderholm M., Maunsbach A.B. (1988): Three-dimensional structure of renal Na,K-ATPase determined from two-dimensional membrane crystals of the p1 form. *Journal of Ultrastructure Research and Molecular Structure Research* **100**, 86–93.

Heger T. (2019): Studium inhibice sodno-draselné ATPasy rostlinnými extrakty a jejich antiproliferační aktivity. *Diploma's thesis*, Palacký University, Olomouc, Czech Republic.

Helfrich E.J.N., Vogel C.M., Ueoka R., Schäfer M., Ryffel F., Müller D.B., Probst S., Kreuzer M., Piel J., Vorholt J.A. (2018): Bipartite interactions, antibiotic production and biosynthetic potential of the *Arabidopsis* leaf microbiome. *Nature Microbiology* **3**, 909–919.

Hellenbrand N., Sendker J., Lechtenberg M., Petereit F., Hensel A. (2015): Isolation and quantification of oligomeric and polymeric procyanidins in leaves and flowers of Hawthorn (*Crataegus* spp.). *Fitoterapia* **104**, 14–22.

Herbert H., Skriver E., Maunsbach A.B. (1985): Three-dimensional structure of renal Na,K-ATPase determined by electron microscopy of membrane crystals. *FEBS Letters* **187**, 182–186.

Heyse S., Wuddel I., Apell H., Stürmer W. (1994): Partial reactions of the Na, K-ATPase: Determination of rate constants. *Journal of General Physiology* **104**, 197–240.

Hilbers F., Kopec W., Isaksen T.J., Holm T.H., Lykke-Hartmann K., Nissen P., Khandelia H., Poulsen H. (2016): Tuning of the Na,K-ATPase by the beta subunit. *Scientific Reports* **6**, 1–11.

Holt R.R., Lazarus S.A., Cameron Sullards M., Zhu Q.Y., Schramm D.D., Hammerstone J.F., Fraga C.G., Schmitz H.H., Keen C.L. (2002): Procyanidin dimer B2 [epicatechin-(4β-8)-epicatechin] in human plasma after the consumption of a flavanol-rich cocoa. *American Journal of Clinical Nutrition* **76**, 798–804.

Horisberger J.D. (2004): Recent insights into the structure and mechanism of the sodium pump. *Physiology* **19**, 377–387.

Hou Y., Braun D.R., Michel C.R., Klassen J.L., Adnani N., Wyche T.P., Bugni T.S. (2012): Microbial strain prioritization using metabolomics tools for the discovery of natural products. *Analytical Chemistry* **84**, 4277–4283.

Hubert J., Nuzillard J.M., Renault J.H. (2017): Dereplication strategies in natural product research: How many tools and methodologies behind the same concept? *Phytochemistry Reviews* **16**, 55–95.

Huigens R.W., Morrison K.C., Hicklin R.W., Timothy T.A., Richter M.F., Hergenrother P.J. (2013): A ring-distortion strategy to construct stereochemically complex and structurally diverse compounds from natural products. *Nature Chemistry* **5**, 195–202.

Ingólfsson H.I., Thakur P., Herold K.F., Hobart E.A., Ramsey N.B., Periole X., De Jong D.H., Zwama M., Yilmaz D., Hall K., Maretzky T., Hemmings H.C., Blobel C., Marrink S.J., Koçer A., Sack J.T., Andersen O.S. (2014): Phytochemicals perturb membranes and promiscuously alter protein function. *ACS Chemical Biology* **9**, 1788–1798.

Ino Y., Gotoh M., Sakamoto M., Tsukagoshi K., Hirohashi S. (2002): Dysadherin, a cancer-associated cell membrane glycoprotein, down-regulates E-cadherin and promotes metastasis. *Proceedings of the National Academy of Sciences of the United States of America* **99**, 365–370.

Irwin J.J., Duan D., Torosyan H., Doak A.K., Ziebart K.T., Sterling T., Tumanian G., Shoichet B.K. (2015): An Aggregation Advisor for Ligand Discovery. *Journal of Medicinal Chemistry* **58**, 7076–7087.

Itkin M., Heinig U., Tzfadia O., Bhide A.J., Shinde B., Cardenas P.D., Bocobza S.E., Unger T., Malitsky S., Finkers R., Tikunov Y., Bovy A., Chikate Y., Singh P., Rogachev I., Beekwilder J., Giri A.P., Aharoni A. (2013): Biosynthesis of antinutritional alkaloids in solanaceous crops is mediated by clustered genes. *Science* **341**, 175–179.

Ito T., Masubuchi M. (2014): Dereplication of microbial extracts and related analytical technologies. *Journal of Antibiotics* **67**, 353–360.

Izumi T., Terauchi M. (2020): The diverse efficacy of food-derived proanthocyanidins for middle-aged and elderly women. *Nutrients* **12**, 1–17.

Jadhav A., Ferreira R.S., Klumpp C., Mott B.T., Austin C.P., Inglese J., Thomas C.J., Maloney D.J., Shoichet B.K., Simeonov A. (2010): Quantitative analyses of aggregation, autofluorescence, and reactivity artifacts in a screen for inhibitors of a thiol protease. *Journal of Medicinal Chemistry* **53**, 37–51.

Jang J.P., Nogawa T., Uramoto M., Okano A., Futamura Y., Shimizu T., Takahashi S., Jang J.H., Ahn J.S., Osada H. (2014): RK-270A-C, new oxindole derivatives isolated from a microbial metabolites fraction library of *Streptomyces* sp. RK85-270. *Journal of Antibiotics* **68**, 293–295.

Jensen A.-M.L., Sørensen T.L.-M., Olesen C., Møller J.V., Nissen P. (2006): Modulatory and catalytic modes of ATP binding by the calcium pump. *The EMBO Journal* **25**, 2305–2314.

Jez J.M., Noel J.P. (2002): Reaction mechanism of chalcone isomerase: pH dependence, diffusion control, and product binding differences. *Journal of Biological Chemistry* **277**, 1361–1369.

Jiang B., Xu D., Allocco J., Parish C., Davison J., Veillette K., Sillaots S., Hu W., Rodriguez-Suarez R., Trosok S., Zhang L., Li Y., Rahkhoodaee F., Ransom T., Martel N., Wang H., Gauvin D., Wiltsie J., Wisniewski D., Salowe S., Kahn J.N., Hsu M.J., Giacobbe R., Abruzzo G., Flattery A., Gill C., Youngman P., Wilson K., Bills G., Platas G., Pelaez F., Diez M.T., Kauffman S., Becker J., Harris G., Liberator P., Roemer T. (2008): PAP Inhibitor with *In Vivo* Efficacy Identified by *Candida albicans* Genetic Profiling of Natural Products. *Chemistry and Biology* **15**, 363–374.

Jimenez T., McDermott J.P., Sánchez G., Blanco G. (2011): Na, K-ATPase α4 isoform is essential for sperm fertility. *Proceedings of the National Academy of Sciences of the United States of America* **108**, 644–649.

Kanai R., Ogawa H., Vilsen B., Cornelius F., Toyoshima C. (2013): Crystal structure of a Na^+-bound Na^+,K^+-ATPase preceding the E_1P state. *Nature* **502**, 201–206.

Kaplan J.H. (2002): Biochemistry of Na,K-ATPase. *Annual Review of Biochemistry* **71**, 511–535.

Katoch M., Singh A., Singh G., Wazir P., Kumar R. (2017): Phylogeny, antimicrobial, antioxidant and enzyme-producing potential of fungal endophytes found in *Viola odorata*. *Annals of Microbiology* **67**, 529–540.

Katz A., Tal D.M., Heller D., Habeck M., Zeev E. Ben, Rabah B., Kana Y.B., Marcovich A.L., Karlish S.J.D. (2015): Digoxin derivatives with selectivity for the α2β3 isoform of Na,K-ATPase potently reduce intraocular pressure. *Proceedings of the National Academy of Sciences of the United States of America* **112**, 13723–13728.

Kennedy J., Marchesi J.R., Dobson A.D.W. (2008): Marine metagenomics: Strategies for the discovery of novel enzymes with biotechnological applications from marine environments. *Microbial Cell Factories* **7**, 27.

Kim E., Moore B.S., Yoon Y.J. (2015): Reinvigorating natural product combinatorial biosynthesis with synthetic biology. *Nature Chemical Biology* **11**, 649–659.

Kintses B., Jangir P.K., Fekete G., Számel M., Méhi O., Spohn R., Daruka L., Martins A., Hosseinnia A., Gagarinova A., Kim S., Phanse S., Csörgő B., Györkei Á., Ari E., Lázár V., Nagy I., Babu M., Pál C., Papp B. (2019): Chemical-genetic profiling reveals limited cross-resistance between antimicrobial peptides with different modes of action. *Nature Communications* **10**, 1–13.

Kitamura N., Ikekita M., Sato T., Akimoto Y., Hatanaka Y., Kawakami H., Inomata M., Furukawa K. (2005): Mouse Na^+/K^+-ATPase β1-subunit has a K^+-dependent cell adhesion activity for β-GlcNac-terminating glycans. *Proceedings of the National Academy of Sciences of the United States of America* **102**, 2796–2801.

Koch E., Malek F.A. (2011): Standardized extracts from hawthorn leaves and flowers in the treatment of cardiovascular disorders preclinical and clinical studies. *Planta Medica* **77**, 1123–1128.

Koch M.A., Schuffenhauer A., Scheck M., Wetzel S., Casaulta M., Odermatt A., Ertl P., Weldmann H. (2005): Charting biologically relevant chemical space: A structural classification of natural products (SCONP). *Proceedings of the National Academy of Sciences of the United States of America* **102**, 17272–17277.

Kongkamnerd J., Milani A., Cattoli G., Terregino C., Capua I., Beneduce L., Gallotta A., Pengo P., Fassina G., Monthakantirat O., Umehara K., De-Eknamkul W., Miertus S. (2011): The quenching effect of flavonoids on 4-methylumbelliferone, a potential pitfall in fluorimetric neuraminidase inhibition assays. *Journal of Biomolecular Screening* **16**, 755–764.

Konoki M.H.K., Tachibana K. (1996): Cholesterol-independent membrane disruption caused by triterpenoid saponins. *Biochimica et Biophysica Acta - Lipids and Lipid Metabolism* **1299**, 252–258.

Kosińska A., Andlauer W. (2012): Cocoa polyphenols are absorbed in Caco-2 cell model of intestinal epithelium. *Food Chemistry* **135**, 999–1005.

Kraus T.E.C., Zasoski R.J., Dahlgren R.A., Horwath W.R., Preston C.M. (2004): Carbon and nitrogen dynamics in a forest soil amended with purified tannins from different plant species. *Soil Biology and Biochemistry* **36**, 309–321.

Kubala M. (2006): ATP-binding to P-type ATPases as revealed by biochemical, spectroscopic, and crystallographic experiments. *Proteins: Structure, Function, and Bioinformatics* **64**, 1–12.

Kubala M., Čechová P., Geletičová J., Biler M., Štenclová T., Trouillas P., Biedermann D. (2016): Flavonolignans As a Novel Class of Sodium Pump Inhibitors. *Frontiers in Physiology* **7**, 115.

de la Iglesia R., Milagro F.I., Campión J., Boqué N., Martínez J.A. (2010): Healthy properties of proanthocyanidins. *BioFactors* **36**, 159–168.

Larsen B.R., Assentoft M., Cotrina M.L., Hua S.Z., Nedergaard M., Kaila K., Voipio J., MacAulay N. (2014): Contributions of the Na^+/K^+-ATPase, NKCC1, and Kir4.1 to hippocampal K^+ clearance and volume responses. *Glia* **62**, 608–622.

Larsen B.R., Stoica A., MacAulay N. (2016): Managing brain extracellular K^+ during neuronal activity: The physiological role of the Na^+/K^+-ATPase subunit isoforms. *Frontiers in Physiology* **7**, 141.

Laursen M., Yatime L., Nissen P., Fedosova N.U. (2013): Crystal structure of the high-affinity Na^+,K^+-ATPase–ouabain complex with Mg^{2+} bound in the cation binding site. *Proceedings of the National Academy of Sciences of the United States of America* **110**, 10958–10963.

Lee A.Y., St.Onge R.P., Proctor M.J., Wallace I.M., Nile A.H., Spagnuolo P.A., Jitkova Y., Gronda M., Wu Y., Kim M.K., Cheung-Ong K., Torres N.P., Spear E.D., Han M.K.L., Schlecht U., Suresh S., Duby G., Heisler L.E., Surendra A., Fung E., Urbanus M.L., Gebbia M., Lissina E., Miranda M., Chiang J.H., Aparicio A.M., Zeghouf M., Davis R.W., Cherfils J., Boutry M., Kaiser C.A., Cummins C.L., Trimble W.S., Brown G.W., Schimmer A.D., Bankaitis V.A., Nislow C., Bader G.D., Giaever G. (2014): Mapping the cellular response to small molecules using chemogenomic fitness signatures. *Science* **344**, 208–211.

Lee K.W., Kim Y.J., Kim D.O., Lee H.J., Lee C.Y. (2003): Major Phenolics in Apple and Their Contribution to the Total Antioxidant Capacity. *Journal of Agricultural and Food Chemistry* **51**, 6516–6520.

Lewis L.K., Yandle T.G., Lewis J.G., Richards A.M., Pidgeon G.B., Kaaja R.J., Nicholls M.G. (1994): Ouabain is not detectable in human plasma. *Hypertension* **24**, 549–555.

Li B., Cui G., Shen G., Zhan Z., Huang L., Chen J., Qi X. (2017): Targeted mutagenesis in the medicinal plant *Salvia miltiorrhiza*. *Scientific Reports* **7**, 1–9.

Li F., Wang Y., Li D., Chen Y., Dou Q.P. (2019): Are we seeing a resurgence in the use of natural products for new drug discovery? *Expert Opinion on Drug Discovery* **14**, 417–420.

Li S., Sui Y., Xiao J., Wu Q., Hu B., Xie B., Sun Z. (2013): Absorption and urinary excretion of A-type procyanidin oligomers from *Litchi chinensis* pericarp in rats by selected ion monitoring liquid chromatography-mass spectrometry. *Food Chemistry* **138**, 1536–1542.

Li Z., Nair S.K. (2015): Structural Basis for Specificity and Flexibility in a Plant 4-Coumarate:CoA Ligase. *Structure* **23**, 2032–2042.

Li Z., Tamari K., Seo Y., Minami K., Takahashi Y., Tatekawa S., Otani K., Suzuki O., Isohashi F., Ogawa K. (2020): Dihydroouabain, a novel radiosensitizer for cervical cancer identified by automated high-throughput screening. *Radiotherapy and Oncology* **148**, 21–29.

Li Z., Zhao C., Zhao X., Xia Y., Sun X., Xie W., Ye Y., Lu X., Xu G. (2018): Deep Annotation of Hydroxycinnamic Acid Amides in Plants Based on Ultra-High-Performance Liquid Chromatography-High-Resolution Mass Spectrometry and Its in Silico Database. *Analytical Chemistry* **90**, 14321–14330.

Lim C.L., Nogawa T., Okano A., Futamura Y., Kawatani M., Takahashi S., Ibrahim D., Osada H. (2016): Unantimycin A, a new neoantimycin analog isolated from a microbial metabolite fraction library. *Journal of Antibiotics* **69**, 456–458.

Lim C.L., Nogawa T., Uramoto M., Okano A., Hongo Y., Nakamura T., Koshino H., Takahashi S., Ibrahim D., Osada H. (2014): RK-1355A and B, novel quinomycin derivatives isolated from a microbial metabolites fraction library based on NPPlot screening. *Journal of Antibiotics* **67**, 323–329.

Lin L.Z., Sun J., Chen P., Monagas M.J., Harnly J.M. (2014): UHPLC-PDA-ESI/HRMSn profiling method to identify and quantify oligomeric proanthocyanidins in plant products. *Journal of Agricultural and Food Chemistry* **62**, 9387–9400.

Lipinski C.A., Lombardo F., Dominy B.W., Feeney P.J. (1997): Experimental and computational approaches to estimate solubility and permeability in drug discovery and development settings. *Advanced Drug Delivery Reviews* **23**, 3–25.

Liu L., Xie B., Cao S., Yang E., Xu X., Guo S. (2007): A-type procyanidins from *Litchi chinensis* pericarp with antioxidant activity. *Food Chemistry* **105**, 1446–1451.

Lu Z., Jia Q., Wang R., Wu X., Wu Y., Huang C., Li Y. (2011): Hypoglycemic activities of A- and B-type procyanidin oligomer-rich extracts from different Cinnamon barks. *Phytomedicine* **18**, 298–302.

Luo Y., Enghiad B., Zhao H. (2016): New tools for reconstruction and heterologous expression of natural product biosynthetic gene clusters. *Natural Product Reports* **33**, 174–182.

Luo Y., Li B.Z., Liu D., Zhang L., Chen Y., Jia B., Zeng B.X., Zhao H., Yuan Y.J. (2015): Engineered biosynthesis of natural products in heterologous hosts. *Chemical Society Reviews* **44**, 5265–5290.

Mackenzie G.G., Delfino J.M., Keen C.L., Fraga C.G., Oteiza P.I. (2009): Dimeric procyanidins are inhibitors of NF-κB-DNA binding. *Biochemical Pharmacology* **78**, 1252–1262.

Mang C., Jakupovic S., Schunk S., Ambrosi H.D., Schwarz O., Jakupovic J. (2006): Natural products in combinatorial chemistry: An andrographolide-based library. *Journal of Combinatorial Chemistry* **8**, 268–274.

Manivasagan P., Venkatesan J., Sivakumar K., Kim S.K. (2014): Pharmaceutically active secondary metabolites of marine actinobacteria. *Microbiological Research* **169**, 262–278.

Marles M.A.S., Ray H., Gruber M.Y. (2003): New perspectives on proanthocyanidin biochemistry and molecular regulation. *Phytochemistry* **64**, 367–383.

McGovern S.L., Caselli E., Grigorieff N., Shoichet B.K. (2002): A common mechanism underlying promiscuous inhibitors from virtual and high-throughput screening. *Journal of Medicinal Chemistry* **45**, 1712–1722.

Medema M.H., Kottmann R., Yilmaz P., Cummings M., Biggins J.B., Blin K., De Bruijn I., Chooi Y.H., Claesen J., Coates R.C., Cruz-Morales P., Duddela S., Düsterhus S., Edwards D.J., Fewer D.P., Garg N., Geiger C., Gomez-Escribano J.P., Greule A., Hadjithomas M., Haines A.S., Helfrich E.J.N., Hillwig M.L., Ishida K., Jones A.C., Jones C.S., Jungmann K., Kegler C., Kim H.U., Kötter P., Krug D., Masschelein J., Melnik A. V., Mantovani S.M., Monroe E.A., Moore M., Moss N., Nützmann H.W., Pan G., Pati A., Petras D., Reen F.J., Rosconi F., Rui Z., Tian Z., Tobias N.J., Tsunematsu Y., Wiemann P., Wyckoff E., Yan X., Yim G., Yu F., Xie Y., Aigle B., Apel A.K., Balibar C.J., Balskus E.P., Barona-Gómez F., Bechthold A., Bode H.B., Borriss R., Brady S.F., Brakhage A.A., Caffrey P., Cheng Y.Q., Clardy J., Cox R.J., De Mot R., Donadio S., Donia M.S., Van Der Donk W.A., Dorrestein P.C., Doyle S., Driessen A.J.M., Ehling-Schulz M., Entian K.D., Fischbach M.A., Gerwick L., Gerwick W.H., Gross H., Gust B., Hertweck C., Höfte M., Jensen S.E., Ju J., Katz L., Kaysser L., Klassen J.L., Keller N.P., Kormanec J., Kuipers O.P., Kuzuyama T., Kyrpides N.C., Kwon H.J., Lautru S., Lavigne R., Lee C.Y., Linquan B., Liu X., Liu W., Luzhetskyy A., Mahmud T., Mast Y., Méndez C., Metsä-Ketelä M., Micklefield J., Mitchell D.A., Moore B.S., Moreira L.M., Müller R., Neilan B.A., Nett M., Nielsen J., O'Gara F., Oikawa H., Osbourn A., Osburne M.S., Ostash B., Payne S.M., Pernodet J.L., Petricek M., Piel J., Ploux O., Raaijmakers J.M., Salas J.A., Schmitt E.K., Scott B., Seipke R.F., Shen B., Sherman D.H., Sivonen K., Smanski M.J., Sosio M., Stegmann E., Süssmuth R.D., Tahlan K., Thomas C.M., Tang Y., Truman A.W., Viaud M., Walton J.D., Walsh C.T., Weber T., Van Wezel G.P., Wilkinson B., Willey J.M., Wohlleben W., Wright G.D., Ziemert N., Zhang C., Zotchev S.B., Breitling R., Takano E., Glöckner F.O. (2015): Minimum Information about a Biosynthetic Gene cluster. *Nature Chemical Biology* **11**, 625–631.

Mendoza-Wilson A.M., Carmelo-Luna F.J., Astiazarán-García H., Mata-Haro V., Espinosa-Plascencia A., del Carmen Bermúdez-Almada M., Rascón-Durán M.L. (2016): Absorption of dimers, trimers and tetramers of procyanidins present in apple skin by IEC-18 cell monolayers. *Journal of Functional Foods* **27**, 386–391.

Mignani S., Rodrigues J., Tomas H., Jalal R., Singh P.P., Majoral J.P., Vishwakarma R.A. (2018): Present drug-likeness filters in medicinal chemistry during the hit and lead optimization process: how far can they be simplified? *Drug Discovery Today* **23**, 605–615.

Miller T.J., Davis P.B. (2008): FXYD5 modulates Na^+ absorption and is increased in cystic fibrosis airway epithelia. *American Journal of Physiology - Lung Cellular and Molecular Physiology* **294**, L654–L664.

Mishra N.K., Habeck M., Kirchner C., Haviv H., Peleg Y., Eisenstein M., Apell H.J., Karlish S.J.D. (2015): Molecular mechanisms and kinetic effects of FXYD1 and phosphomimetic mutants on purified human Na,K-ATPase. *Journal of Biological Chemistry* **290**, 28746–28759.

Mizukasi S., Tanabe Y., Noguchi M., Tamaki E. (1971): *p*-coumaroylputrescine, caffeoylputrescine and feruloylputrescine from callus tissue culture of *Nicotiana tabacum*. *Phytochemistry* **10**, 1347–1350.

Molday L.L., Wu W.W.H., Molday R.S. (2007): Retinoschisin (RS1), the protein encoded by the X-linked retinoschisis gene, is anchored to the surface of retinal photoreceptor and bipolar cells through its interactions with a Na/K ATPase-SARM1 complex. *Journal of Biological Chemistry* **282**, 32792–32801.

Monti J.L.E., Montes M.R., Rossi R.C. (2018): Steady-state analysis of enzymes with non-Michaelis-Menten kinetics: The transport mechanism of Na^+/K^+-ATPase. *Journal of Biological Chemistry* **293**, 1373–1385.

Morineau C., Bellec Y., Tellier F., Gissot L., Kelemen Z., Nogué F., Faure J.D. (2017): Selective gene dosage by CRISPR-Cas9 genome editing in hexaploid *Camelina sativa*. *Plant Biotechnology Journal* **15**, 729–739.

Morth J.P., Pedersen B.P., Buch-Pedersen M.J., Andersen J.P., Vilsen B., Palmgren M.G., Nissen P. (2011): A structural overview of the plasma membrane Na^+,K^+-ATPase and H^+-ATPase ion pumps. *Nature Reviews Molecular Cell Biology* **12**, 60–70.

Mózsik L., Hoekzema M., de Kok N.A.W., Bovenberg R.A.L., Nygård Y., Driessen A.J.M. (2021): CRISPR-based transcriptional activation tool for silent genes in filamentous fungi. *Scientific Reports* **11**, 1118.

Na W., Ma B., Shi S., Chen Y., Zhang H., Zhan Y., An H. (2020): Procyanidin B1, a novel and specific inhibitor of Kv10.1 channel, suppresses the evolution of hepatoma. *Biochemical Pharmacology* **178**, 114089.

Nakamura T., Kawai Y., Kitamoto N., Osawa T., Kato Y. (2009): Covalent modification of lysine residues by allyl isothiocyanate in physiological conditions: Plausible transformation of isothiocyanate from thiol to amine. *Chemical Research in Toxicology* **22**, 536–542.

Narayani M., Chadha A., Srivastava S. (2017): Cyclotides from the Indian Medicinal Plant *Viola odorata* (Banafsha): Identification and Characterization. *Journal of Natural Products* **80**, 1972–1980.

Newman D.J., Cragg G.M. (2020): Natural Products as Sources of New Drugs over the Nearly Four Decades from 01/1981 to 09/2019. *Journal of Natural Products* **83**, 770–803.

Nicolaou K.C., Hale C.R.H., Nilewski C., Ioannidou H.A. (2012): Constructing molecular complexity and diversity: Total synthesis of natural products of biological and medicinal importance. *Chemical Society Reviews* **41**, 5185–5238.

Nie Y., Bai F., Chaudhry M.A., Pratt R., Shapiro J.I., Liu J. (2020): The Na/K-ATPase α1 and c-Src form signaling complex under native condition: A crosslinking approach. *Scientific Reports* **10**, 1–14.

Nilubol N., Zhang L., Shen M., Zhang Y.Q., He M., Austin C.P., Kebebew E. (2012): Four clinically utilized drugs were identified and validated for treatment of adrenocortical cancer using quantitative high-throughput screening. *Journal of Translational Medicine* **10**, 198.

Nishizuka T., Fujita Y., Sato Y., Nakano A., Kakino A., Ohshima S., Kanda T., Yoshimoto R., Sawamura T. (2011): Procyanidins are potent inhibitors of LOX-1: A new player in the French Paradox. *Proceedings of the Japan Academy Series B: Physical and Biological Sciences* **87**, 104–113.

Nogawa T., Okano A., Takahashi S., Uramoto M., Konno H., Saito T., Osada H. (2010): Verticilactam, a new macrolactam isolated from a microbial metabolite fraction library. *Organic Letters* **12**, 4564–4567.

Nogawa T., Takahashi S., Okano A., Kawatani M., Uramoto M., Saito T., Osada H. (2012): Spirotoamides A and B, novel 6,6-spiroacetal polyketides isolated from a microbial metabolite fraction library. *Journal of Antibiotics* **65**, 123–128.

Nonaka S., Arai C., Takayama M., Matsukura C., Ezura H. (2017): Efficient increase of γ-aminobutyric acid (GABA) content in tomato fruits by targeted mutagenesis. *Scientific Reports* **7**, 1–14.

Nothias L.F., Nothias-Esposito M., Da Silva R., Wang M., Protsyuk I., Zhang Z., Sarvepalli A., Leyssen P., Touboul D., Costa J., Paolini J., Alexandrov T., Litaudon M., Dorrestein P.C. (2018): Bioactivity-Based Molecular Networking for the Discovery of Drug Leads in Natural Product Bioassay-Guided Fractionation. *Journal of Natural Products* **81**, 758–767.

Ogawa H., Stokes D.L., Sasabe H., Toyoshima C. (1998): Structure of the Ca^{2+} pump of sarcoplasmic reticulum: A view along the lipid bilayer at 9-Å resolution. *Biophysical Journal* **75**, 41–52.

Ohnuma T., Nakayama S., Anan E., Nishiyama T., Ogura K., Hiratsuka A. (2010): Activation of the Nrf2/ARE pathway via S-alkylation of cysteine 151 in the chemopreventive agent-sensor Keap1 protein by falcarindiol, a conjugated diacetylene compound. *Toxicology and Applied Pharmacology* **244**, 27–36.

Ondeyka J., Harris G., Zink D., Basilio A., Vicente F., Bills G., Platas G., Collado J., González A., De La Cruz M., Martin J., Kahn J.N., Galuska S., Giacobbe R., Abruzzo G., Hickey E., Liberator P., Jiang B., Xu D., Roemer T., Singh S.B. (2009): Isolation, structure elucidation, and biological activity of virgineone from *Lachnum virgineum* using the genome-wide *Candida albicans* fitness test. *Journal of Natural Products* **72**, 136–141.

Osada H., Nogawa T. (2012): Systematic isolation of microbial metabolites for natural products depository (NPDepo). *Pure and Applied Chemistry* **84**, 1407–1420.

Ottaviani J.I., Actis-Goretta L., Villordo J.J., Fraga C.G. (2006): Procyanidin structure defines the extent and specificity of angiotensin I converting enzyme inhibition. *Biochimie* **88**, 359–365.

Ottaviani J.I., Kwik-Uribe C., Keen C.L., Schroeter H. (2012): Intake of dietary procyanidins does not contribute to the pool of circulating flavanols in humans. *The American Journal of Clinical Nutrition* **95**, 851–858.

Ou K., Percival S.S., Zou T., Khoo C., Gu L. (2012): Transport of cranberry A-type procyanidin dimers, trimers, and tetramers across monolayers of human intestinal epithelial caco-2 cells. *Journal of Agricultural and Food Chemistry* **60**, 1390–1396.

Páez O., Martínez-Archundia M., Villegas-Sepúlveda N., Roldan M.L., Correa-Basurto J., Shoshani L. (2019): A model for the homotypic interaction between Na^+,K^+-ATPase β1 subunits reveals the role of extracellular residues 221-229 in its Ig-like domain. *International Journal of Molecular Sciences* **20**.

Palmgren M.G., Nissen P. (2011): P-Type ATPases. *Annual Review of Biophysics* **40**, 243–266.

Pang Y.P., Park J.G., Wang S., Vummenthala A., Mishra R.K., McLaughlin J.E., Di R., Kahn J.N., Tumer N.E., Janosi L., Davis J., Millard C.B. (2011): Small-molecule inhibitor leads of Ribosome-inactivating proteins developed using the doorstop approach. *PLoS ONE* **6**, e17883.

Parsley N.C., Kirkpatrick C.L., Crittenden C.M., Rad J.G., Hoskin D.W., Brodbelt J.S., Hicks L.M. (2018): PepSAVI-MS reveals anticancer and antifungal cycloviolacins in *Viola odorata*. *Phytochemistry* **152**, 61–70.

Parsons A.B., Lopez A., Givoni I.E., Williams D.E., Gray C.A., Porter J., Chua G., Sopko R., Brost R.L., Ho C.H., Wang J., Ketela T., Brenner C., Brill J.A., Fernandez G.E., Lorenz T.C., Payne G.S., Ishihara S., Ohya Y., Andrews B., Hughes T.R., Frey B.J., Graham T.R., Andersen R.J., Boone C. (2006): Exploring the Mode-of-Action of Bioactive Compounds by Chemical-Genetic Profiling in Yeast. *Cell* **126**, 611–625.

De Pascale G., Nazi I., Harrison P.H.M., Wright G.D. (2011): β-Lactone natural products and derivatives inactivate homoserine transacetylase, a target for antimicrobial agents. *Journal of Antibiotics* **64**, 483–487.

Pedersen P.L., Carafoli E. (1987): Ion motive ATPases. I. Ubiquity, properties, and significance to cell function. *Trends in Biochemical Sciences* **12**, 146–150.

Petersen M. (2003): Cinnamic acid 4-hydroxylase from cell cultures of the hornwort *Anthoceros agrestis*. *Planta* **217**, 96–101.

Pfeiffer J., Kühnel C., Brandt J., Duy D., Punyasiri P.A.N., Forkmann G., Fischer T.C. (2006): Biosynthesis of flavan 3-ols by leucoanthocyanidin 4-reductases and anthocyanidin reductases in leaves of grape (*Vitis vinifera* L.), apple (*Malus* x *domestica* Borkh.) and other crops. *Plant Physiology and Biochemistry* **44**, 323–334.

Plössl K., Royer M., Bernklau S., Tavraz N.N., Friedrich T., Wild J., Weber B.H.F., Friedrich U. (2017): Retinoschisin is linked to retinal Na/K-ATPase signaling and localization. *Molecular Biology of the Cell* **28**, 2178–2189.

Pohjala L., Tammela P. (2012): Aggregating Behavior of Phenolic Compounds — A Source of False Bioassay Results? *Molecules* **17**, 10774–10790.

Post R.L., Kume S., Tobin T., Orcutt B., Sen A.K. (1969): Flexibility of an active center in sodium-plus-potassium adenosine triphosphatase. *Journal of General Physiology* **54**, 306–326.

Prasain J.K., Peng N., Dai Y., Moore R., Arabshahi A., Wilson L., Barnes S., Michael Wyss J., Kim H., Watts R.L. (2009): Liquid chromatography tandem mass spectrometry identification of proanthocyanidins in rat plasma after oral administration of grape seed extract. *Phytomedicine* **16**, 233–243.

Prassas I., Diamandis E.P. (2008): Novel therapeutic applications of cardiac glycosides. *Nature Reviews Drug Discovery* **7**, 926–935.

Prassas I., Paliouras M., Datti A., Diamandis E.P. (2008): High-throughput screening identifies cardiac glycosides as potent inhibitors of human tissue kallikrein expression: Implications for cancer therapies. *Clinical Cancer Research* **14**, 5778–5784.

Prior R.L., Gu L. (2005): Occurrence and biological significance of proanthocyanidins in the American diet. *Phytochemistry* **66**, 2264–2280.

Prior R.L., Lazarus S.A., Cao G., Muccitelli H., Hammerstone J.F. (2001): Identification of procyanidins and anthocyanins in blueberries and cranberries (*Vaccinium* spp.) Using high-performance liquid chromatography/mass spectrometry. *Journal of Agricultural and Food Chemistry* **49**, 1270–1276.

Qi X., Bakht S., Leggett M., Maxwell C., Melton R., Osbourn A. (2004): A gene cluster for secondary metabolism in oat: Implications for the evolution of metabolic diversity in plants. *Proceedings of the National Academy of Sciences of the United States of America* **101**, 8233–8238.

Quinn R.J., Carroll A.R., Pham N.B., Baron P., Palframan M.E., Suraweera L., Pierens G.K., Muresan S. (2008): Developing a drug-like natural product library. *Journal of Natural Products* **71**, 464–468.

Rahman I.U., Ijaz F., Afzal A., Iqbal Z., Ali N., Khan S.M. (2016): Contributions to the phytotherapies of digestive disorders: Traditional knowledge and cultural drivers of Manoor Valley, Northern Pakistan. *Journal of Ethnopharmacology* **192**, 30–52.

Rajasekaran S.A., Gopal J., Willis D., Espineda C., Twiss J.L., Rajasekaran A.K. (2004): Na,K-ATPase β1-subunit increases the translation efficiency of the α1-subunit in MSV-MDCK cells. *Molecular Biology of the Cell* **15**, 3224–3232.

Rajasekaran S.A., Palmer L.G., Quan K., Harper J.F., Ball J., Bander N.H., Peralta Soler A., Rajasekaran A.K. (2001): Na,K-ATPase β-subunit is required for epithelial polarization, suppression of invasion, and cell motility. *Molecular Biology of the Cell* **12**, 279–295.

Rárová L., Ncube B., Van Staden J., Fürst R., Strnad M., Gruz J. (2019): Identification of Narciclasine as an *in Vitro* Anti-Inflammatory Component of Cyrtanthus contractus by Correlation-Based Metabolomics. *Journal of Natural Products* **82**, 1372–1376.

Rath C.M., Janto B., Earl J., Ahmed A., Hu F.Z., Hiller L., Dahlgren M., Kreft R., Yu F., Wolff J.J., Kweon H.K., Christiansen M.A., Håkansson K., Williams R.M., Ehrlich G.D., Sherman D.H. (2011): Meta-omic characterization of the marine invertebrate microbial consortium that produces the chemotherapeutic natural product ET-743. *ACS Chemical Biology* **6**, 1244–1256.

Rauf A., Imran M., Abu-Izneid T., Iahtisham-Ul-Haq, Patel S., Pan X., Naz S., Sanches Silva A., Saeed F., Rasul Suleria H.A. (2019): Proanthocyanidins: A comprehensive review. *Biomedicine and Pharmacotherapy* **116**, 108999.

Rios L.Y., Bennett R.N., Lazarus S.A., Rémésy C., Scalbert A., Williamson G. (2002): Cocoa procyanidins are stable during gastric transit in humans. *American Journal of Clinical Nutrition* **76**, 1106–1110.

Rizwan K., Khan S.A., Ahmad I., Rasool N., Ibrahim M., Zubair M., Jaafar H.Z., Manea R. (2019): A Comprehensive Review on Chemical and Pharmacological Potential of *Viola betonicifolia*: A Plant with Multiple Benefits. *Molecules* **24**, 3138.

Roemer T., Xu D., Singh S.B., Parish C.A., Harris G., Wang H., Davies J.E., Bills G.F. (2011): Confronting the challenges of natural product-based antifungal discovery. *Chemistry and Biology* **18**, 148–164.

Rohn S., Rawel H.M., Kroll J. (2002): Inhibitory effects of plant phenols on the activity of selected enzymes. *Journal of Agricultural and Food Chemistry* **50**, 3566–3571.

Rue E.A., Glinski J.A., Glinski V.B., van Breemen R.B. (2020): Ion mobility-mass spectrometry for the separation and analysis of procyanidins. *Journal of Mass Spectrometry* **55**, e4377.

Rupaimoole R., Yoon B., Zhang W.C., Adams B.D., Slack F.J. (2020): A High-Throughput Small Molecule Screen Identifies Ouabain as Synergistic with miR-34a in Killing Lung Cancer Cells. *iScience* **23**, 100878.

Ryabinin A.A., Il'Ina E.M. (1949): The alkaloid of Salsola subaphylla. *Dok Akad Nauk SSSR* **67**, 513–516.

Ryan A.J., Gray N.M., Lowe P.N., Chung C.W. (2003): Effect of detergent on 'promiscuous' inhibitors. *Journal of Medicinal Chemistry* **46**, 3448–3451.

Saint-Lary L., Paris J.-P., Tournayre P., Berdagué J.-L., Thomas O.P., Fernandez X. (2014): Volatile Compounds of *Viola odorata* Absolutes: Identification of Odorant Active Markers to Distinguish Plants Originating from France and Egypt. *Chemistry and biodiversity* **11**, 843–860.

Saint-Lary L., Roy C., Paris J.P., Martin J.F., Thomas O.P., Fernandez X. (2016): Metabolomics for the Authentication of Natural Extracts Used in Flavors and Fragrances: the Case Study of Violet Leaf Absolutes from *Viola odorata*. *Chemistry and Biodiversity* **13**, 737–747.

Salentin S., Schreiber S., Haupt V.J., Adasme M.F., Schroeder M. (2015): PLIP: Fully automated protein-ligand interaction profiler. *Nucleic Acids Research* **43**, W443–W447.

Salles P., Fernandez H.H. (2020): Untangling the complicated web of ATP1A3 mutations. *Parkinsonism and Related Disorders* **78**, 186–188.

Sankar M.G., Mantilli L., Bull J., Giordanetto F., Bauer J.O., Strohmann C., Waldmann H., Kumar K. (2015): Stereoselective synthesis of a natural product inspired tetrahydroindolo[2,3-a]-quinolizine compound library. *Bioorganic and Medicinal Chemistry* **23**, 2614–2620.

Sano A., Yamakoshi J., Tokutake S., Tobe K., Kubota Y., Kikuchi M. (2003): Procyanidin B1 is detected in human serum after intake of proanthocyanidin-rich grape seed extract. *Bioscience, Biotechnology and Biochemistry* **67**, 1140–1143.

Sassano M.F., Doak A.K., Roth B.L., Shoichet B.K. (2013): Colloidal aggregation causes inhibition of G protein-coupled receptors. *Journal of Medicinal Chemistry* **56**, 2406–2414.

Sato M., Maulik G., Ray P.S., Bagchi D., Das D.K. (1999): Cardioprotective effects of grape seed proanthocyanidin against ischemic reperfusion injury. *Journal of Molecular and Cellular Cardiology* **31**, 1289–1297.

Satoh K., Nagai F., Ushiyama K., Kano I. (1996): Specific inhibition of Na^+,K^+-ATPase activity by Atractylon, a major component of Byaku-jutsu, by interaction with enzyme in the E_2 state. *Biochemical Pharmacology* **51**, 339–343.

Schack V.R., Morth J.P., Toustrup-Jensen M.S., Anthonisen A.N., Nissen P., Andersen J.P., Vilsen B. (2008): Identification and function of a cytoplasmic K^+ site of the Na^+,K^+-ATPase. *Journal of Biological Chemistry* **283**, 27982–27990.

Schilling S., Sigolotto C.I., Carle R., Schieber A. (2008): Characterization of covalent addition products of chlorogenic acid quinone with amino acid derivatives in model systems and apple juice by high-performance liquid chromatography/electrospray ionization tandem mass spectrometry. *Rapid Communications in Mass Spectrometry* **22**, 441–448.

Schlenk D., Sapozhnikova Y., Irwin M.A., Xie L., Hwang W., Reddy S., Brownawell B.J., Armstrong J., Kelly M., Montagne D.E., Kolodziej E.P., Sedlak D., Snyder S. (2005): *In vivo* bioassay-guided fractionation of marine sediment extracts from the Southern California Bight, USA, for estrogenic activity. *Environmental Toxicology and Chemistry* **24**, 2820–2826.

Schmitz R. (1985): Friedrich Wilhelm Sertürner and the Discovery of Morphine. *Pharmacy in History* **27**, 61–74.

Schneditz G., Elias J.E., Pagano E., Zaeem Cader M., Saveljeva S., Long K., Mukhopadhyay S., Arasteh M., Lawley T.D., Dougan G., Bassett A., Karlsen T.H., Kaser A., Kaneider N.C. (2019): GPR35 promotes glycolysis, proliferation, and oncogenic signaling by engaging with the sodium potassium pump. *Science Signaling* **12**.

Schneider P., Schneider G. (2003): Collection of Bioactive Reference Compounds for Focused Library Design. *QSAR & Combinatorial Science* **22**, 713–718.

Schoenbohm C., Martens S., Eder C., Forkmann G., Weisshaar B. (2000): Identification of the arabidopsis thaliana flavonoid 3'-hydroxylase gene and functional expression of the encoded P450 enzyme. *Biological Chemistry* **381**, 749–753.

Schoner W. (2002): Endogenous cardiac glycosides, a new class of steroid hormones. *European Journal of Biochemistry* **269**, 2440–2448.

Schrimpe-Rutledge A.C., Sherrod S.D., McLean J.A. (2018): Improving the discovery of secondary metabolite natural products using ion mobility–mass spectrometry. *Current Opinion in Chemical Biology* **42**, 160–166.

Schwinger R.H.G., Pietsch M., Frank K., Brixius K. (2000): Crataegus special extract WS 1442 increases force of contraction in human myocardium cAMP-independently. *Journal of Cardiovascular Pharmacology* **35**, 700–707.

Segall L., Mezzetti A., Scanzano R., Gargus J.J., Purisima E., Blostein R. (2005): Alterations in the α2 isoform of Na,K-ATPase associated with familial hemiplegic migraine type 2. *Proceedings of the National Academy of Sciences of the United States of America* **102**, 11106–11111.

Seidler J., McGovern S.L., Doman T.N., Shoichet B.K. (2003): Identification and prediction of promiscuous aggregating inhibitors among known drugs. *Journal of Medicinal Chemistry* **46**, 4477–4486.

Serra A., MacI A., Romero M.P., Valls J., Bladé C., Arola L., Motilva M.J. (2010): Bioavailability of procyanidin dimers and trimers and matrix food effects in *in vitro* and *in vivo* models. *British Journal of Nutrition* **103**, 944–952.

Serra A., Macià A., Romero M.P., Salvadó M.J., Bustos M., Fernández-Larrea J., Motilva M.J. (2009): Determination of procyanidins and their metabolites in plasma samples by improved liquid chromatography-tandem mass spectrometry. *Journal of Chromatography B: Analytical Technologies in the Biomedical and Life Sciences* **877**, 1169–1176.

Serra A., Macià A., Rubió L., Anglès N., Ortega N., Morelló J.R., Romero M.P., Motilva M.J. (2013): Distribution of procyanidins and their metabolites in rat plasma and tissues in relation to ingestion of procyanidin-enriched or procyanidin-rich cocoa creams. *European Journal of Nutrition* **52**, 1029–1038.

Sferrazza G., Corti M., Andreola F., Giovannini D., Nicotera G., Zonfrillo M., Serra M., Tengattini S., Calleri E., Brusotti G., Pierimarchi P., Serafino A. (2020): Bioassay-Guided Isolation of Nigracin, Responsible for the Tissue Repair Properties of *Drypetes Klainei* Stem Bark. *Frontiers in Pharmacology* **10**, 1.

Shinoda T., Ogawa H., Cornelius F., Toyoshima C. (2009): Crystal structure of the sodium-potassium pump at 2.4 Å resolution. *Nature* **459**, 446–450.

Shoichet B.K. (2006): Interpreting steep dose-response curves in early inhibitor discovery. *Journal of Medicinal Chemistry* **49**, 7274–7277.

Shoji T., Masumoto S., Moriichi N., Akiyama H., Kanda T., Ohtake Y., Goda Y. (2006): Apple procyanidin oligomers absorption in rats after oral administration: Analysis of procyanidins in plasma using the porter method and high-performance liquid chromatography/tandem mass spectrometry. *Journal of Agricultural and Food Chemistry* **54**, 884–892.

Simeonov A., Jadhav A., Thomas C.J., Wang Y., Huang R., Southall N.T., Shinn P., Smith J., Austin C.P., Auld D.S., Inglese J. (2008): Fluorescence spectroscopic profiling of compound libraries. *Journal of Medicinal Chemistry* **51**, 2363–2371.

Simpson C.D., Mawji I.A., Anyiwe K., Williams M.A., Wang X., Venugopal A.L., Gronda M., Hurren R., Cheng S., Serra S., Zavareh R.B., Datti A., Wrana J.L., Ezzat S., Schimmer A.D. (2009): Inhibition of the sodium potassium adenosine triphosphatase pump sensitizes cancer cells to anoikis and prevents distant tumor formation. *Cancer Research* **69**, 2739–2747.

Skou J.C. (1957): The influence of some cations on an adenosine triphosphatase from peripheral nerves. *BBA - Biochimica et Biophysica Acta* **23**, 394–401.

Somanadhan B., Leong C., Whitton S.R., Ng S., Buss A.D., Butler M.S. (2011): Identification of a naturally occurring quinazolin-4(3*H*)-one firefly luciferase inhibitor. *Journal of Natural Products* **74**, 1500–1502.

Søndergaard D., Pedersen C.N.S. (2015): PATBox: A Toolbox for Classification and Analysis of P-Type ATPases. *PLOS ONE* **10**, e0139571.

Song Y., Lee S.Y., Kim S., Choi I., Kim S.H., Shum D., Heo J., Kim A.R., Kim K.M., Seo H.R. (2020): Inhibitors of Na^+/K^+ ATPase exhibit antitumor effects on multicellular tumor spheroids of hepatocellular carcinoma. *Scientific Reports* **10**, 1–16.

Sørensen D.M., Holen H.W., Pedersen J.T., Martens H.J., Silvestro D., Stanchev L.D., Costa S.R., Günther Pomorski T., López-Marqués R.L., Palmgren M. (2019): The P5A ATPase Spf1p is stimulated by phosphatidylinositol 4-phosphate and influences cellular sterol homeostasis H. Riezman, ed. *Molecular Biology of the Cell* **30**, 1069–1084.

Sørensen Thomas Lykke Møller, Clausen J.D., Jensen A.M.L., Vilsen B., Møller J.V., Andersen J.P., Nissen P. (2004): Localization of a K^+-binding site involved in dephosphorylation of the sarcoplasmic reticulum Ca^{2+}-ATPase. *Journal of Biological Chemistry* **279**, 46355–46358.

Sørensen Thomas Lykke Moller, Møller J.V., Nissen P. (2004): Phosphoryl transfer and calcium ion occlusion in the calcium pump. *Science* **304**, 1672–1675.

Souccar C., Cysneiros R.M., Tanae M.M., Torres L.M.B., Lima-Landman M.T.R., Lapa A.J. (2008): Inhibition of gastric acid secretion by a standardized aqueous extract of *Cecropia glaziovii* Sneth and underlying mechanism. *Phytomedicine* **15**, 462–469.

Suvanto J., Karppinen K., Riihinen K., Jaakola L., Salminen J.P. (2020): Changes in the Proanthocyanidin Composition and Related Gene Expression in Bilberry (*Vaccinium myrtillus* L.) Tissues. *Journal of Agricultural and Food Chemistry* **68**, 7378–7386.

Svedström U., Vuorela H., Kostiainen R., Huovinen K., Laakso I., Hiltunen R. (2002): High-performance liquid chromatographic determination of oligomeric procyanidins from dimers up to the hexamer in hawthorn. *Journal of Chromatography A* **968**, 53–60.

Svedström U., Vuorela H., Kostiainen R., Laakso I., Hiltunen R. (2006): Fractionation of polyphenols in hawthorn into polymeric procyanidins, phenolic acids and flavonoids prior to high-performance liquid chromatographic analysis. *Journal of Chromatography A* **1112**, 103–111.

Tamura T., Ozawa M., Kobayashi S., Watanabe H., Arai S., Mura K. (2015): Inhibitory effect of oligomeric polyphenols from peanut-skin on sugar digestion enzymes and glucose transport. *Food Science and Technology Research* **21**, 111–115.

Tanaka N., Sekiya N., Hattori M., Goto H., Shibahara N., Shimada Y., Terasawa K. (2003): Measurement of plasma procyanidin B-2 and procyanidin B-3 levels after oral administration in rat. *Phytomedicine* **10**, 122–126.

Tanaka T., Kondou K., Kouno I. (2000): Oxidation and epimerization of epigallocatechin in banana fruits. *Phytochemistry* **53**, 311–316.

Thorne N., Shen M., Lea W.A., Simeonov A., Lovell S., Auld D.S., Inglese J. (2012): Firefly luciferase in chemical biology: A compendium of inhibitors, mechanistic evaluation of chemotypes, and suggested use as a reporter. *Chemistry and Biology* **19**, 1060–1072.

Tian J., Cai T., Yuan Z., Wang H., Liu L., Haas M., Maksimova E., Huang X.Y., Xie Z.J. (2006): Binding of Src to Na^+/K^+-ATPase forms a functional signaling complex. *Molecular Biology of the Cell* **17**, 317–326.

Timcenko M., Lyons J.A., Januliene D., Ulstrup J.J., Dieudonné T., Montigny C., Ash M.R., Karlsen J.L., Boesen T., Kühlbrandt W., Lenoir G., Moeller A., Nissen P. (2019): Structure and autoregulation of a P4-ATPase lipid flippase. *Nature* **571**, 366–370.

Tokhtaeva E., Clifford R.J., Kaplan J.H., Sachs G., Vagin O. (2012): Subunit isoform selectivity in assembly of Na,K-ATPase α-β heterodimers. *Journal of Biological Chemistry* **287**, 26115–26125.

Tokhtaeva E., Sachs G., Souda P., Bassilian S., Whitelegge J.P., Shoshani L., Vagin O. (2011): Epithelial junctions depend on intercellular trans-interactions between the Na,K-ATPase β1 subunits. *Journal of Biological Chemistry* **286**, 25801–25812.

Tokhtaeva E., Sun H., Deiss-Yehiely N., Wen Y., Soni P.N., Gabrielli N.M., Marcus E.A., Ridge K.M., Sachs G., Vazquez-Levin M., Sznajder J.I., Vagin O., Dada L.A. (2016): The O-glycosylated ectodomain of FXYD5 impairs adhesion by disrupting cell-cell trans-dimerization of Na,K-ATPase β1 subunits. *Journal of Cell Science* **129**, 2394–2406.

Tomochika K., Shimizu-Ibuka A., Tamura T., Mura K., Abe N., Onose J., Arai S. (2011): Effects of Peanut-Skin Procyanidin A1 on Degranulation of RBL-2H3 Cells. *Bioscience, Biotechnology, and Biochemistry* **75**, 1644–1648.

Toustrup-Jensen M.S., Holm R., Einholm V.R., Morth P.J., Nissen P., Andersen J.P., Vilsen B. (2009): The C terminus of Na^+,K^+-ATPase controls Na^+ affinity on both sides of the membrane through Arg935. *Journal of Biological Chemistry* **284**, 18715–18725.

Toyoshima C., Kanai R., Cornelius F. (2011): First Crystal Structures of Na^+,K^+-ATPase: New Light on the Oldest Ion Pump. *Structure* **19**, 1732–1738.

Toyoshima C., Nakasako M., Nomura H., Ogawa H. (2000): Crystal structure of the calcium pump of sarcoplasmic reticulum at 2.6 Å resolution. *Nature* **405**, 647–655.

Toyoshima C., Nomura H., Tsuda T. (2004): Lumenal gating mechanism revealed in calcium pump crystal structures with phosphate analogues. *Nature* **432**, 361–368.

Toyoshima C., Sasabe H., Stokes D.L. (1993): Three-dimensional cryo-electron microscopy of the calcium ion pump in the sarcoplasmic reticulum membrane. *Nature* **362**, 469–471.

Trott O., Olson A.J. (2009): AutoDock Vina: Improving the speed and accuracy of docking with a new scoring function, efficient optimization, and multithreading. *Journal of Computational Chemistry* **31**, NA-NA.

Tsang C., Auger C., Mullen W., Bornet A., Rouanet J.-M., Crozier A., Teissedre P.-L. (2005): The absorption, metabolism and excretion of flavan-3-ols and procyanidins following the ingestion of a grape seed extract by rats. *British Journal of Nutrition* **94**, 170–181.

Tulp M., Bohlin L. (2005): Rediscovery of known natural compounds: Nuisance or goldmine? *Bioorganic and Medicinal Chemistry* **13**, 5274–5282.

Turek-Etienne T.C., Small E.C., Soh S.C., Xin T.A., Gaitonde P. V., Barrabee E.B., Hart R.F., Bryant R.W. (2003): Evaluation of fluorescent compound interference in 4 fluorescence polarization assays: 2 Kinases, 1 protease, and 1 phosphatase. *Journal of Biomolecular Screening* **8**, 176–184.

Turnbull J.J., Nakajima J.I., Welford R.W.D., Yamazaki M., Saito K., Schofield C.J. (2004): Mechanistic studies on three 2-oxoglutarate-dependent oxygenases of flavonoid biosynthesis: Anthocyanidin synthase, flavonol synthase, and flavanone 3β-hydroxylase. *Journal of Biological Chemistry* **279**, 1206–1216.

Uddin M.J., Kokubo S., Ueda K., Suenaga K., Uemura D. (2001): Haterumaimides F-I, four new cytotoxic diterpene alkaloids from an ascidian *Lissoclinum* species. *Journal of Natural Products* **64**, 1169–1173.

Vagin O., Tokhtaeva E., Sachs G. (2006): The role of the β1 subunit of the Na,K-ATPase and its glycosylation in cell-cell adhesion. *Journal of Biological Chemistry* **281**, 39573–39587.

Vartoukian S.R., Palmer R.M., Wade W.G. (2010): Strategies for culture of 'unculturable' bacteria. *FEMS Microbiology Letters* **309**, no-no.

Verma G., Dua V.K., Agarwal D.D., Atul P.K. (2011): Anti-malarial activity of *Holarrhena antidysenterica* and *Viola canescens*, plants traditionally used against malaria in the Garhwal region of north-west Himalaya. *Malaria Journal* **10**, 1–5.

Wall M.E., Wani M.C., Brown D.M., Fullas F., Olwald J.B., Josephson F.F., Thornton N.M., Pezzuto J.M., Beecher C.W.W., Farnsworth N.R., Cordell G.A., Kinghorn A.D. (1996): Effect of tannins on screening of plant extracts for enzyme inhibitory activity and techniques for their removal. *Phytomedicine* **3**, 281–285.

Wang H., Cong W.L., Fu Z.L., Chen D.F., Wang Q. (2017): Anti-complementary constituents of *Viola kunawarensis*. *Natural Product Research* **31**, 2312–2315.

Wang L., Yamashita Y., Komeda S., Saito A., Ashida H. (2018): Absorption, metabolism, distribution and faecal excretion of B-type procyanidin oligomers in mice after a single oral administration of black soybean seed coat extract. *Food and Function* **9**, 5362–5370.

Wang Q.Q., Gao H., Yuan R., Han S., Li X.X., Tang M., Dong B., Li J.X., Zhao L.C., Feng J., Yang S. (2020): Procyanidin A2, a polyphenolic compound, exerts anti-inflammatory and anti-oxidative activity in lipopolysaccharide-stimulated RAW264.7 cells. *PLoS ONE* **15**.

Wang R., Wang J., Liu Y., Zhang X., Liang X. (2019): Resonant waveguide grating based assays for colloidal aggregate detection and promiscuity characterization in natural products. *RSC Advances* **9**, 38055–38064.

Wani M.C., Taylor H.L., Wall M.E., Coggon P., Mcphail A.T. (1971): Plant Antitumor Agents. VI. The Isolation and Structure of Taxol, a Novel Antileukemic and Antitumor Agent from Taxus brevifolia. *Journal of the American Chemical Society* **93**, 2325–2327.

Welling M.T., Liu L., Rose T.J., Waters D.L.E., Benkendorff K. (2016): Arbuscular mycorrhizal fungi: effects on plant terpenoid accumulation. *Plant Biology* **18**, 552–562.

Wha Jun D., Hwang M., Kim H.J., Hwang S.K., Kim S., Lee C.-H. (2013): Ouabain, a Cardiac Glycoside, Inhibits the Fanconi Anemia/BRCA Pathway Activated by DNA Interstrand Cross-Linking Agents P. Fei, ed. *PLoS ONE* **8**, e75905.

Wilde S.C., Treitz C., Keppler J.K., Koudelka T., Palani K., Tholey A., Rawel H.M., Schwarz K. (2016): β-Lactoglobulin as nanotransporter - Part II: Characterization of the covalent protein modification by allicin and diallyl disulfide. *Food Chemistry* **197**, 1022–1029.

Willer E.A., Malli R., Bondarenko A.I., Zahler S., Vollmar A.M., Graier W.F., Fürst R. (2012): The vascular barrier-protecting hawthorn extract WS 1442 raises endothelial calcium levels by inhibition of SERCA and activation of the IP3 pathway. *Journal of Molecular and Cellular Cardiology* **53**, 567–577.

Williams D.H., Stone M.J., Hauck P.R., Rahman S.K. (1989): Why are secondary metabolites (Natural Products) biosynthesized. *Journal of Natural Products* **52**, 1189–1208.

Wilson B.A.P., Thornburg C.C., Henrich C.J., Grkovic T., O'Keefe B.R. (2020): Creating and screening natural product libraries. *Natural Product Reports* **37**, 893–918.

Winzer T., Gazda V., He Z., Kaminski F., Kern M., Larson T.R., Li Y., Meade F., Teodor R., Vaistij F.E., Walker C., Bowser T.A., Graham I.A. (2012): A *papaver somniferum* 10-gene cluster for synthesis of the anticancer alkaloid noscapine. *Science* **336**, 1704–1708.

Wolfender J.L., Marti G., Thomas A., Bertrand S. (2015): Current approaches and challenges for the metabolite profiling of complex natural extracts. *Journal of Chromatography A* **1382**, 136–164.

Xie D.Y., Dixon R.A. (2005): Proanthocyanidin biosynthesis - Still more questions than answers? *Phytochemistry* **66**, 2127–2144.

Xie Z., Askari A. (2002): Na^+/K^+-ATPase as a signal transducer. *European Journal of Biochemistry* **269**, 2434–2439.

Yang B., Liu P. (2012): Composition and health effects of phenolic compounds in hawthorn (*Crataegus* spp.) of different origins. *Journal of the Science of Food and Agriculture* **92**, 1578–1590.

Yang H., Tuo X., Wang L., Tundis R., Portillo M.P., Simal-Gandara J., Yu Y., Zou L., Xiao J., Deng J. (2021): Bioactive procyanidins from dietary sources: The relationship between bioactivity and polymerization degree. *Trends in Food Science and Technology* **111**, 114–127.

Yap J.Q., Seflova J., Sweazey R., Artigas P., Robia S.L. (2021): FXYD proteins and sodium pump regulatory mechanisms. *Journal of General Physiology* **153**.

Yatime L., Laursen M., Morth J.P., Esmann M., Nissen P., Fedosova N.U. (2011): Structural insights into the high affinity binding of cardiotonic steroids to the Na^+,K^+-ATPase. *Journal of Structural Biology* **174**, 296–306.

Yokomichi T., Morimoto K., Oshima N., Yamada Y., Fu L., Taketani S., Ando M., Kataoka T. (2011): Ursolic acid inhibits Na^+/K^+-ATPase activity and prevents TNF-α-induced gene expression by blocking amino acid transport and cellular protein synthesis. *Biomolecules* **1**, 32–47.

Yosef E., Katz A., Peleg Y., Mehlman T., Karlish S.J.D. (2016): Do Src kinase and caveolin interact directly with Na,K-ATPase? *Journal of Biological Chemistry* **291**, 11736–11750.

Young V.C., Artigas P. (2021): Displacement of the Na^+/K^+-Pump'S Transmembrane Domains Demonstrate Conserved Conformational Changes in P-Type 2 ATPases. *Biophysical Journal* **120**, e2019317118.

Yu F., Li B., Yin M., Lu W., Li X., Cheng M., Gao H. (2020): Proteomic analysis of liver mitochondria of db/db mice treated with grape seed procyanidin B2. *Journal of Food Biochemistry* **44**, 13443.

Yudowski G.A., Efendiev R., Pedemonte C.H., Katz A.I., Berggren P.O., Bertorello A.M. (2000): Phosphoinositide-3 kinase binds to a proline-rich motif in the Na^+,K^+-ATPase α subunit and regulates its trafficking. *Proceedings of the National Academy of Sciences of the United States of America* **97**, 6556–6561.

Zdravkovic I., Zhao C., Lev B., Cuervo J.E., Noskov S.Y. (2012): Atomistic models of ion and solute transport by the sodium-dependent secondary active transporters. *Biochimica et Biophysica Acta - Biomembranes* **1818**, 337–347.

Zhang H., Fang L., Osburne M.S., Pfeifer B.A. (2016): The continuing development of *E. coli* as a heterologous host for complex natural product biosynthesis. In: *Methods in Molecular Biology*. Totowa, New Jersey, USA, Humana Press Inc., pp. 121–134.

Zhang L., He M., Zhang Y., Nilubol N., Shen M., Kebebew E. (2012): Quantitative high-throughput drug screening identifies novel classes of drugs with anticancer activity in thyroid cancer cells: Opportunities for repurposing. *Journal of Clinical Endocrinology and Metabolism* **97**, E319.

Zhang Mingzi M, Qiao Y., Ang E.L., Zhao H. (2017): Using natural products for drug discovery: the impact of the genomics era. *Expert Opinion on Drug Discovery* **12**, 475–487.

Zhang Mingzi M., Wong F.T., Wang Y., Luo S., Lim Y.H., Heng E., Yeo W.L., Cobb R.E., Enghiad B., Ang E.L., Zhao H. (2017): CRISPR-Cas9 strategy for activation of silent Streptomyces biosynthetic gene clusters. *Nature Chemical Biology* **13**, 607–609.

Zhang P., Toyoshima C., Yonekura K., Green N.M., Stokes D.L. (1998): Structure of the calcium pump from sarcoplasmic reticulum at 8-Å resolution. *Nature* **392**, 835–839.

Zhang S., Malmersjö S., Li J., Ando H., Aizman O., Uhlén P., Mikoshiba K., Aperia A. (2006): Distinct role of the N-terminal tail of the Na,K-ATPase catalytic subunit as a signal transducer. *Journal of Biological Chemistry* **281**, 21954–21962.

Zhang X.C., Zhang H. (2019): P-type ATPases use a domain-association mechanism to couple ATP hydrolysis to conformational change. *Biophysics Reports* **5**, 167–175.

Zhao L., Wen L., Lu Q., Liu R. (2020): Interaction mechanism between α-glucosidase and A-type trimer procyanidin revealed by integrated spectroscopic analysis techniques. *International Journal of Biological Macromolecules* **143**, 173–180.

Zhu Y., Zhao L., Wang X., Li P. (2016): Pharmacognostical and phytochemical studies of *Viola tianschanica* Maxim. - An Uyghur ethnomedicinal plant. *Journal of Pharmacy & Pharmacognosy Research* **4**, 95–106.

Zubek S., Rola K., Szewczyk A., Majewska M.L., Turnau K. (2015): Enhanced concentrations of elements and secondary metabolites in *Viola tricolor* L. induced by arbuscular mycorrhizal fungi. *Plant and Soil* **390**, 129–142.

Zumdick S., Petereit F., Luftmann H., Hensel A. (2009): Preparative isolation of oligomeric procyanidins from Hawthorn (*Crataegus* spp.). *Pharmazie* **64**, 286–288.

8 ABBREVIATIONS

A-domain	actuator domain
AO	anthroyl ouabain
DW	dry weight
M-domain	membrane domain
N-domain	nucleotide-binding domain
NKA	Na^+,K^+-ATPase
PC1	procyanidin C1
P-domain	phosphorylation domain
pNPP	*p*-nitrophenyl phosphate
R-domain	regulator domain
S-domain	support domain
SERCA	sarco/endoplasmic reticulum Ca^{2+}-ATPase
T-domain	transport domain